博士論文（要約）

A Study of Redirected Walking With Individual Characteristics of the Sensory Systems

（感覚系の個人特性を考慮したリダイレクテッドウォーキングの研究）

松本 啓吾

A Study of Redirected Walking With Individual Characteristics of the Sensory Systems (Summary)

by

Keigo Matsumoto

A dissertation submitted to
the Department of Mechano-Informatics,
the Graduate School of Information Science and Technology,
the University of Tokyo, Tokyo, Japan
in Partial Fulfillment of the Requirements
for the Degree of Doctor of Philosophy
in Information Science and Technology

March 2021

Acknowledgement

I would like to express my gratitude to Prof. Dr. Takuji Narumi for his patience, encouragement, and guidance as my supervisor throughout my time as his student. I am fortunate to learn from an enthusiastic supervisor who values my research independence and always responds quickly to my questions and concerns. I would also like to express my deepest appreciation to the remaining members of my thesis committee: Prof. Dr. Yasuo Kuniyoshi, Prof. Dr. Masahiko Inami, Prof. Dr. Takeshi Naemura, and Prof. Dr. Hideaki Kuzuoka. Their comments, advice, as well as broad and in-depth insights have immensely helped me with the discussion of this dissertation.

I am also grateful to the members and alumni of the Cyber Interface Laboratory at the University of Tokyo, with whom I have had the pleasure of working together. In particular, I would like to thank Prof. Dr. Hideaki Kuzuoka, Prof. Dr. Kazuma Aoyama, Prof. Dr. Yuki Ban, and Prof. Dr. Michitaka Hirose. Prof. Kuzuoka offered me insightful advice on the overall structure of this dissertation. Prof. Aoyama was very generous with his cooperation in developing Chapter 5. Prof. Ban provided useful guidance for the research in Chapter 7. Prof. Hirose very kindly taught me about the philosophy of research. I am fortunate to have had the opportunity to collaborate with such great members and receive support from them. I am also particularly grateful for the administrative assistance given by Yoshiyuki Nakagaki, Yasuko Hanabusa, Natsumi Hatsuya, and Yuka Kato.

Furthermore, I would like to thank the external collaborators who assisted with my research. I would also like to express my gratitude to Prof. Dr. Frank Steinicke, Dr. Eike Langbehn, and Mr. Yohei Yanase for their academic and industrial assistance. The success of this dissertation is also owed to the Global Creative Leaders (GCL) program at the University of Tokyo. I am thankful to Prof. Tanikawa and the other faculty members of the GCL program for their advice. I also spent a considerable amount of time with the GCL students on joint projects and discussions, and I

gratefully acknowledge them for helping me in every way they could. Many of them have also become close friends of mine during this time. I thank the Japan Society for the Promotion of Science (a Grant-in-Aid for JSPS Fellows; 18J21379). Finally, I am indebted to my family, without whose understanding, support, and encouragement, I could not have got here. Lastly, I would like to once again thank all the people involved in the laboratory and projects, everyone who cooperated with the experiments, and my family and friends, who have immensely supported me.

Abstract

Redirected walking (RDW) is a set of technologies that enables users to walk freely within a virtual environment (VE) by controlling the spatial correspondence of virtual and real environments. The ultimate goal of the RDW is to enable users to explore an arbitrary virtual reality (VR) space in a room-scale real space while maintaining a natural gait. Extensive research has been conducted in this field over the past 20 years, and various algorithms, techniques, and evaluation methods have been proposed. However, there are still numerous unsolved problems in achieving the ultimate goal of RDW.

One of the major problems of RDW is detection thresholds, which are the smallest manipulations that a user can detect. In general, manipulations of RDWs are performed below a detection threshold because performing manipulations beyond the threshold may decrease the sense of presence and cause cybersickness. A large number of studies have estimated the value of the detection threshold or proposed methods to estimate the detection threshold. According to these studies, the detection threshold is not constant, and it is strongly affected by equipment, VEs, and individual differences. In particular, it has been shown that there are significant individual differences in detection thresholds. The effectiveness of the conventional RDW method that uses only visual manipulations is limited, and it is not always possible to compress an arbitrary VR space into a room-scale real space using manipulations below the perceptual threshold.

In this work, we addressed the aforementioned issues using findings from physiology and psychology. We addressed the issues of individual differences in detection thresholds in terms of sensory characteristics (Chapter 3). In addition, on the basis of physiology, the effects of an RDW technique were estimated using physiological and behavioral indices (Chapter 4).

We attempted to improve the limited effectiveness of RDW using senses other than vision. We used the findings of cognitive science for this purpose, i.e., spatial

perception consists of vision, vestibular perception, somatosensory perception, and hearing. In recent years, the maximum likelihood estimation (MLE) model has been presented as a versatile model of sensory integration in the field of perceptual psychology. We used the MLE model to develop the novel RDW methods, which used vestibular perception (Chapter 5), auditory perception (Chapter 6), and haptic perception (Chapter 7). We evaluated these methods using the estimation methods proposed in Chapters 3 and 4 and the conventional psychophysical method.

In Chapter 3, we evaluated the relationship between detection thresholds, cybersickness, and perceptual characteristics. In the field of developmental psychology, it is well known that there is a relationship between perceptual characteristics and spatial perception. Therefore, we considered that there is a relationship between sensory characteristics and RDW, which is a type of spatial perceptual manipulation. A psychophysical experiment was conducted to estimate the detection thresholds of an RDW technique, and a questionnaire was used to evaluate the individual perceptual characteristics. Our results suggested that participants with a higher propensity for sensory sensitivity and sensory avoidance were more likely to notice RDW manipulation.

In Chapter 4, we investigated the relationship between redirection thresholds and physiological and behavioral indices and discussed the method for inferring redirection thresholds based on physiological and behavioral indices. The pupil diameter and microsaccades were selected as physiological indices, and walking speed and head sway were selected as behavioral indices. Experimental results showed a correlation between walking speed, head sway and redirection thresholds.

In Chapter 5, based on the MLE theory, we hypothesized that reducing the reliability of vestibular sensation would improve the effectiveness of RDW and reduce cybersickness. Noisy galvanic vestibular stimulation (nGVS) was used to reduce the reliability of vestibular sensation. We conducted a psychophysical experiment to estimate the detection thresholds of curvature gain and measure cybersickness under two nGVS conditions. The results suggested that nGVS might affect the detection thresholds of curvature gain.

In Chapter 6, we first investigated whether MLE could be applied to incongruent visuo-auditory integration in a VR environment. Then, we proposed a novel method that introduced visual noise and incongruence between the visual and auditory cues of an object in a VE while applying curvature gain. We verified the effectiveness of this method by comparing it with existing psychophysical methods.

Finally, in Chapter 7, we explored the possibility of visuo-haptic RDW. We verified the effectiveness of this method through psychophysical and behavioral evaluations. Then, we created *Unlimited Corridor*, which was a type of media art based on visuo-haptic RDW. Unlimited Corridor enabled users to freely explore an immersive corridor by touching walls or handrails. In addition, we conducted a workshop about Unlimited Corridor. People associated with VR work, curators, attendants, individuals, and developers participated in the workshop to discuss the operation and experience of Unlimited Corridor in an art museum. This workshop enabled us to identify the strengths and challenges of VR exhibitions in general society, such as in museums.

Overall, even though there were individual differences, the results showed that perceptual characteristics influenced the effectiveness of RDW and there was a correlation between behavioral indices and the perceptual threshold of RDW. Furthermore, psychophysical experiments and behavioral indices showed that our new multimodal RDW technology improved the effectiveness of RDW. These findings emphasize the importance of considering individual differences in perception and optimizing the type and amount of stimuli for each individual in the design of virtual experiences.

Contents

List of Figures

List of Tables

List of Abbreviations

AASP Adolescent Adult Sensory Profile.

DT Detection Threshold.

GVS Galvanic Vestibular Stimulation.

HMD Head Mounted Display.

IPQ iGroup Presence Questionnaire.

JND Just-noticeable Difference.

MAP Maximum A Posteriori.

MLE Maximum Likelihood Estimation.

nGVS Noisy Galvanic Vestibular Stimulation.

PSE Point of Subjective Equality.

RDW Redirected Walking.

SP Sensory Profile.

SSQ Simulator Sickness Questionnaire.

VE Virtual Environment.

VR Virtual Reality.

Chapter 1

Introduction

1.1 Background

In 1965, Ivan Sutherland presented the concept of Virtual Reality (VR) in his essay *The Ultimate Display* [1]. Over the next half-century, numerous researchers have attempted to realize the future of VR proposed by Sutherland. *The Ultimate Display* concludes with the following sentence: "With appropriate programming such a display could be the Wonderland into which Alice walked." Thus, the concept of walking around a virtual environment (VE) was initially presented, and it was expected that realistic walking would play an essential role in VR in the future of VR.

Several methods have been proposed to enable VR walking, such as walking-in-place [2], omnidirectional treadmills [3], and friction-free platforms[1][2]. However, "real walking", is considered to be the most realistic and natural [4]. In VEs, real walking can be realized by one-to-one mapping, which involves mapping the position and orientation of the user's head position using a one-to-one correspondence to the virtual camera. For example, walking forward one meter in the physical world is mapped to walking forward one meter in the virtual world. One-to-one mapping provides the user with a near-natural proprioceptive and vestibular sensations that are similar to real walking. However, this method does not allow us to walk a virtual space that is larger than the physical space.

To solve this problem, in 2001, Razzaque et al. proposed the first concept of Redirected Walking (RDW) [5]. RDW is a set of technologies that enables users to walk within a vast VE by controlling the virtual and real environments' spatial

[1]Virtuix Omni: http://www.virtuix.com/
[2]Cyberith Virtualizer: http://www.cyberith.com/

correspondence. It allows users to have a natural walking experience by successfully mapping a vast virtual space to a limited real space. Thus, RDW is precisely the technology that can realize the experience predicted in *The Ultimate Display*.

In addition to its engineering significance, the RDW offers physiological and psychological advantages. The physiological benefit of the RDW is that it can be used to investigate gait, postural control, and sensory integration. RDW is also expected to be applied to the evaluation and rehabilitation of gait function in the elderly and patients with Parkinson's disease [6,7]. The psychological aspect of the RDW is that, in addition to the use of experimental psychological methods for its evaluation, it may provide a supplementary method for sensory evaluation in developmental psychology.

The ultimate goal of the RDW is to be able to explore an arbitrary VR space at the room scale while maintaining a natural gait [5, 8]. Substantial has been conducted in the RDW field over the past two decades to achieve this goal, with various techniques, control methods, and evaluation methods having been proposed [8]. However, many challenges in realizing ultimate goal of RDW have also been identified in the process.

One of the significant problems of RDW is the Detection Threshold (DT). The DT is the point of intensity at which subjects can barely detect an RDW manipulation. Applying the amount of manipulation above the DT will cause the user to notice the RDW, which will reduce the sense of presence and cause VR sickness. Many studies have been conducted on DTs [9–11]. However, it is known that DTs are strongly influenced by equipment, VEs, and individual differences. In particular, individual differences have a significant impact on DTs. Therefore, it is necessary to estimate the individual DTs and use the optimal amount of sensory manipulation. Moreover, the existing methods are not effective enough to compress an arbitrary VR space to room-scale size. Even though spatial perception is composed of vision, proprioception, vestibular perception, and auditory perception, conventional research has mainly focused on visual manipulation, and little research has been conducted using the other senses [8]. There is a possibility that we can manipulate spatial perception

more effectively by using multiple senses.

Therefore, in this study, we propose a method to improve the effect of RDW according to each user in order to realize the ultimate RDW that can compress an arbitrary VR space into a room-scale size. In addition to developing a method of utilizing multiple modals to improve the effectiveness of RDW, we investigate the relationship between the perceptual characteristics of each individual and the responses to the RDW manipulation and the perceptual threshold of the RDW in order to apply the optimal combination of modals and amount of manipulation for each user.

Besides, from the viewpoint of sensory-motor coupling, RDW is performed by a loop of sensory input, sensory processing, and response. In this paper, we summarize the issues of RDW and these solutions from the viewpoint of sensory-motor coupling.

1.2 Research Objectives

This dissertation discusses the individual perceptual thresholds of RDW, as well as methods to improve the effectiveness of RDW using multimodality. It is necessary to apply appropriate amount of manipulation according to the individual's perceptual characteristics in RDW. In the field of psychology, it is known that individual differences exist in perception and cognition. Although it has been suggested that there are also individual differences in spatial perception, these have rarely been considered. Therefore, a certain number of users have not achieved the desired effect despite using the manipulation quantities that have been demonstrated effective for several other users. In this study, we propose a methodology that enables participants to achieve a better effect by using different modalities and varying amounts of manipulation according to their perceptual characteristics.

In Chapters 3 and 4, we discuss individual perceptual thresholds in the RDW and how to estimate them. Chapter 3 addresses the relationship between the RDW thresholds and sensory characteristics. We study individual thresholds in spatial perception by focusing on curvature manipulation in RDW, and by comparing the

individual perceptual thresholds with individual sensory profiles. Next, in Chapter 4, to solve the problem of measuring threshold values, which have previously been determined by psychophysical experiments — they requires a large number of trials, thereby compromising the user experience — methods for measuring the threshold values using physiological and behavioral indices were investigated. The estimation method using physiological and behavioral indicators is expected to reduce the burden on the user, and simultaneously make it possible to estimate the threshold online.

Chapters 5–7 present techniques to improve the effectiveness of RDW through multimodality. In Chapter 5, based on the sensory integration model, we examine whether electrical noise on vestibular perception can enhance the effectiveness of RDW by reducing the reliability of vestibular sensation. In Chapter 6, considering that spatial perception consists of auditory as well as visual, vestibular, and proprioceptive perception, we examine whether the appropriate stimulation of auditory perception, in addition to visual perception can enhance the effectiveness of RDW. Furthermore, we examine the optimal presentation of auditory stimuli based on the sensory integration model. Finally, in Chapter 7, we examine whether the appropriate stimulation of haptic perception can enhance the effectiveness of RDW. In addition, we propose a VR demonstration using a visuo-haptic RDW and introduce a workshop on this demonstration.

1.3 Contributions

This dissertation examines the relationship between individual perceptual thresholds of RDW and sensory characteristics (Chapter 3) and proposed and evaluated methods for estimating the thresholds based on physiological and behavioral indices (Chapter 4). Further, we proposed, implemented, and evaluated methods to improve the effectiveness of RDW using multiple senses such as vestibular (Chapter 5), Auditory (Chapter 6) and Haptic sensation (Chapter 7).

Besides, from the perspective of physiology, the research addressed in this study

was corresponded in sensory-motor coupling as follows: Chapter 3 is related to sensory processing, Chapter 4 is related to response, and Chapters 5-7 is related to sensory input and sensory processing. Thus, by viewing and organizing RDW from the perspective of sensory-motor coupling, we proposed a methodology to improve the effectiveness of RDW throughout the sensory-motor loop.

Specifically, Chapter 3 evaluated the relationship between the individual detection thresholds and sensory characteristics. We conducted a psychophysical experiment to estimate individual perceptual thresholds of RDW and used a questionnaire to evaluate the individual perceptual characteristics. The results suggest that the participants with a higher propensity for sensory sensitivity and sensory avoidance were more likely to notice the RDW techniques.

In Chapter4, we evaluated the association between individual threshold of curvature RDW, physiological indices (pupil diameter and microsaccades), and behavioral indices (walking speed and head sway) to develop a method for estimating an individual's perceptual threshold by using the physiological and behavioral indices. A conventional psychophysical experiment was conducted to estimate the curvature RDW thresholds. Then, we examined the correlations between the pupil diameter, microsaccades, walking speed, and head sway data measured during the psychophysical experiments and the curvature thresholds obtained from these experiments. The results show a significant correlation between the curvature RDW threshold and the mean of walking speed and the standard deviation of head sway.

Chapter 5 proposed a visuo-vestibular RDW technique using noisy galvanic vestibular stimulation. In the experiments, the effect of nGVS on RDW thresholds was investigated using two current value conditions. The results suggested that the use of nGVS might improve the effectiveness of the RDW. In addition, the results of the sensory profile suggested that the effect of nGVS tended to be lower for users with a higher tendency toward sensory sensitivity.

In Chapter 6, we proposed and evaluated a visuo-auditory RDW technique based on sensory integration models. We first investigated whether MLE could be adapted to incongruent visual-auditory integration in VR environment. Then, we proposed a

novel method that introduced visual noise and incongruence between visual and auditory cues of the object in VR when applying curvature manipulation. We verified the effectiveness of this method by conducting a psychophysical experiment. Therefore, the effectiveness of curvature RDW was improved by presenting auditory cues incongruent with visual manipulation, and the minimum walking radius became 12.1 m under normal vision conditions and 9.8 m under noisy vision conditions, which is more effective than conventional methods that use only visual manipulation.

Chapter 7 introduced and evaluated a novel visuo-haptic RDW technique, proposed a VR demonstration using the visuo-haptic RDW technique, and described a workshop on the demonstration. For visuo-haptic RDW, the results suggest that the use of haptic cues improves the effectiveness of curvature RDW. In "Unlimited Corridor," a VR demo utilizing visuo-haptic interaction, the improved effectiveness of RDW enabled us to build a large-scale virtual environment in a relatively small real space without interrupting the experience or reorienting the user. We also conducted a workshop on the Unlimited Corridor to gain insights into the challenges to the technology, staff, and users regarding VR exhibitions in museums.

Together, these studies provide insight that there was a relationship between sensory characteristics, the optimal type, and amount of sensory stimulation. Besides, we found that there was a relationship between the behavioral indices and the RDW threshold in several experimental environments. In addition, we proposed multimodal RDW methods that can be used depending on the constraints of the content and the size of the VR space presented and confirmed their effectiveness. The experimental findings suggest that when applying RDW, appropriate senses and amounts of manipulation should be used depending on individual differences in users and the content to be presented, rather than uniformly using specific methods and amounts of manipulation.

1.4 Overview

The remainder of this dissertation is structured as follows. Chapter 1 focuses on fundamental background information and states the purpose of the thesis. Chapter 2 first reviewed the related work in the field of perception from the perspective of psychology and neuroscience. Thereafter, the existing literature on RDW is summarized. Chapter 3 investigates the individual differences in the RDW technique by assessing the relationship between the RDW technique and sensory profiles. Chapter 4 evaluates the changes in physiological behavioral indices in the RDW techniques. Chapter 5 discusses how to improve the effectiveness of RDW by using noisy vestibular stimuli based on the sensory integration theory. Chapter 6 introduces concepts for improving the effectiveness of RDW by using auditory stimuli and noisy visual stimuli based on the sensory integration theory. Chapter 7 investigates how to improve the effectiveness of RDW by using haptic stimuli and proposes a novel RDW demonstration. Chapter 8 summarizes the findings in Chapters 3, 4, 5, 6, and 7, and revisits the significance of RDW in engineering, physiology, and psychology. Chapter 9 concludes the thesis by discussing the limitations and future studies.

Chapter 2

Literature Review

In this chapter, the spatial perception research is first reviewed from the perspective of psychology and physiology. Next, the existing literature on redirected walking is categorized and summarized in terms of perceptual experience. Finally, a summary of the literature in the context of this thesis is provided.

2.1 Spatial Perception

This section discusses the characteristics of perception, cognition, and motor control related to spatial perception in terms of psychology and physiology.

2.1.1 Spatial Senses

Spatial perception consists of the integration of external and internal information obtained through various sensory organs by the central nervous system. In the following, the role of visual, auditory, vestibular, and proprioceptive senses in spatial perception and the characteristics of internal information are described.

Vision

Vision is a sense that can be used to acquire various types of spatial information, such as the absolute distance from images on the retina, a focus adjustment, and convergence, as well as the relative distance of an object from motion disparity and binocular disparity, and the spatial extent from visual field and eye movements [12]. In addition to static spatial information such as the spatial extent and depth, vision

is also superior in terms of motion perception, such as the perception of an object's movement [13].

Vision forms a visual space, which is a type of perceptual space. A visual space is characterized by the anisotropic nature of a visual space, in which the size and distance of an object are perceived differently depending on the direction and distance from the object. The most famous example of anisotropy is a phenomenon called Helmholtz's horopter, in which a horizontal line that appears to be straight on a subjective frontal parallel plane is not always straight in the physical world, and the shape of the line depends on the distance from the observer [14].

The anisotropy of perception is observed not only in real environments (REs) but also in VEs [15,16]. In a (Head Mounted Display (HMD)) VE, a distance perception such that a distance underestimation in the HMD-VE generalizes to intervals in the depth plane, but not to intervals in the frontal plane [15]

In addition, there is a phenomenon called *size constancy*, in which the size of the image in the retina differs between near and far views, but the perceived size of the object does not change significantly [17]. The phenomenon called a *moon illusion* in which the moon appears larger when it is closer to the horizon than when it is in the middle of the sky is thought to be due to this characteristic [18].

In term of physiology, the stimuli of the visual system can be divided into a ventral stream for perception and recognition, and a dorsal stream for computing the spatial information for motor action [19]. Of these, the dorsal cortical auditory pathway is also called the "where pathway" and is closely related to spatial perception.

Auditory

It is known that the auditory system can perceive the localization of sound sources and the spatial extent of sound pressure differences between the left and right ears through the head and auricles. The accuracy of auditory localization is said to be approximately 1° degree [20], which is less accurate than the accuracy of visual localization, which is approximately 1' [21]. However, the space available to the

auditory system is much larger than that of the visual system, and it is possible to localize using sound sources from the whole space.

The auditory system also forms an auditory space, which is a type of perceptual space. Similar to a visual space, an auditory space is known to have anisotropy [22]. In the auditory system, as in the case of vision, stimuli are divided into the dorsal and ventral cortical auditory tracts through the primary auditory cortex [23].

Vestibule

A vestibular sensation is perceived as a rotation by the three semicircular canals of the inner ear and as acceleration by the vestibular organs. The three semicircular canals are arranged at right angles to each other, and a rotation is sensed by the inertia of the lymph and hair cells in the semicircular canals. By contrast, the vestibular system contains hair cells and equilibrium sand, through which it senses acceleration from the inertia. A vestibular sensation forms a visual space along with vision.

Proprioception

Proprioception is a sensation caused by mechanical stimuli such as the amount of stretching or contraction of a muscle, the amount of load applied to a muscle, and the angle of a joint. This is due to the proprioceptive sensation by which we can know the relative position of our body when we close our eyes. The proprioceptive sensations are classified into position, motion, force, and weight [24]. In addition, proprioception and haptic sensation constitute the tactile space.

Efference Copy

An efference copy is a copy of motor commands for making adjustments to sensory information in order to reflect a more stable external space in the brain in response to changes in sensory information induced through motion [25]. For instance, the image on the retina can oscillate slightly when the eye is saccaded, but the brain

uses its own eye movement motor commands to affect the visual input. Sperry used the term *corollary discharge* to describe signals associated with one's own motion that influence the processing of sensory information [26].

2.1.2 Spatial Ability

Spatial ability is one of the major fields of psychology [27–30]. Although various methods for classifying measures of spatial ability have been presented, the classification method that has currently achieved a large consensus was introduced by Linn and Petersen [29], who referred to spatial ability as skills in representing, transforming, generating, and recalling symbolic, nonlinguistic information, and distinguished spatial ability into three categories, i.e., *spatial perception*, *mental rotation*, and *spatial visualization* based on the similarity of the processes used for an individual ability [29]. In this section, we will briefly describe spatial perception, mental rotation, and spatial visualization.

Spatial Perception

According to Linn and Petersen ' s categorization, spatial perception is defined as the ability to determine spatial relations despite distracting information [29]. For measuring spatial perception, the rod-and-frame and water level tests are well known [31]. The rod-and-frame test consists of a frame and a movable rod in the frame, and the participant is required to adjust the rod such that it is perpendicular to the frame [32]. In the water level test, participants are shown illustrations of bottles of various shapes with the water level marked, and are then shown illustrations of bottles tilted at different angles without the water level marked and asked to mark where the water level would be [33].

Many studies have shown that spatial perception in VR is different from reality [34,35]. It has been shown that depth perception in a (Virtual Environment (VE)) is extremely different from that in the real world and that distances in the peripersonal space are often overestimated, whereas distances in extrapersonal space tend to be

underestimated [36]. Depth estimation in VE also depends on the quality of the VE, i.e., a richer and more realistic virtual world might provide a more accurate depth estimation [37].

Mental Rotation

The mental rotation was defined as the ability to rotate a two- or three-dimensional object within the mind [29]. A mental rotation test was originally presented by Shepard and Metzler [38], who examined the reaction times of the participants to determine whether pairs of images depicting objects rotated in two- or three-dimensions matched, and showed that the time increased linearly as the object was rotated from its original position to determine whether the two images were the same object. It is known that there is a large difference in this ability between men and women, and many studies have been conducted in this area [29, 31].

Spatial Visualization

Spatial visualization was defined as the ability to manipulate complex spatial information when several stages are needed to produce the correct solution [31]. Mental rotation tasks and cognitive tests such as the form board, paper folding, and surface development tests are used to evaluate spatial visualization [39]. Increased age was associated with lower levels of performance on several tests of such visualization [39].

Environmental Spatial Abilities

While the studies discussed thus far have primarily focused on small-scale spatial capabilities, the main discussion in this thesis is walking in a VE, which requires large-scale spatial abilities, i.e., environmental spatial abilities. Environmental spatial abilities include wayfinding and navigation abilities. These abilities are called a sense of direction (SOD), and the Santa Barbara Sense of Direction (SBSOD) has been proposed as a method for measuring this capability [40].

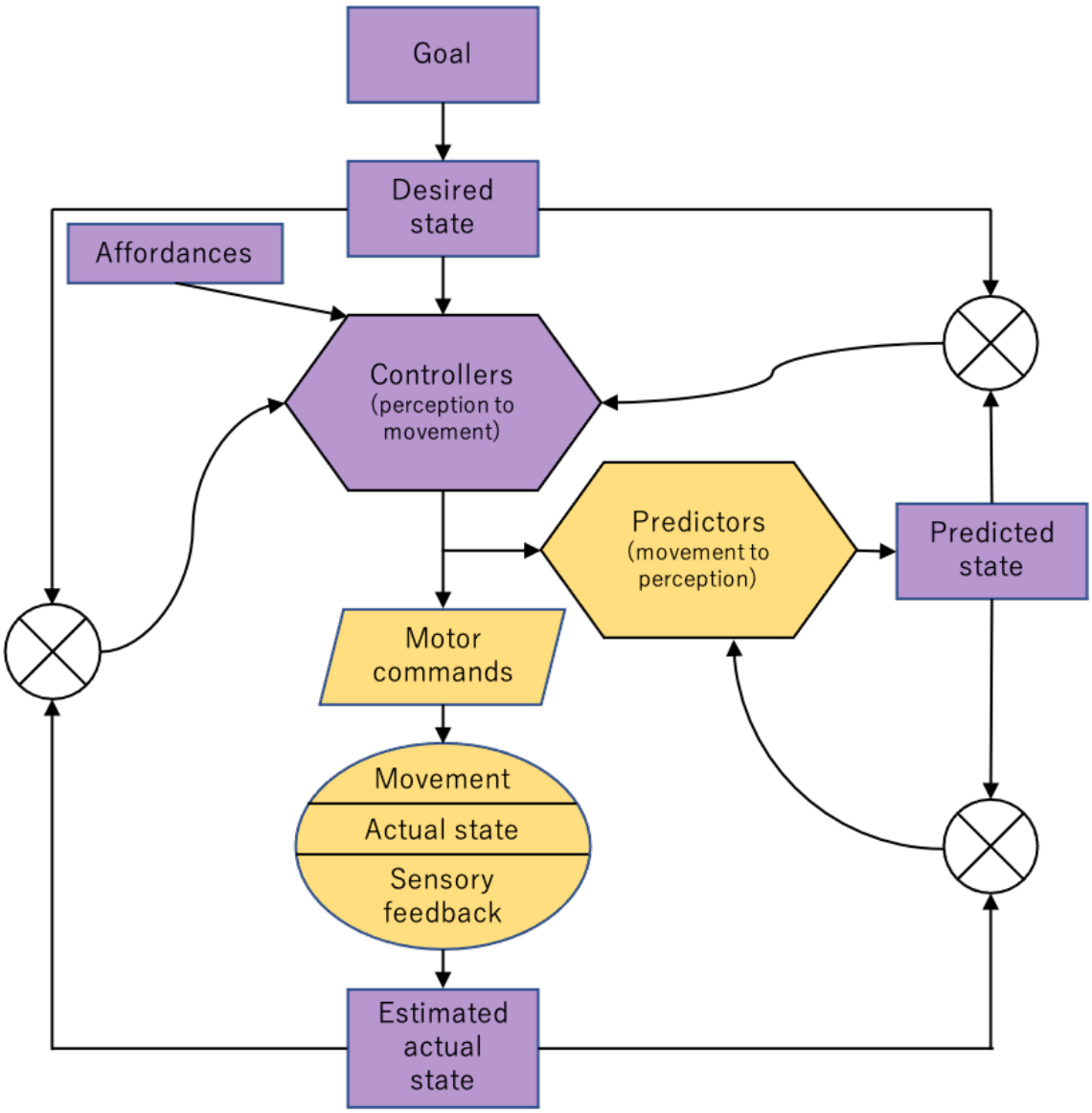

Fig. 2.1: Motor control system based on studies conducted by Frith et al. [41] and Blakemore et al. [42]

2.1.3 Sensory-motor Coupling

Sensation and perception do not exist on their own and are altered by movements. This relationship between sensation, perception, and movement is called sensory-motor coupling. Therefore, motor control must be considered when working with

sensation and perception. Various models have been proposed for motor control systems [41–43].

Figure 2.1 shows the framework of a motor control system based on studies conducted by Frith et al. [41] and Blakemore et al. [42]. Studies have shown that different motor representations exist. Some of these representations are available to awareness (in purple), whereas others are not (in yellow). The purpose of the system is to derive the desired state. The controllers integrate inputs from the desired state, affordances, and feedback, and issue motor commands. Then, a reference copy is transmitted to the predictors. The motor commands produce movements, which act on the environment, to generate sensory feedback. The estimated actual state is inferred based on such feedback. The predictors derive the predicted state of the system using an efference copy and feedback. The motion control system operates by feeding the errors in these states to the controllers and predictors.

This mechanism is considered to be closely related to the response to the RDW. For example, when the desired state, which is composed of motor intentions, and the estimated actual state, which comprises sensory feedback, are consistent, then users do not notice the RDW manipulation. However, when there is a discrepancy between the desired state and the estimated actual state, the users notice the manipulation.

2.1.4 Perception Model

As mentioned above, spatial perception consists of stimuli from almost all sensations, such as visual, auditory, vestibular, and proprioceptive sensations. Studies in the field of psychology and neuroscience, however, have revealed that these sensations are not perceived alone but interact with each other [44, 45]. This sensory integration is also called cross-modal/multimodal and plays an important role in spatial perception [46]. Here, we introduce models for sensory integration.

Maximum Likelihood Estimation

With a (Maximum Likelihood Estimation (MLE)) [47–49], it has been proposed that each modality affects the users' estimate of the target object independently and that the weight of each modality in the integration is determined based on their relative reliability.

The MLE model was first validated through a visual-haptic shape recognition task [48]. In this study, the participants visually observed the width of a rectangle in a mirror while touching a haptic stimulus behind the mirror. The participants were presented with incongruent visual and haptic cues, and corrupting the visual scene with noises caused the participants to weigh the haptic cues more highly. This study showed that the perceptual shape changed with the weight of the visual and tactile cues as expected in the MLE, demonstrating the validity of the MLE as a sensory integration model.

This model is often used when there is no prior information about the target object. A considerable amount of research has investigated this topic and a variety of sensory modalities have been used [48,50–52]. For instance, it was also shown that the MLE was partially correct for a visual-auditory spatial localization task [52].

According to the MLE, the estimated values of different modalities to the same event in a specific scene are statistically independent of each other. Instead of an absolute value, the estimate of each modality about the target is considered a normal distribution with its own mean and variance. The mean value of the distribution represents the estimated value with the highest probability. The uncertainty of the estimated value of each modality is represented by the variance, with a smaller variance representing a lower uncertainty and higher reliability. Moreover, the integrated estimates of multiple modalities can be considered as a normal distribution with a higher bias toward modalities with higher reliability.

Mathematically, s_i is the mean value of the estimated distribution of the ith modality, and $\hat{s}$ is the mean value of the integrated distribution. The optimal

estimate of the target event is given by the following equation:

$$\hat{s} = \sum_{i}^{n} w_i s_i \quad \text{and} \quad w_i = \frac{1/\sigma_i^2}{\sum_j^n 1/\sigma_j^2} \tag{2.1}$$

where w_i denotes how much the ith modality is weighted in the final integration, and $\hat{s}$ is the linear summation weighted according to the reliability of each modality.

In the context of the visual-auditory spatial localization task, both visual and auditory estimates of the location of an event can be considered a normal distribution but with independent mean (p_v, p_a) and variance (σ_v^2 and σ_a^2) values. The variance of the final integrated estimate σ^2 is given by the following:

$$\frac{1}{\sigma^2} = \frac{1}{\sigma_v^2} + \frac{1}{\sigma_a^2} \tag{2.2}$$

From this equation, because the variance of the integrated estimate is smaller than any of the independent estimates, the MLE supposes that a human enhances the reliability of the final estimate by integrating information from multiple senses about the same event.

Maximum A Posteriori Estimation

Although the MLE does not use a priori information about the object, there are many situations in our daily lives in which we have a priori information about an object (e.g., objects are stationary in most cases). A (Maximum A Posteriori (MAP)) estimation is a model that maximizes the posterior probability given the a priori probability. The posterior probability can be obtained from the likelihood and prior probability using Bayes' theorem as follows:

$$p(x|z) = \frac{p(z|x)p(x)}{p(z)} \tag{2.3}$$

Therefore, the MAP can be calculated as follows:

$$x_{MAP} = \text{argmax}_\text{x} p(x|z) = \text{argmax}_\text{x} p(z|x)p(x) \tag{2.4}$$

We take the aperture problem as an example of how a MAP estimation can interpret perceptual phenomena. The aperture problem is a problem of a motion perception in which multiple local motion directions are integrated to compute the total motion direction [53]. Two methods have been proposed to solve the window problem in the brain: a vector-average method, which takes the average of the directions of motion, and a crossover method, which is constrained by the direction of motion, and supports the vector-average method under some experimental conditions and the crossover method under other experimental conditions. Weiss et al. successfully formulated the window problem as a MAP estimation problem [54]. They showed that vector averaging and crossing methods appear as special cases of MAP estimation by incorporating into the prior an assumption for the external world in which objects are mostly stationary having a Gaussian distribution with a zero mean-velocity. Thus, assuming that models based on a Bayesian estimation such as the MLE and MAP are used in the brain, various mechanisms of sensory integration can be explained.

2.1.5 Psychophysics

Psychophysics is the study of deriving the laws between a stimulus and sensation [55]. Weber's law [56] is the fundamental theory in this field, which states that the perceived change in stimuli is proportional to the initial stimuli. Letting the intensity of the stimulus added at the beginning be noted as S and the corresponding discrimination threshold be represented as Δ S, the following equation holds regardless of the value of R. This constant value is referred to as the Weber ratio.

$$\frac{\Delta S}{S} = \text{constant} \tag{2.5}$$

By integrating this expression, the Weber-Fechner law is obtained as follows:

$$E = k \log S + C \tag{2.6}$$

where C is a constant of integration and the constant k is sensation-specific and depends on the type of sensation or stimulus. This equation does not hold for stimuli

that are smaller than the perceivable stimulus [57]. This minimum perceivable stimuli is called a (Just-noticeable Difference (JND)), difference limen, difference threshold, or least perceptible difference. In the field of (Redirected Walking (RDW)), we usually refer to this limen as a detection threshold (DT). Various methods have been proposed to measure DT, e.g., the method of constant stimulus [58], the staircase method [59], or the method of adjustment [60]. By contrast, in the field of RDW, the pseudo-two-alternative forced-choice task method has become the de facto standard.

Two-Alternative Forced Choice

The two-alternative forced-choice (2AFC) method is used for measuring the DT. In the original 2AFC task, subjects are presented with two options, only one of which contained a target stimulus, and are forced to choose which is the correct option. By contrast, the pseudo-2AFC used in the RDW field is different from the original 2AFC. In the pseudo-2AFC, the subjects perform an action once and then choose one of the two options presented to them. For example, when the pseudo-2AFC is used to measure the thresholds of the curvature gain, which is an RDW technique (see subsection 2.2.1), the participants walk on a straight path in the virtual environment, while walking along a left or right curved path in the real environment. They then have to determine whether the physical path was turned "left" or "right." The participants could not answer in another way, such as "I don't know" or "straight." Assuming that they respond randomly when they feel they are walking straight, the probability of answering "right" is expected to be 50%. The point at which this response reaches 50% is called the (Point of Subjective Equality (PSE)). However, there is a DT between the PSE and the number of stimuli with almost 100% correct answers. Typically, the DT is defined as the number of stimuli that result in a 75% correct response rate [9]. In general, to compute the DT, the pooled data are fitted to the cumulative normal distribution, logistic functions, Weibull functions, Gumbel functions, and hyperbolic proper division functions [61]. In the field of redirection, logistic functions have usually been used for fitting [9,62], and thus we also use logistic functions in this thesis.

Although this method is much similar to a yes/no format, where targets from a list are randomly intermixed with lures, and such items are presented one at a time for a decision [63], in the area of RDW it is called pseudo-2AFC, a convention we follow in the present thesis.

2.1.6 Cybersickness

Our spatial perception consists of an integration of multisensory information from a variety of senses, including vision, hearing, vestibule, and proprioception. When vision signals conflict with other signals such as proprioceptive and vestibular signals, visual information often becomes dominant. However, this evokes a subjective awareness of the conflict [64–66]. However, when the displacement increases, the vision, vestibule, and proprioception are no longer integrated. Consequently, the remapped movements cannot be considered the same movements, and evoke cybersickness [67].

Cybersickness, also known as virtual reality sickness, occurs when inputs from conflict from visual and vestibular stimuli. Symptoms caused by cybersickness include eyestrain, headache, pallor, sweating, dryness of mouth, fullness of stomach, disorientation, vertigo, ataxia, nausea, and vomiting [67].

Age is associated with cybersickness, with children between the ages of 2 and 12 being the most susceptible to cybersickness, and decreases rapidly between 12 and 21 years of age or later [68]. With regard to gender, women are more likely to have a wider field of view, which makes them more prone to the effects of vection and thus more susceptible to cybersickness [67]. In addition, previous studies have measured the association between presence and cybersickness and have concluded that the balance of evidence favors a negative relationship between the two factors [69].

The (Simulator Sickness Questionnaire (SSQ)) of Kennedy et al. [70] is often used as a standard measurement for cybersickness. The SSQ categorizes symptoms into nausea (e.g., stomach awareness and nausea), eye movements (e.g., headaches and eyestrain), and disorientation (e.g., dizziness and vertigo), and rates the severity of

these symptoms on a scale of zero to 3 [70].

2.2 Redirected Walking

Walking is one of the most fundamental interactions with the outside world. This is not only appropriate for the physical world, but for the virtual world as well. Nilsson proposed a taxonomy of virtual travel techniques and virtual travel techniques classified by *Vehicular* and *Body-centric*, *Mundane* and *Magical*, *Mobile*, and *Stationary* [71](see Figure 2.2). This study aims to achieve a natural walking experience without complex equipment, and thus we focus on real walking and redirected walking included in the intersection of the Body-centric, Mundane, and Mobile techniques.

As the advantage of real walking, the physical movements coincide with the virtual movements, and thus the visual, vestibular, and proprioceptive information coincide with each other, improving the natural sense of walking. However, to apply real walking, a physical tracking space that is larger than the virtual environment is required. Therefore, this technique must either require an extremely large tracking space or limit the size of the virtual world.

To solve the limitations of real walking, RDW has been proposed [5]. RDW is a set of techniques for intentionally creating subtle or overt discrepancies between the spatial senses, distorting the perception-action mappings during movements in a virtual environment (VE), or dynamically rearranging the geometry and affordances of a virtual world [8]. Using RDW, users can walk through a vast VE in a limited real environment (RE).

Since Razzaque et al. first proposed the concept of RDW [5], a number of RDW techniques have been proposed. These techniques can be classified into two categories: (i) RDW techniques that manipulate the mapping between the user's real and virtual position and orientation, and (ii) RDW techniques that self-over-lap VEs for compression into a smaller tracking space.

A taxonomy of redirection techniques (see Figure 2.3) is introduced by Suma et

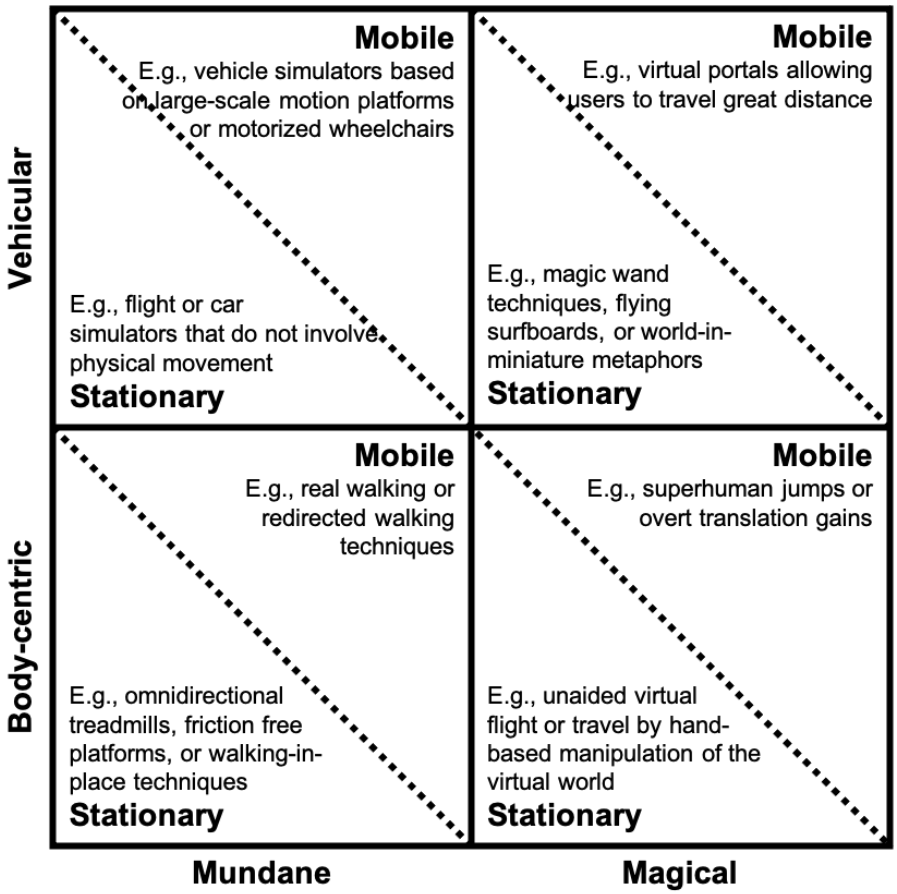

Fig. 2.2: Taxonomy of Virtual Travel Techniques based on Nilsson [71]

al., and these techniques are classified as *repositioning* and *reorientation*, *overt* and *subtle*, and *discrete* and *continuous* [72]. In this paper, we mainly focus on subtle techniques because to realize a natural walking experience it is necessary for the user to be unaware of the manipulation.

2.2.1 Subtle Continuous Techniques

Figure 2.4 shows subtle continuous techniques. Steinicke et al. defined subtle continuous techniques for the first time [73]. They proposed expressing the operations in terms of ratios and classified them into translation, rotation, and curvature gains. Later, Langbehn et al. proposed a bending gain that extends the curvature

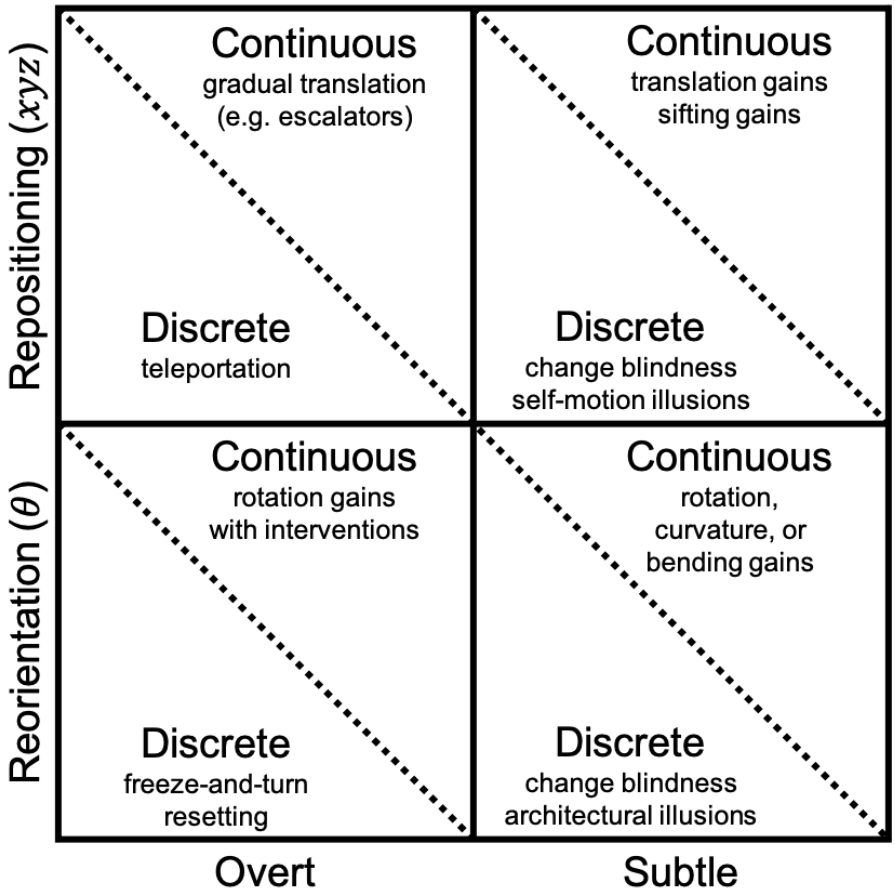

Fig. 2.3: Taxonomy of Redirection Techniques based on Suma et al. [72]

gain [74]. In this subsection, these four techniques are explained along with other approaches.

Translation Gain

A translation gain is defined as the ratio of the amount of translation in real and virtual spaces. The translation gain can be applied in three directions: walking direction, vertical (gravity), and a left-to-right (lateral) direction perpendicular to each direction. Unless otherwise stated, a translation gain refers to gain applied to the walking direction. The translation gain is defined by the following equation: $g_T := \frac{T_{virtual}}{T_{real}}$, where $T_{virtual}$ and T_{real} represent the amount of translation in the

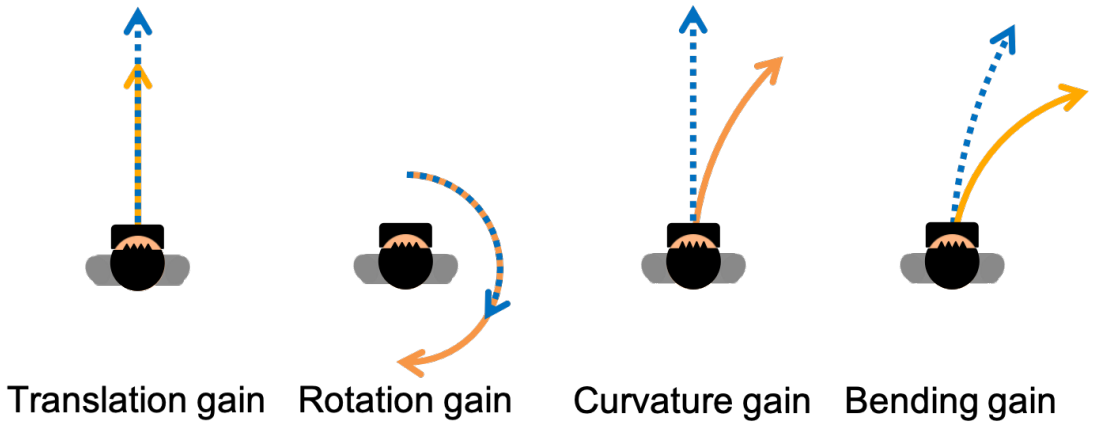

Fig. 2.4: Subtle Continuous Techniques. Blue lines show virtual routes and orange lines show real routes.

virtual and real worlds, respectively.

Rotation Gain

Rotation gain g_R is defined as the ratio of the amount of rotation in real and virtual spaces. The translation gain can also be applied in three axes: yaw, pitch, and roll. Unless otherwise stated, rotation gain refers to gain applied to the yaw axis. The rotation gain is defined by the following equation: $g_T := \frac{R_{virtual}}{R_{real}}$, where $R_{virtual}$ and R_{real} represent the amount of rotation in the virtual and real worlds, respectively.

Curvature Gain

Curvature gain g_C is defined as the amount of curvature in a real space. Although the curvature gain can be defined in several ways, herein we define a curvature gain as follows: $g_C := \frac{1}{r_{real}}$, where r_{real} is the radius of the circle to which the user is guided in the RE. Therefore, the curvature gain has a dimension of m^{-1}, unlike the dimensionless translation and rotation gains.

Bending Gain

Langbehn et al. proposed the use of a bending gain [74]. The bending gain is an extension of the curvature gain to enable walking along a curved path in a VE. The bending gain is defined by the following equation: $g_B := \frac{r_{virtual}}{r_{real}}$, where $r_{virtual}$ and r_{real} represent the radius of the circle to which the user is guided in the VE and RE, respectively.

Other Subtle Continuous Techniques

In addition to the above approaches, other methods have been proposed. One such method allows users to walk a curved path on a VE on a treadmill that can only move back and forth by reversing the curvature gain [75]. Another method called strafing gain steers users diagonally by adding a sideways translation to their forward movement [76].

2.2.2 Subtle Discrete Techniques

Subtle discrete techniques exploit cognitive as well as perceptual properties. In this subsection, we introduce two of the most popular techniques, change blindness and architectural illusions.

Change Blindness

Change blindness for RDW was proposed by Suma et al., a technique for rearranging space by changing the position of doors and furniture when the user is looking in a different direction [77]. This technique is based on the phenomenon of change blindness, in which the vision perceives perceptible changes but is unable to notice them. Although this method is extremely effective, it imposes certain constraints on the spatial structure, content, and user movement paths.

Architectural Illusions

Architectural illusions are techniques for compressing the VE by dynamically changing the VE itself, reversing the preconceived notion that the space is static, and proposing a space-saving method by moving the rooms within the VE. Suma et al. proposed the first concept of an architectural illusion called an "impossible space" to save space by overlapping the rooms in the VE [72]. They reported that the users did not notice the spatial arrangement operation when the ratio of overlapping of two rooms was less than 50%. Later, Vasylevska et al. proposed a technique called "Flexible Spaces" [78]. With this method, the arrangement of rooms and corridors on the VE can be superimposed or transformed according to the user's position in the real space to explore a large VE.

2.2.3 Resetting

Subtle techniques can be used to manipulate the amount and direction of the user's movement without the user being aware of it. However, these techniques alone cannot necessarily keep the user in a limited tracking space. Therefore, a *resetting* was needed, which is a series of methods applied to force the user to change direction at the boundaries of the tracking space [79].

Williams et al. proposed three resetting methods: Freeze-Backup, Freeze-Turn, and 2:1-Turn [79]. With the Freeze-Backup method, when the user has reached the boundaries of the tracking area, the user is instructed to step back in the RE, whereas the user ' s position in the VE remains frozen. When a sufficient number of steps are taken, the user is informed to stop, and the display is unfrozen, and the user will be able to continue along the same path again. With the Freeze-Turn method, when the user has reached the boundaries of the tracking area, the user is instructed to reset by turning 180 degrees. While the user is rotating, the VE remains stationary, and when the user finishes a 180-degree rotation, the VE reflects the user's position and orientation again, and the user is able to continue walking along the same path. With the 2:1-Turn method, when the user has reached the

boundaries of the tracking area, the user is instructed to reset by turning 180 degrees. As long as the user is rotating, the rotation gain is applied and the VE rotates twice as much as the user. Therefore, when the user finishes a 180-degree rotation, the VE has rotated 360 degrees and then the user is able to continue walking along the same route.

2.2.4 Redirection Controller

A successful combination of subtle manipulation techniques and resetting allows users to walk around a given VE, but it is necessary to control what operations are performed and at what time. To solve this problem, various redirection controllers have been proposed. The redirection controller can be classified into scripted, generalized, and predictive controllers [8].

Scripted Controller

Scripted controllers allow users to explore space along physical and virtual paths that are largely predetermined by the developers [5]. This ensures that the virtual experience stays within the tracking area as long as the user is behaving as the developer expected. However, if the user deviates from the pre-defined path, the correspondence between the RE and VE might break down, and the user might not be able to continue the virtual experience. In addition, such controllers are not easily reusable across different VEs and REs and require an extensive customization for each environment.

Generalized Controller

Generalized controllers use subtle manipulation techniques used to guide the user to a specific physical location or pattern, regardless of the user's intended virtual movement [8]. Because it does not use information about the spatial configuration of the VE or the user's movements, it cannot be optimized in a generalized controller

as in a scripted controller, but has the versatility of being able to be used regardless of the shape of the VE and is sufficiently practical if the RE is of a simple structure, such as a square shape.

Typical general controllers include steer-to-center, steer-to-multiple-targets, and steer-to-orbit. The basic concept of steer-to-center was proposed by Razzaque et al. [5]. The steer-to-center algorithm currently in use is a modification of Razzaque's algorithm developed by Hodgson et al. [80]. The primary steering target is the physical center of the tracking area; however, additional targets are temporarily and dynamically generated off-center to overcome some limitations such as a rapid oscillation (see [80] for details). Steer-to-multiple-targets is an extension of steer-to-center. In steer-to-center, a target is set at the center of the tracking area, whereas in steer-to-multiple-targets, multiple targets are set near the center of the tracking area and the user is directed to the nearest target. Steer-to-orbit differs from the above two methods in that it guides the user to draw an orbital path around a point [81]. Combinations of these algorithms such as steer-to-multiple+center [81] have also been developed. These algorithms generally use a curvature gain to guide the user to the target.

Hodgson and Bachmann compared steer-to-center, steer-to-multiple-targets, steer-to-multiple+center, and steer-to-orbit using simulations and live user data. They concluded that in most cases steer-to-center performed the best, and in some cases, steer-to-orbit also performed well [81].

Predictive Controller

Predictive controllers analyze the physical and virtual environments to determine where users can and cannot go and where they are likely to move, using such information to control a redirection [8]. Predictive controllers can be divided into two categories: optimal control and reinforcement learning. FORCE [82] and MPCRed [83] are given as optimal controls. Several researchers have proposed controllers based on reinforcement learning [84–87].

2.2.5 Detection Threshold

subsection 2.2.5 shows detection thresholds of subtle manipulation techniques: translation, rotation, curvature, and bending gains. In general, in the field of redirection, the DT is analyzed using a two-alternative forced-choice (2AFC) task. Steinicke et al. conducted several experiments to determine the DTs for translation, rotation, and curvature gain using the 2AFC [73]. The effect of the presence of a virtual body and the visual cue of VEs on the DT has also been investigated [88]. In the subsection 2.2.5, those that are not mentioned in the comments section applied subtle manipulation techniques using only visual stimulation with the HMD and analyzed the DTs using 2AFC tasks. By contrast, those remarked in the comments as blinks [62] and saccades [89] are not gains but the amount of movement or angle. In other words, these values indicate the extent to which the user does not notice the translation or rotation while blinking or experiencing saccades. The DT for curvature gain has been shown to depend on the walking speed [90]. Grechkin et al. analyzed the DT of the curvature gain using the maximum likelihood procedure [10]. Zhang et al. investigated the effect of a 360° video-based telepresence environment on the DTs [91]. The thresholds for auditory-only, visual, and auditory redirection were also analyzed [92, 93]. In addition, the DTs for bending gain were studied [74, 94]. It has also been suggested that acclimation to redirection increases the DT [95]. The DT for the same manipulation may vary depending on the equipment used, as well as the VE, RE, and experimental conditions. In addition, some studies have shown that DTs may be different for individual users [96,97]. Moreover, some studies have investigated whether these individual differences in DTs correlate with other indicators [98, 99].

2.2.6 Multimodal Redirected Walking

Redirected walking is a method that makes use of the predominance of vision in spatial perception, although research is also being conducted on methods for presenting senses other than vision. Nilsson et al. investigated whether the threshold

Table 2.1: Detection Thresholds of Redirection Techniques based on [100]. For translation and rotation gains, the range of undetectable gain is stated. For bending gains, the maximal gain is stated. For curvature gains, the radius of the resulting arc in the real world is stated. In addition, for blinks and saccades, the maximal offset in centimeters or ° is stated.

Gain	**Comment**	**Thresholds**[1]	**Source**
Translation	-	0.78 - 1.22	[9]
Translation	Virtual Feet	0.88 - 1.15	[88]
Translation	Low-cue VE	0.73 - 1.25	[88]
Translation	360° video	0.94 - 1.10	[91]
Translation	Saccades	-50 cm - 50 cm	[89]
Translation	Eye Blinks	-9.75 cm - 7.71 cm	[62]
Rotation	-	0.67 - 1.24	[9]
Rotation	Audio only	0.88 - 1.20	[101]
Rotation	Audio & Vision	0.68 - 1.36	[93]
Rotation	360° video	0.88 - 1.09	[91]
Rotation	Saccades	-5° - 5°	[89]
Rotation	Eye Blinks	-4.76° - 5.78°	[62]
Curvature	-	$r > 22.03m$	[9]
Curvature	$v = 0.75ms^{-1}$	$r > 10.57m$	[90]
Curvature	$v = 1.00ms^{-1}$	$r > 23.75m$	[90]
Curvature	$v = 1.25ms^{-1}$	$r > 26.99m$	[90]
Curvature	-	$r > 11.61m$	[10]
Curvature	Maximum likelihood	$r > 6.4m$	[10]
Curvature	Audio only	$r > 16m$	[101]
Curvature	Audio & Vision	$r > 6.0m$	[93]
Curvature	-	$r > 21.7m$	Chapter 5
Curvature	Audio & Vision	$r > 12.1m$	Chapter 5
Curvature	-	$r > 26.5m$	Chapter 6
Curvature	nGVS	$r > 22.7m$	Chapter 6
Bending	$r_{real} = 1.25$ m	3.25	[74]
Bending	$r_{real} = 2.5$ m	4.35	[74]
Bending	$r_{virtual} = 3$ m	1.63	[94]
Bending	tDCS, $r_{virtual} = 3$ m	1.61	[94]

for rotation gain varies with the presence of sound and positional manipulation of the sound source and reported that auditory presentation does not affect the redirected walking [92]. Meyer et al. investigated the thresholds for rotation and curvature gains with a positional manipulation of sound and found that an auditory presentation affects the threshold of curvature gain [93]. Dynamic audio for RDW was also proposed [92, 102]. Kohli et al. proposed a visuo-haptic presentation of a single cylindrical object as if it exists in multiple locations by combining the rotation gain and passive haptic presentation [103]. Finally, we also proposed a curvature gain based on a visuo-haptic interaction [104] (see Appendix).

2.3 Summary

In this chapter, we first introduced studies on perception research. Section 2.1 discussed human perception, particularly spatial perception, from the perspective of psychology and neuroscience. Subsection 2.1.2 described spatial abilities from the perspective of psychology. These are related to previous studies on individual differences in RDW thresholds, which will be discussed in Chapter 3. Next, in Subsection 2.1.2, we introduced the senses that shape the spatial perception from the perspective of neuroscience. In Subsection 2.1.4, we described the perception model, particularly the sensory integration. These subsections are deeply involved in the studies described in Chapters 5 and 6, which deal with multimodal RDW techniques. Meanwhile, in Subsection 2.1.5, we introduced individual differences of spatial perception. Subsection 2.1.3 described sensory-motor coupling. These subsections are linked to the analysis of individual differences in RDW thresholds treated in Chapter 3 and the estimation of such thresholds treated in Chapter 4. In Subsection 2.1.6, we discussed cybersickness, which is relevant to all RDW technologies.

Section 2.2 introduced the RDW techniques. Subsection 2.2.1 described subtle continuous techniques. Among them, curvature gain is particularly relevant to this entire study. In Subsection 2.2.2, change blindness and architectural illusions among subtle discrete techniques were then introduced. Subsection 2.2.3 introduced a reset-

ting, which is a series of methods applied to force the user to change the direction of movement at the boundaries of the tracking space. In Subsection 2.2.4, we described a redirection controller that controls the RDW technology according to the VE, RE, and user's position and attitude. In Subsection 2.2.5, the DT applied in RDW techniques was introduced. This is linked to the analysis of individual differences in RDW thresholds in Chapter 3, and an estimation of the threshold was analyzed by using physiological behavioral indices in Chapter 4. Subsection 2.2.6 introduced multimodal redirected walking techniques. This is deeply relevant to Chapters 5-7, which propose visuo-vestibular, visuo-auditory, and visuo-haptic RDW techniques.

Chapter 3

Sensory Characteristics and RDW

3.1 Introduction

This chapter examines the relationship between the sensory characteristics and the effects of redirected walking (RDW). Research efforts have been devoted to identifying the DT of the RDW techniques, and a wide range of thresholds have been reported in different studies (see subsection 2.2.5. Steinicke et al. first investigated the detection thresholds (DTs) of the RDW techniques using a pseudo two-alternative forced choice (2AFC) method and reported that the DTs of the translation, rotation, and curvature gain are 0.78-1.22, 0.67-1.24, and r $>$ 22 m, respectively [9]. Grechkin et al. reexamined the curvature gain thresholds by using psuedo-2AFC and Green's maximum likelihood methods. They reported that the DTs of the curvature gain are r $>$ 11.6 m and r $>$ 11.6 m depending on the estimation method [10]. Many other studies have also calculated the DTs; however, most of these thresholds were calculated from the pooled results of the participants, and the individual differences in the thresholds were discarded.

In recent years, the individual differences in the redirection thresholds have been addressed. Schmitz et al. analyzed the correlation between the age and rotation gain thresholds and reported a negative correlation between the age and the threshold for limited immersion in increasing conditions [98]. Nguyen et al. investigated the effect of gender on the curvature gain thresholds and showed that there is a high variability in the individuals' DTs and women tend to have a higher DT for the curvature gain than men [105].

In addition, several studies have examined the relationship between the spatial ability and the redirection thresholds. Schmitz et al. examined the relationship

between the mental rotation (see section 2.1.2 and the DT of the rotation gain, a method of RDW, but no correlation was found [98]. Rothacher et al. investigated the relationship between the DT of the curvature gain, the visual-dependency measures, blind locomotion control, and the interoceptive awareness. Rotchacher et al. found that the rod-and-frame test (see section 2.1.2) had the strongest relationship with the redirection detection thresholds; the higher the visual dependency, the higher the detection threshold [99].

Besides, the spatial perception is also affected by the neurological differences. For instance, individuals with autism spectrum disorders were superior to the control group for certain spatial abilities [106,107]. Shah and Frith showed that the autistic subjects, regardless of their age and ability, displayed a better performance than the controls when presented with unsegmented designs [106]. Caron et al. reported that patients with high-functioning autism are superior to a control group for tasks that involve information transfer between the micro-and macro-scales. This exhibited a superior accuracy in the graphic cued recall for a path, and a shorter learning time for the map learning tasks [107]. Thus, neurological characteristics might be closely related to the effects of the RDW techniques.

This chapter examines the individual differences in the curvature gain thresholds based on the neurological characteristics and it discusses the causes of the individual differences.

As a theory that integrates the neurological characteristics and behavioral responses, Dunn's model of sensory processing has been proposed [108]. In the next subsection, Dunn's model is introduced.

3.2 Dunn's Model of Sensory Processing

There are individual differences in sensory processing and behavioral responses. Some people have difficulty detecting faint smells, while others are more sensitive to small sounds. Some people like busy places, while others prefer to stay away from noisy places. According to Dunn et al., these individual differences are caused

Table 3.1: Dunn's Model of Sensory Processing adapted from [108]

		Behavioral Response Continuum	
		Accordance	Counteract
Neurological Threshold Continuum	High	Low Registration	Sensation Seeking
	Low	Sensory Sensitivity	Sensation Avoiding

by a combination of sensory processing and behavioral responses [108]. They have proposed a theory that integrates sensory processing and behavioral responses [108]. This model provides a broad interpretation of the individual behavior by viewing the neuroscientific thresholds and behavioral responses/self-regulation as a continuum that interacts with each other.

Table 3.2 shows Dunn's model of sensory processing [108] and its elements. In Dunn's model, sensory processing is divided into four quadrants: low registration, sensory seeking, sensory sensitivity, and sensory avoidance, which depend on the continuum of the neurological threshold and the behavioral responses. The neurological threshold is the amount of stimulation that is required for a neuron or neuronal system to respond. A high neurological threshold means that the neurons require several stimuli to be excited (i.e., difficult to notice a faint light, sound, scent, etc.) On the other hand, a low neurological threshold means that neurons are more likely to be excited (i.e., easy to notice the slightest light, noise, smell, etc.) The behavioral response is a tendency to respond to a stimulus. A counteract behavioral response means that the user responds actively to the stimuli (i.e., when he or she notices the scent of a flower, he or she will come closer to sniff it.) On the other hand, an accordance behavioral response means that the user responds passively to the stimuli (i.e., do not notice it even if it makes a sound).

The (Sensory Profile (SP)) [109] and (Adolescent Adult Sensory Profile (AASP)) [110], which are based on this conceptual model, have a widespread influence on the entire field of occupational therapy. In addition, they are becoming an integral part of many therapists' practices and a central source of research and theory generation [111]. AASP is designed to measure the sensory processing patterns and their impact

on the functional performance and it consists of a set of four scores for each sensory processing pattern [110]. AASP is a questionnaire for 11–82 years old and it consists of 60 questions and it is based on the SP for children that are aged 3–10 years. The SP is a questionnaire for parents, while AASP is a self-response questionnaire.

In this experiment, we used the Japanese version of the AASP [112] because the cut level and content of the questionnaire differs for different cultures. The original version classified the cut score into five levels according to three age groups: much less than most people (<2% of the study population), less than most people (between 2% and 16% of the study population), similar to most people (between 16% and 84% of the study population), more than most people (between 84% and 98% of the study population), and much more than most people (>98% of the study population). In the Japanese version, the four age groups were classified into five levels by using a cumulative frequency distribution [112].

3.3 Experiment

In this study, we investigated whether there was an association between the RDW thresholds and the neurological thresholds. In addition, we examined if there was an association between cybersickness and the neurological thresholds.

3.3.1 Participants

To use the Japanese version of the AASP and from the point of view of the physical burden, the participants in the experiment consisted of Japanese people that ranged between 20 to 65 years old. In addition, pregnant women and people with any known disorders that involve the vision, vestibule, and locomotion systems were not permitted to participate in the experiment.

In this experiment, 19 participants attended. The participants were students or staff at a local campus that received 1,500 JPY Amazon gift cards (approximately 14 USD). One participant of the initial 19 participants dropped out due to trouble with

the head mounted display (HMD). Thus, 18 participants completed the experiment and were included in the analyses (gender: 3 females and 15 males, age: M = 25.3, SD = 4.01, body height: M = 1.69 m, SD = 0.066 m).

All the participants had a normal or corrected-to-normal vision. Five participants wore glasses during the experiment and nine wore contact lenses. One participant reported having color blindness, but this disorder was not considered to be sufficient to exclude the participant from the analysis. No other vision disorders were reported by the participants. In addition, 17 participants were right-handed, and 15 participants had a right dominant foot.

Six participants played 3D computer games more than once a week, and 11 played more than once a month. Six participants watched 3D stereoscopic displays more than once a week and 12 watched 3D stereoscopic displays more than once a month. In addition, 17 participants have previously used HMDs. Eight participants used HMDs more than once a week, and fourteen used HMDs more than once a month.

3.3.2 Materials

The experiment took place in a 6 m × 8 m laboratory room. A Lighthouse tracking system to track the user's location was installed so that there was a walking space of 5 × 7m. The participants wore a HP VR Backpack G2, which contained an Intel Core i7 vPro processor, 32 GB of main memory, and an NVIDIA GeForce RTX 2080 graphics card, and an HTC Vive Pro Eye HMD, which provides a resolution of 1440 × 1660 pixels per eye with 615 PPI and an approximately 110° diagonal field of view and a refresh rate of 90 Hz (see Fig.3.1(a)). The HTC Vive controller, which was used as an input device, was utilized by the participants to convey their responses.

The VE was rendered by using the Unity3D engine 2019.4, and it had a space that reproduced a subway station in front of the participant (see Fig.3.1(b)). The scenery consisted of an environment in which the user performed the walking task and the target object that emitted the visual cue to the participant. A subway scene

(a) (b)

Fig. 3.1: Experimental setup: (a) A participant wears an HMD and a Backpack PC, and (b) the participant's view on the HMD during the experiment.

was created, since it is an indoor environment in which trains, benches, and pillars were placed as landmarks in the scene. A poster stand was placed to instruct the user about the target they should walk toward.

3.3.3 Methods

We used a between-subjects experimental design. We tested nine different gains: $g_C \in -0.2, -0.1, -0.05, -0.025, 0, 0.025, 0.05, 0.1, 0.2$. These gains were chosen based on what has been reported in the literature [9, 10]. The participants were presented with one set of the above nine conditions. Each set was repeated 10 times. All trials in one set were randomized.

3.3.4 Procedure

Before the experiment, all participants filled out an informed consent form and received a detailed explanation about the experiment and instructions on how to perform the experimental tasks. Furthermore, they answered: a questionnaire about their experiences with virtual reality (VR), stereoscopic displays, games; a

handedness questionnaire; a questionnaire about vision impairments; and a general questionnaire about diseases. Before and after the experiment, the participants completed the simulator sickness questionnaire (SSQ) [70].

In this study, 90 trials were conducted throughout the experiment, which consisted of nine conditions for the curvature gain. The curvature gains that were used in this experiment include $g_C \in \{-0.2, -0.1, -0.05, -0.025, 0, 0.025, 0.05, 0.1, 0.2\}$. These gains were chosen based on previous works [9, 10]. The participants were presented with one set of the above nine conditions. Each condition was repeated ten times; thus, each participant performed a total of 90 trials. All trials in one set were randomized.

Each trial consisted of the following steps:

1. A participant walks to a black arrow (start point) and faces the direction of the arrow.
2. The walking scenery (a subway station) and the target (a poster stand) appear.
3. The participant walks toward the target for 6.5 m while the curvature gain is implemented for the last 5 m (see item 3.3.4.
4. A questionnaire appears and the participant answers it by using a controller.
5. The walking scenery and target disappear.

There were four possible starting points, and the one that was close to the participant and where the participant's path was expected to fit into the tracking space in the next trial was selected as the starting point. This intervention ensured that the participants were unaware of their position and orientation in the RE. This also makes them unable to identify the amount of redirection that was applied. The next trial started once the participants reached the new start position and were directed in the right direction.

In each trial, the participants were asked to complete the following questionnaire: "Did you feel like walking to the left or to the right?" This question is for a pseudo-2AFC task (see subsection 2.1.5 for details).

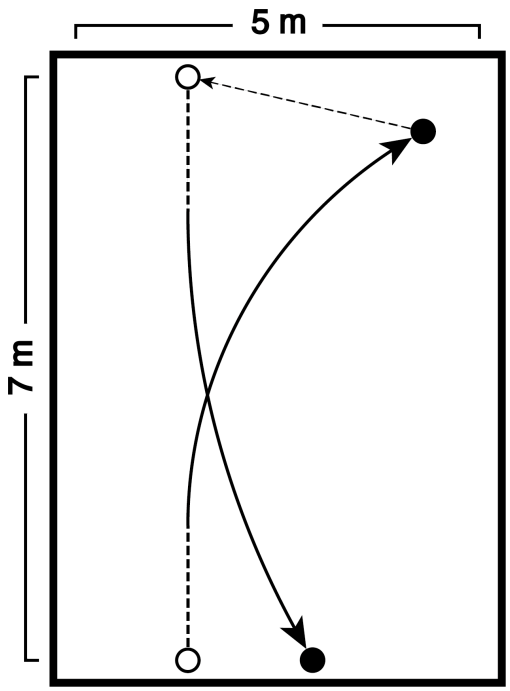

Fig. 3.2: Bird's-eye view of the 5 m × 7 m tracked walking area. The participants started from the white point at the bottom and walked 1.5 m without a curvature gain, and then they walked 5 m with the implemented curvature gain. After the first trial, the participants navigated to the next starting point (upper white point) and started the next trial.

The participants completed a set of training trials before the actual experimental trials. By including the time to answer the question after the 6.5 m walk, each trial took about 20 s. Each participant could take a break when half of the trials were completed. After all the sets, the participants filled out the SSQ again, the iGroup Presence Questionnaire [113], and answered the oral questionnaire. Thus, the total experiment time for one participant was approximately 60 to 90 min, in which approximately 30 min were spent in VR.

3.3.5 Working Hypotheses

Our working hypotheses that were tested in this experiment are as follows:

H1 there is an association between the detection thresholds and the neurological thresholds

H2 there is an association between cybersickness and the neurological thresholds

3.3.6 Results

This section describes the results of the experiment with respect to AASP, the estimated detection thresholds, and cybersickness. For the continuous variables, the analysis of variance (ANOVA) was conducted when the normality assumption (Shapiro–Wilk's normality test) was not violated ($p > .05$). In cases in which a Shapiro-Wilk test revealed that the data were not normally distributed, we analyzed the results with a Friedman test at the 5 % significance level. In order to test whether the results were significantly different, we ran a t-test at the 5% significance level. When the Shapiro-Wilk test showed that the data were not normally distributed, we used a Wilcoxon test at the 5% significance level.

AASP

We calculated the raw scores for each quadrant and classified the appropriate columns (e.g., much more than most people, more than most people, etc.) for each participant. In regard to the low registration, one participant was classified as much more than most people, one participant was classified as more than most people, and the others were classified as similar to most people. For sensory seeking, one participant was classified as much more than most people, four participants were classified as more than most people, one participant was classified as less than most people, and others were classified as similar to most people. In regard to the sensory sensitivity, one participant was classified as much more than most people, five participants were classified as more than most people, and the others were classified as similar to most people. In sensory avoiding, two participants were classified as much more than most people, four participants were classified as more

than most people, one participant was classified as less than most people, and the others were classified as similar to most people.

Detection Thresholds

In the experiment, three participants provided completely opposite responses (i.e., answering that they were bent to the left when they were bent to the right). These participants' responses were inverted and analyzed. section 3.3.6 shows the pooled results of the 2AFC task for four quadrants of the AASP. The x-axis shows the applied curvature gains $g_C \in \{-0.2, -0.1, -0.05, -0.025, 0, 0.025, 0.05, 0.1, 0.2\}$. The y-axis indicates the probability of the correct answer. Each curve was fitted with a sigmoidal psychometric function that determines the DT. Figure 3.3.6 shows the PSEs and DTs for the four quadrants of the AASP. Because the number of trials per condition for each participant is as low as ten, the values served as a reference. The values in parentheses can be used as a reference because only one person was sampled.

We also calculated the DTs for each participant. Because the number of trials per condition for each participant is as low as ten, the values serve as a reference. These DTs were used to perform a significance test to compare the thresholds between the level of each quadrant of the AASP. The DTs were analyzed by performing a one-way ANOVA. For the low registration, no significant differences were found between the levels ($F = 1.19$, $p = .332$). In regard to sensory seeking, no significant differences were found between the levels ($F = .152$, $p = .926$). Regarding the sensory sensitivity, no significant differences were found between the levels ($F = .558$, $p = .584$). In sensory avoidance, no significant differences were found between the levels ($F = .332$, $p = .802$).

Cyber Sickness

We calculated the SSQ total score before and after the experiment for each participant. The mean of the pre-SSQ total scores was 7.84, and the mean of the post-SSQ

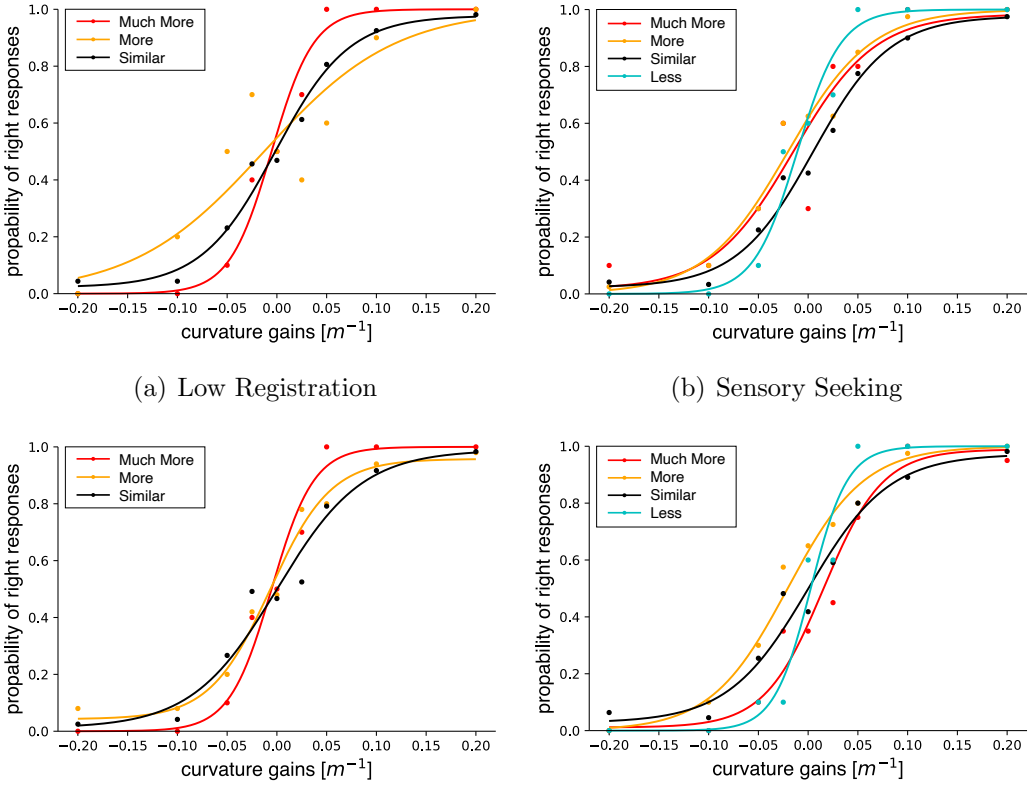

(a) Low Registration

(b) Sensory Seeking

(c) Sensory Sensitivity

(d) Sensory Avoidance

Fig. 3.3: Fitted psychometric functions fitted according to the four quadrants of the AASP

Table 3.2: The pooled results of the 2AFC task for the four quadrants of the AASP. The values in parentheses serve as a reference.

	Low Registration			**Sensory Seeking**			
	Much more	**More**	**Similar**	**Much more**	**More**	**Similar**	**Less**
PSE	(-.005)	(-.013)	-.002	(-.015)	-.020	.005	(-.011)
DT	(.023)	(.072)	.043	(.047)	.046	.045	(.024)
	Sensory Sensitivity			**Sensory Avoiding**			
	Much more	**More**	**Similar**	**Much more**	**More**	**Similar**	**Less**
PSE	(-.005)	-.007	.000	.015	-.021	.000	(.003)
DT	(.023)	.037	.048	.033	.042	.048	(.020)

Table 3.3: The levels of each quadrant of the AASP and the difference between pre- and post- SSQ TS. The values in parentheses serve as a reference.

	Low Registration			**Sensory Seeking**			
	Much more	**More**	**Similar**	**Much more**	**More**	**Similar**	**Less**
Mean	(13.48)	(2)	14.02	(50.4)	10.43	11.52	(9.48)
SD	-	-	17.13	-	7.75	16.22	-

	Sensory Sensitivity			**Sensory Avoiding**			
	Much more	**More**	**Similar**	**Much more**	**More**	**Similar**	**Less**
Mean	(13.48)	23.46	9.09	13.35	6.12	16.18	(10.74)
SD	-	25.84	10.16	.183	9.62	19.89	-

total score was 21.2. There was a significant difference between the scores before and after the experiment ($t = 3.46$, $p = .003$). The levels of each quadrant of the AASP and the difference in the scores before and after the experiment are shown in Table 3.3. Because the number of trials per condition for each participant is as low as ten, the values serve as a reference. These scores were used to perform a significance test to compare the thresholds between the levels of each quadrant of the AASP. These scores were analyzed by performing a one-way ANOVA test. For the low registration, no significant differences were found between the levels ($F = .232$, $p = .796$). In regard to sensory seeking, no significant differences were found between the levels ($F = 2.22$, $p = .131$). Regarding sensory sensitivity, no significant differences were found between the levels ($F = 1.43$, $p = .269$). For sensory avoidance, no significant differences were found between the levels ($F = .335$, $p = .800$).

Presence

Although there are other questionnaires to measure the presence, such as the Witmer and Singer presence questionnaire [114] and the Slater-Usoh-Steed presence questionnaire [115], previous studies recommend using the (iGroup Presence Questionnaire (IPQ)) [113] to measure the presence [116]. Therefore, we used IPQ

Table 3.4: Presence scores. PRES: Presence, SP: Spatial Presence, INV: Involvement, REAL: Experienced realism

	PRES	SP	INV	REAL
Mean	3.48	4.41	2.82	2.64
SD	.72	.73	1.17	.94

for measuring the presence. The questionnaire consisted of fourteen questions with seven point Likert scales.

The results of the IPQ are shown in section 3.3.6. The mean IPQ presence score was 3.48 (SD = .72), which means that the participants had a moderate presence. In the subcategories, the spatial presence had the highest score, and the experienced realism had the lowest score.

3.3.7 Discussion

The purpose of this experiment was to investigate that **H1**: there is an association between the RDW thresholds and the neurological thresholds, and **H2**: there is an association between cybersickness and the neurological thresholds.

From our results, the pooled results for each quadrant of the AASP showed no differences between the levels for the low registration and sensory seeking. Thus, there was no association between the low neurological threshold quadrant and the RDW threshold. On the other hand, the pooled results for each quadrant of the AASP showed differences in the sensory sensitivity and sensory avoiding between the levels. For the sensory sensitivity, the DT of participants who were similar to most people was $g_C = 0.48$ and the DT for more than most people was $g_C = 0.37$. The results suggest that the threshold was 22% lower for those who were prone to sensory sensitivity in comparison to most people. For the sensory sensitivity, the DT of the participants who were similar to most people was $g_C = 0.48$, the DT for more than most people was $g_C = 0.42$, and the DT for much more than most people was $g_C = 0.33$. The results indicate that the threshold was 31% lower for those who were very prone to sensory avoidance and 13% lower for those who were prone to

sensory avoidance in comparison to most people. Thus, there was an association between the neurological threshold and the RDW threshold and a tendency for the groups with lower neurological thresholds to have lower detection thresholds for the curvature gains.

Although the analysis of the individual participants' thresholds did not show significant differences, this might be due to the fact that the constrained number of trials per participant did not allow for reliable estimates of the thresholds. Hence, H1 is partially supported.

Next, an additional working hypothesis, the relationship between cybersickness and the neurological thresholds, is discussed. When comparing the individual pre- and post-experiment SSQ total scores between the levels in each quadrant of the AASP, there were no significant differences between the levels in any quadrant. Therefore, there was no association between cybersickness and the neurological threshold, the behavioral responses, and self-regulation. Therefore, H2 is not supported.

3.4 Conclusion

This chapter evaluated the relationship between the detection thresholds, cybersickness, and the neurological thresholds. We hypothesized an association between the neurological characteristics, RDW thresholds, and cybersickness. We used an AASP to evaluate the neurological thresholds, behavioral responses, and self-regulation, and conducted a psychophysical experiment to estimate the participants' DTs of the curvature gain. We analyzed the DTs and cybersickness for each of the four quadrants of the AASP: low registration, sensory search, sensory sensitivity, and sensory avoidance. Our results demonstrate that there was no significant association between cybersickness and the neurological thresholds. In contrast, the results suggest that the participants who tended to have lower neurological thresholds generally have lower DTs for the curvature gains. In other words, the participants with a higher propensity for sensory sensitivity and sensory avoidance were more likely

to notice the RDW techniques.

Chapter 6

Auditory Redirected Walking

6.1 Introduction

In this chapter, we present a study of redirected walking (RDW) that shifts the positional relationship between visual and auditory cues during curvature manipulation. It has been shown that, when presented with incongruent visual and auditory spatial cues during a localization task, human observers integrate that information based on each cue's relative reliability, which determines their final perception of the target object's location. This multimodal integration model is known as maximum likelihood estimation (MLE). By altering the visual location of objects that users perceive in virtual reality (VR) through auditory cues during redirection manipulation, we expect fewer users to notice the manipulation, which helps increase the usable curvature gain. Most existing studies on MLE in multimodal integration have used random-dot stereograms as visual cues under stable motion states.

In the present study, we first investigated whether this model holds while walking in VR environment. Our results indicate that in a walking state, users' perceptions of the target object's location shift toward auditory cue as the reliability of vision decreases, in keeping with the trend shown in previous studies on MLE. Based on this result, we then investigated the detection threshold (DT) of curvature gains during redirection manipulation under a condition with congruent visuo-auditory cues as well as a condition in which users' location perceptions of the target object are considered to be affected by the incongruent auditory cue. We found that the DT of curvature gains was higher with incongruent visuo-auditory cues than with congruent cues. These results show that incongruent multimodal cues in VR may have a promising application in the area of redirected walking.

6.2 Visuo-auditory Integration

Redirected walking are considered to be based on a phenomenon known as visual dominance [158, 159].Thereafter, in addition to using vision as a cue for redirection, efforts have been made to use visuo-auditory approaches [93, 160] to enhance the amount of redirection. However, most of these approaches have been shown to be inefficient [8]. In this way of thinking, simply appending auditory cues to visual cues may not be sufficient to enhance the amount of redirection.

As a multimodal integration model, maximum-likelihood estimation (MLE) [47] proposes that the weight of each sensory modality during multimodal integration is based on its reliability as describedsection 2.1.4. Visual dominance occurs because the reliability of vision is higher than other modalities, which also explains why audition tends to be inefficient in the area of redirected walking. Therefore, lowering the reliability of visual cues and increasing the relative reliability of auditory cues during visuo-auditory redirection may be a promising approach to enhance the efficacy of auditory cues and enhance the amount of redirection during walking. However, whether the MLE model holds for multimodal integration in VR is unclear. Moreover, most research on the MLE model in multimodal integration has been carried out in a stable motion state and not in a walking state. Previous multimodal integration studies based on MLE mostly used either random-dot stereograms [161] or real-world objects as visual cues during tasks. However, random-dot stereograms are considered to be different from 3D objects in depth constancy, which relates strongly to eye vergence in the perception of objects [162]. As studies have shown that vergence eye movements are generated during self-motion [163], a multimodal integration characteristic using 3D-objects as visual cues in walking tasks may produce different results from those of random-dot stereograms.

Therefore, in this study, we first investigated whether MLE in the multimodal integration model holds for visuo-auditory integration for localization tasks in VR. Then, we presented VR users with a single object with incongruent visual and auditory cues incongruous to each other's location and estimated the DT of the

redirected walking method of curvature manipulation under these conditions.

6.3 Experiment1: The MLE in VR under walking conditions

The aim of Experiment 1 was to investigate whether MLE holds for incongruent visuo-auditory integration of a localization task under walking conditions in VR. The experiment was carried out similarly to those of previous studies investigating visual-haptic integration [48] and visuo-auditory integration [52]. However, this experiment was conducted in a VR environment in a walking state.

6.3.1 Participants

This study had twelve participants.One participant reported color-vision deficiency and failed to conduct the whole experiment, and his data was excluded from the final results. Therefore eleven participants' data entered the analyses. All participants were naive about the purposes of the experiment. Five thousand Japanese yen (approximately 46 USD) were paid to participants after they completed the whole experiment.

6.3.2 Apparatus and Stimuli

The whole environment of this experiment was implemented with Unity3D and using a head-mounted display HTC VIVE PRO, which has a resolution of 1440 $\times$ 1600 pixels for each eye and a refresh rate of 90 Hz. The angle of field is 110°.

We used white noise as the auditory stimulus because previous study by Battaglia et al. investigating the MLE model of visuo-auditory integration [52] used broadband noise as an auditory stimulus. Besides, our preliminary experiment not included in this paper showed that users had no problem performing localization tasks using white noise as auditory stimuli. To realize spatial sound through a binaural

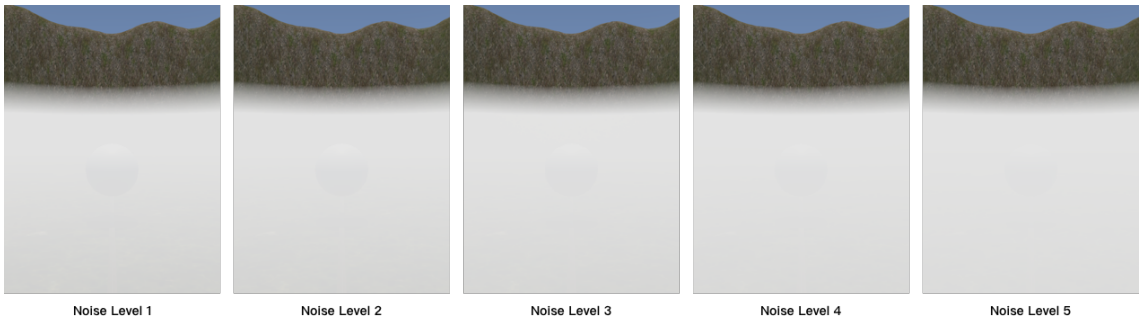

Fig. 6.1: Visual stimulus (the white sphere in the center of each scene) with different fog densities, with the weakest density to the left and the strongest to the right.

sound source, head-related transfer functions were implemented with Steam® Audio SDK[1]

The visual stimulus used in this study is a 3D white sphere 1 m in radius. The distance between the sphere and the participant is about 5 m. To verify the reliability of the visual cue, five different densities of white fog were implemented using the "dynamic fog & mist" asset in Unity. The reliability of the auditory cue was not manipulated because changing the reliability of only vision was enough to change the relative reliability between vision and auditory sensation. This experimental setup followed that of previous studies investigating visual-haptic integration [48] and visuo-auditory integration [52].

The visual scene is shown in Figure 6.1. Noise levels 1 to 5 represent fog density from the thinnest to the thickest. Even at noise level 1, the fog was heavy because lighter fog did not decrease visual reliability sufficiently in the preliminary experiment. Implementing heavy fog even at noise level 1 is acceptable because the examination of the MLE model does not rely on the specific value of visual noise as long as the same visual noise is implemented in both within-modal trials and multimodal trials.

[1]Steam® Audio, Copyright 2017 – 2019, Valve Corp. All rights reserved.

6.3.3 Procedure

The whole experiment was divided into two phases: the within-modal trials and the multimodal trials. The objective of the first phase (within-modal trials) was to measure the probability distribution of every single sensory modality empirically and to predict the probability distribution when participants were presented with multiple modality cues based on the MLE model. Participants were presented with either visual-only or auditory-only cues and asked to perform localizing tasks during the first phase. During the second phase (multimodal trials), participants were presented with visual and auditory cues simultaneously and to perform a similar localizing task. At this step, the empirical probability distribution of visuo-auditory integration was measured. Finally, we investigated whether the distribution predicted in the first phase was consistent with the empirical distribution.

Specifically, in the within-modal trial, participants were presented with two temporally consecutive stimuli, either visually or acoustically, and their task was to judge whether the second stimulus was located to the left or right of the first one and to report their judgment by answering a pseudo two alternative forced choice (2AFC) question. The position of the stimuli is shown in Fig.6.2(a). One of the cues always appeared at the center, which is the standard stimulus, and the comparison stimulus appeared in one of seven different spots: three to the left, three to the right, and one in the center. The spatial interval between two adjacent spots was 1.5° in azimuth angle, so the seven spots were -4.5°, -3°, -1.5°, 0°, 1.5°, 3°, 4.5° in the azimuth angle of the participant. Each comparison stimulus appeared from one of the seven candidate spots, and it was repeated for 15 times for every single spot. Thus, 105 trials were performed in total for the auditory cue. Since the visual scene was affected by five different fog densities, the total number of trials performed with a visual cue was 525.

In the multimodal trial, the participants were presented with stimuli that used visual and auditory cue simultaneously which also appeared twice in temporal sequence. As in within-modal trials, users' task was to judge whether the second

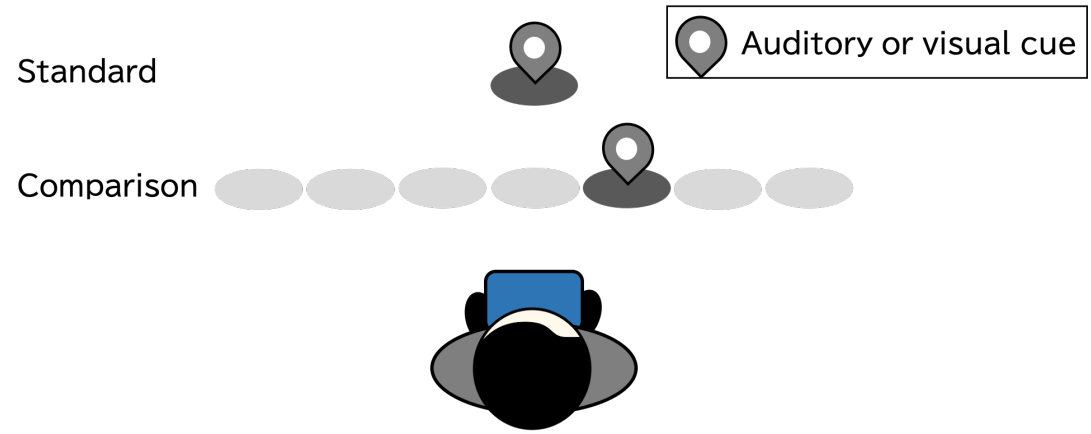

(a) with-in modaltrial

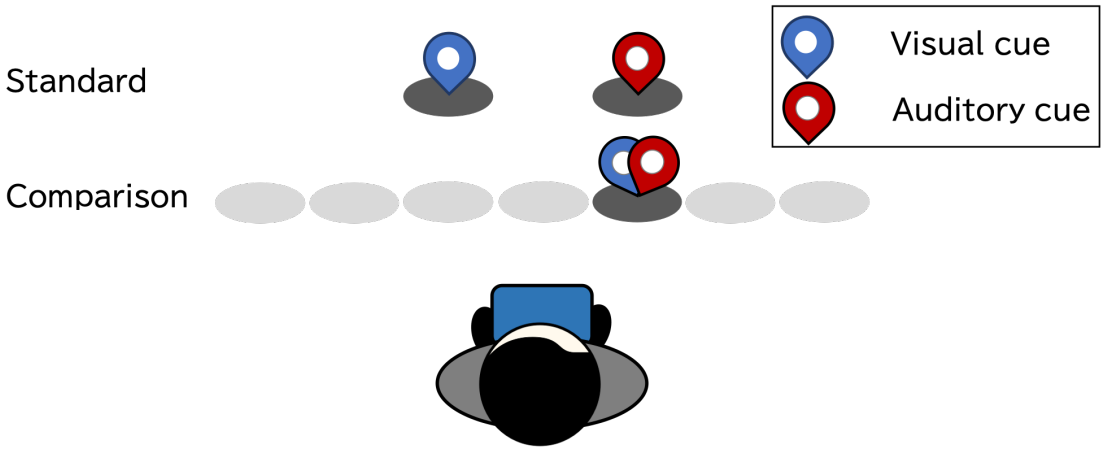

(b) multimodal trial

Fig. 6.2: The position at which the standard stimuli and the comparison stimuli appear.

stimulus was located to the left or the right of the first one and to report this by answering a pseudo-2AFC question. The position of the stimuli is shown in Fig.6.2(b). To investigate the integration of incongruent visuo-auditory cues, the visual event and the auditory event appeared at different spots which is the standard stimulus, where visual event at -1.5° and auditory event at 1.5°. As for the comparison

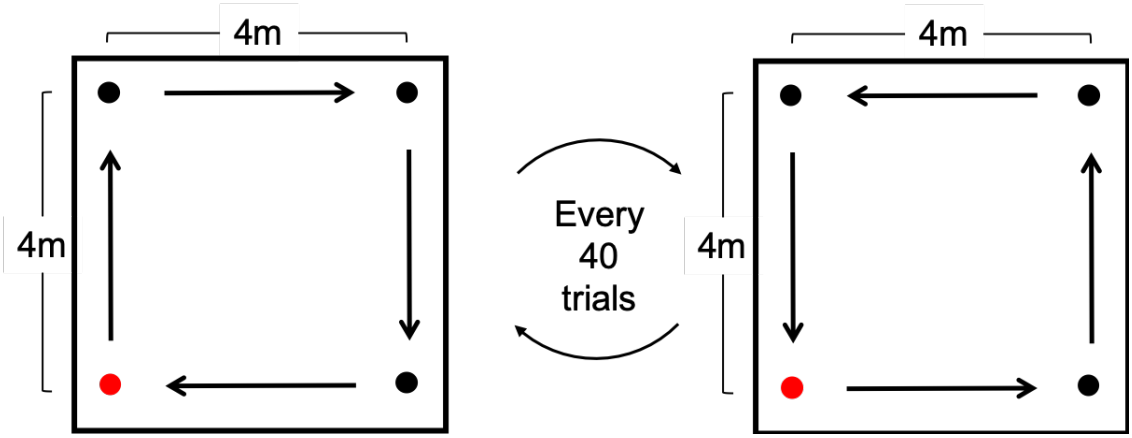

Fig. 6.3: Bird's-eye view of the 4 m × 4 m tracking area. Participants started from the bottom-left red point and walked to each corner of the square area in a clockwise direction at first. Every 40 trials, the direction of walking was shifted between clockwise and counterclockwise.

stimulus, both visual and auditory cues appear at the same spot selected from the seven candidates described above. The standard stimulus and comparison stimulus appeared randomly in sequence. Participants performed 525 trials in total in the multimodal trial. All the trials within each phase were randomized in sequence.

Both the standard stimulus and the comparison stimulus in each trial were presented for 0.5 s, and the temporal interval between the standard and comparison stimuli was 0.5 s. Around 15 minutes were needed for auditory-only trials, and 75 minutes were needed for visual-only and visuo-auditory trials respectively. In addition to a 10-minute rest between the two parts, participants were allowed to rest at any time during the experiment if they asked. Most of the participants took one rest during both the visual-only and the visuo-auditory trials.

In each trial, participants walked along a 4 m straight line while performing the localizing task. Since we expected the task to be done during stable walking, cues appeared after a 1 m free walk. All the trials were conducted in a room with a 4 m × 4 m tracked area. Figure 6.3 shows the bird's-eye view of the experiment area. The participants were asked to start from the lower-left (red) point, and walked along

the side of the square at first, turning 90° to the right-hand side every time they pass the square's vertices. For every 40 trials, we switched participants' walking direction between clockwise and counterclockwise to eliminate its influence on the results and avoid producing dizziness in participants.

6.3.4 Estimation of Normal distribution and Visual weight

Since MLE requires the mean and variance values of the normal distribution of every sensory modality to make predictions, the estimation of the normal distribution from the data obtained by the experiment is a key factor for prediction making. Taking auditory sensation as an example, the procedure is as follows. First, for each azimuth angle where the comparison stimulus appeared, we calculated the ratio of trials in which the participants judged that the comparison stimulus was located to the right of the standard stimulus and put it as p_{right} an then plotted p_{right} with the seven different azimuth angles. It could be expected that p_{right} would be small (near zero) when the comparison stimulus appears at azimuth angle $-4.5°$ and is big (near one) when the comparison stimulus appeared at azimuth angle 4.5°. Then, we fit a cumulative normal distribution curve to the points plotted above, and used 50% x value as estimated mean and "84% value minus mean" as the estimated standard deviation value. This cumulative normal distribution curve is also known as a psychometric function. We took the 50% value as the "point of subjective equality (PSE)" and the difference between the 84% value and the 50% value as the "just noticeable difference (JND)". In a psychophysical experiment, the difference between the 50% value and the 75% value on the psychometric function is mostly considered a JND, which represents the amount of change needed for a difference to be detectable. In a previous study on the MLE model of visual-haptic shape integration [51], JND was treated as the difference between the 50% value and the 84% value in the psychometric function, which was also the case in Experiment 1. In a cumulative normal distribution, the difference between the 84% value and 50% value is also the standard deviation, which is the square root of variance value σ^2.

As for the vision and the visuo-auditory situation, estimation were made for each noise level; thus five psychometric functions at different noise levels were estimated for the two situations.

Another value that had to be estimated from the experimental data was the predicted visual weight value w_v in the visuo-auditory trial. It was calculated as follows using the PSE value gained from the psychometric function.

$$w_v = (PSE - s_v)(s_a - s_v) \tag{6.1}$$

where $s_v = -1.5°$ and $s_a = 1.5°$, according to the experimental setup.

6.3.5 Results and Discussion

Four kinds of analyses were done to investigate the accuracy of MLE in the visuo-auditory localizing task in VR. Firstly, six psychometric functions were fitted to the within-modal trials, with one for the auditory-only trial and five for the visual-only trial under the different visual noise levels. Second, psychometric functions were fitted to multimodal trials under five different visual noise level. Third, the percentage at which vision should be weighted during integration predicted by the MLE model was compared with the empirical one obtained by the experiments. Fourth, the JND of integrated normal distribution predicted by the MLE model was compared with the empirical data obtained by the experiments.

Fig.6.4(a) shows the psychometric functions fitted to within-modal data, one for auditory cue and 5 for the visual cue affected by different fog densities. PSE of all curves are around zero showing an unbiased localization between left and right. The Variance of vision increases as the noise level gets higher. Fig.6.4(b), psychometric functions of multimodal integration are shown. The value of PSE gets nearer to zero as the visual noise level increases, indicating a shift of weight from vision to audition. A plot of visual weight and visual noise level is shown in Fig.6.4(c). In this case, empirical visual weights (red dots) had a higher value than that predicted by the MLE model (yellow shaded area), which indicates that integration of visuo-auditory

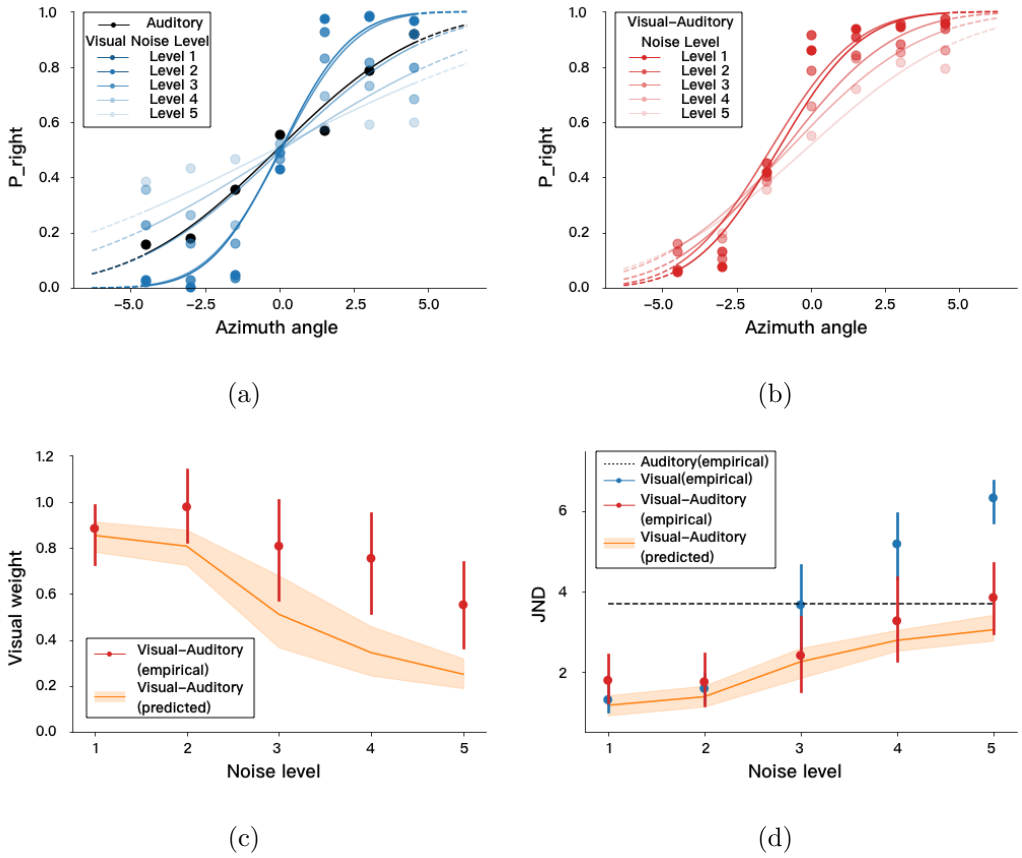

Fig. 6.4: Results of Experiment 1. Top-left figure (a) shows the psychometric functions fitted to the within-modal trials, with black dots and lines representing auditory trials and blue dots and lines different in color intensities representing noised visual trials. Top-right figure (a) shows the psychometric functions fitted to multimodal trials under different visual noise. In the bottom left figure (c), visual weight is plotted against the visual noise level. The yellow shaded area represents the values predicted by MLE based on the within-modal trials. Red dots show the empirical data derived from the visuo-auditory trials. In the bottom-left figure (d), JND of within-modality as well as integrated estimates are plotted against visual noise levels. The dashed line, blue dots, and red dots represent empirical data from the auditory-only, visual-only, and visuo-auditory trials respectively. The yellow shaded area represents the values predicted by MLE from the within-modal trials.

localization is dominated by vision more than MLE expected. Fig.6.4(d) shows the plot of JND and visual noise level. The red dots (empirical JND) almost fall into the

yellow shaded area (predicted JND), which shows that the JND of visuo-auditory integration behaved similarly to the MLE model.

Visual weights were analyzed using 2×5 within-subjects ANOVA. This analysis showed a significant effect of noise level condition, $F(4, 40) = 39.25, p < .001$, a significant effect of "empirical or predicted" condition, $F(1, 10) = 8.39, p < .05$, and a significant interaction effect, $F(4, 40) = 5.97, p < .001$. Since the interaction effect was significant, the difference in visual weight between the empirical and predicted conditions was assessed for each noise level. The difference in visual weight between the empirical and predicted conditions were significant at noise level 3, $F(1, 10) = 6.59, p < .05$, noise level 4, $F(1, 10) = 10.59, p < 0.01$, and noise level 5, $F(1, 10) = 10.17, p < .05$. This result shows that the experimental value of the visual weight (red dot) was higher than the value predicted by the MLE model (yellow shade). A two-sided paired-sample t-test for the visual weights of the two noise levels of the empirical data observed significant difference between noise levels 1 and 5, $p(10) = 3.94, p < .05$, as well as between noise level 2 and 5 $p(10 = 4.05, p < .05)$. This suggests that the weight was shifted from vision to auditory sensation when the visual noise level was high if visual noise was introduced by changing the transparency of fog.

JNDs were analyzed using 2×5 within-subjects ANOVA. This analysis showed a significant effect of noise level conditions, $F(4, 40) = 39.17, p < .001$, while the "empirical or predicted" condition was not significant $F(1, 10) = 6.60, p = 1.15$, and the interaction effect was not significant $F(4, 40) = 1.10, p = 0.37$. Since the experimental value of JND (red dot) fell within the value (yellow shade) predicted by the MLE model, it can be said that the relationship between the reliability during visuo-auditory integration and the reliability of a single modal follows the MLE model.

Under a walking state, the empirical JND meets the predicted value, while visual weight shows a bigger value than expected. Despite the increment in weighting of auditory cues as vision became less reliable, the participants still relied more on vision than audition. It has been previously shown that, during self-motion, eye

movements are triggered by visual and vestibular mechanisms, which are used to compensate for retinal image slip [163]. These eye movements are also considered able to maintain visual acuity, which may influence the ratio at which vision is weighted during visuo-auditory integration.

We can therefore say that lowering visual reliability is an applicable approach to reassigning sensory weights during visuo-auditory localization tasks in VR. Though vision tends to be weighted more highly than predicted by MLE under walking conditions, this remains a promising approach to visuo-auditory redirected walking, as long as the reliability of vision can be manipulated through methods such as introducing noise to the visual scene or changing the resolution of displays.

6.4 Experiment 2: Curvature manipulation with incongruent visuo-auditory cues

Results of Experiment 1 confirmed that the contribution of auditory cues to the visuo-auditory integration of spatial localization tasks increased when the visual reliability was reduced in VR space. Thus, the usefulness of auditory cues may be increased by reducing visual reliability. Since it is possible to change the perception of VR space by manipulating the position perception of objects in VR, we propose a visuo-auditory method redirected walking that presents visual and auditory cues at slightly different spatial positions in a VR environment with low visual reliability. In this experiment, by presenting VR users with an auditory cue that differed from the visual cue of a single object, we manipulated the user's position perception of the target object due to visuo-auditory integration. This experiment aims to investigate the effect of such position perception manipulation on the DT of curvature manipulation, a method of redirected walking. We conducted a user experiment to verify the effectiveness of the proposed method.

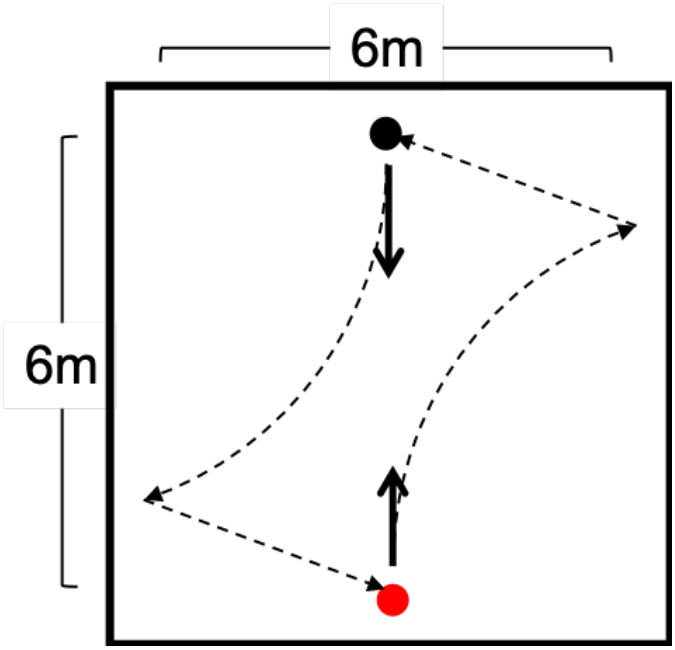

Fig. 6.5: Bird's-eye view of the 6 m × 6 m tracked walking area. Participants started from the red point at the bottom and walked 5 m with the curvature gain implemented. After the first trial, participants navigated to the nearest point (either the black point or the red point) and started the next trial.

6.4.1 Participants

This study had twelve participants (gender: five females and seven males, age: M = 24.3, SD = 4.5). All had normal or corrected-to-normal vision and normal hearing. All participants were right handed. Eight participants had used HMDs before, and three participants were experiences with HMDs more than three times. All the participants were naive to the purpose of the study. One thousand Japanese yen (approximately 9.3 USD) was paid to participants after they completed the whole experiment.

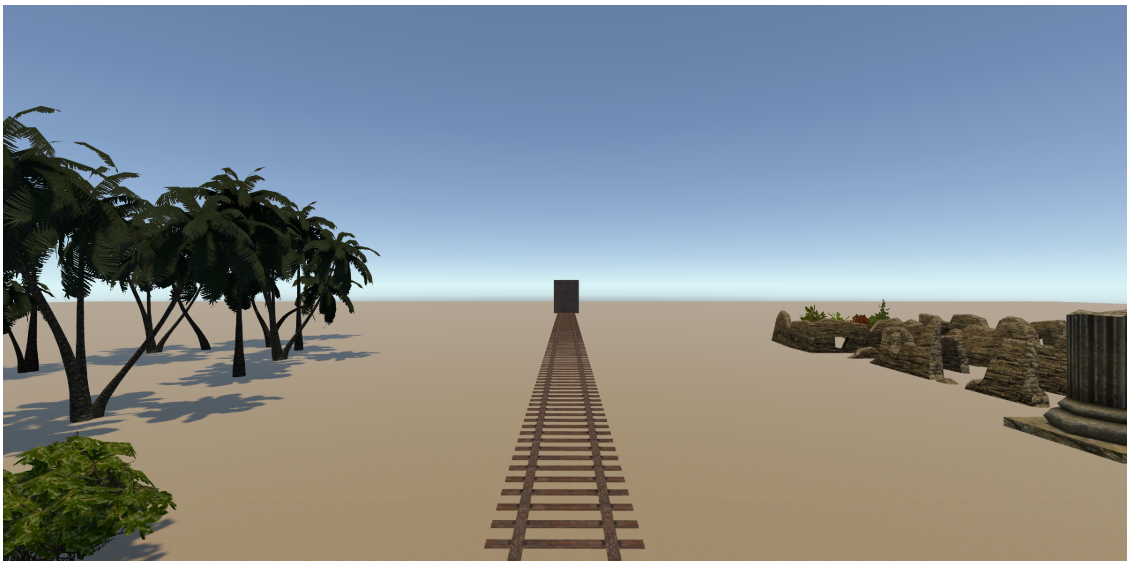

(a) without visual noise

(b) with visual noise

Fig. 6.6: The viewing scenery at the starting point from the participant's perspective. (a) Shows the scene without noise and (b) shows the scene with noise.

6.4.2 Procedure

To manipulate users' visual location perception using auditory cues and investigate its influence on users' DT to curvature manipulation, we conducted Experiment

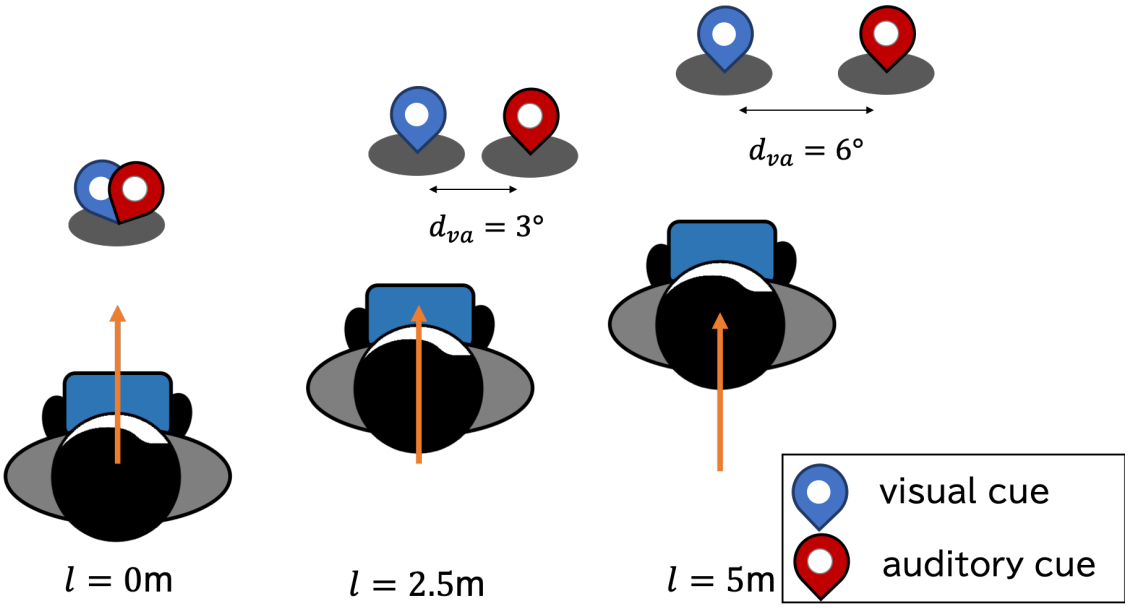

Fig. 6.7: Implementation of incongruent visuo-auditory cues

2 as follows. Two conditions, consisting of congruent conditions and incongruent conditions, were introduced to enable us to investigate the impact of incongruence between visuo-auditory cues. To change the relative reliability between vision and auditory sensations, two conditions "with visual noise" and the "without visual noise" were also introduced in Experiment 2. Unlike the purpose of Experiment 1, which was to verify the MLE model under VR, the purpose of Experiment 2 was to investigate the effectiveness of the proposed method. Therefore, two visual noise levels, two conditions were sufficient. Moreover, since the walking distance of Experiment 2 was longer than that of Experiment 1, reducing conditions and shortening the total experiment time prevented simulator sickness that may be evoked by curvature manipulation. There were a total of 36 conditions throughout the experiment consisting of the combination of two conditions with congruent or incongruent visuo-auditory information, two conditions of with or without visual noise (fog), and nine conditions of curvature gain. The curvature gain used in this experiment were $g_C \in \{-12\pi/180,\ -9\pi/180,\ -6\pi/180,\ -3\pi/180,\ 0,\ 3\pi/180,\ 6\pi/180,\ 9\pi/180,$

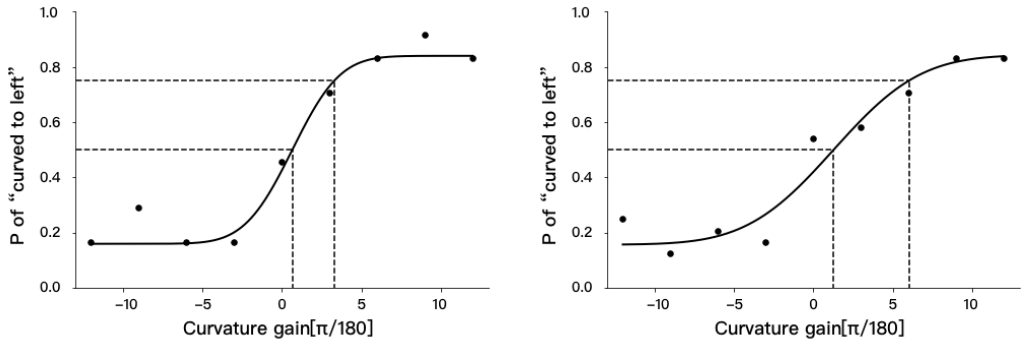

(a) Without visual noise, congruent visuo-auditory cues

(b) Without visual noise, incongruent visuo-auditory cues

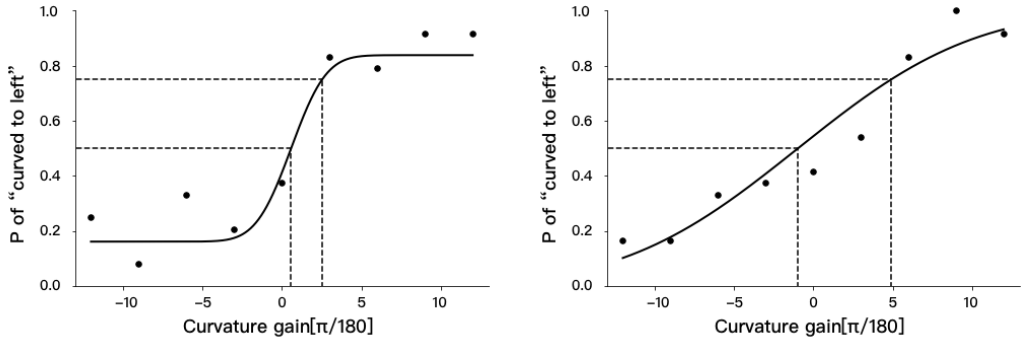

(c) With visual noise, congruent visuo-auditory cues

(d) With visual noise, incongruent visuo-auditory cues

Fig. 6.8: The fitted psychometric function under four conditions. The horizontal axis represents the implemented curvature gain. The vertical axis represents the ratio of reporting "curved to the left" to the question of "Which direction did your walking path turn in the real world?".

$12\pi/180\}$. Each condition was repeated twice, thus each participant performed a total of 72 trials. The trial order was completely randomized.

Each trial consisted of the following steps:

1. Participants walked to the starting point (red) showed in Figure 6.5.
2. Participants turned toward the opposite side of the square area (red arrow).
3. The walking scenery and the visuo-auditory target appeared.

4. Participants walked along the path for 5 m while the curvature gain was implemented.

5. Participants navigated to the nearest point and turned in the direction indicated by the arrow.

During each trial, the instructions given to the participants were as follows:

1. Walk along the railroad track until the train and the engine sound disappear.

2. Answer to the question "Which direction did your walking path turn in the real world turn?" after each 5 m walk.

The purpose of this question was to investigate whether the participants correctly recognized the difference between the real-world walking path and the walking path in VR space. The question was asked as a pseudo-2AFC question. The participants could answer "left" or "right" not to the question, and "I don't know" or "straight" No curvature gain had been applied or the participant did not feel the manipulation, they had to guess. Consequently, when there no curvature gain applied, an equal ratio of "left" and "right" answer expected. The answer to this question was used to estimate the psychometric function, and calculate the DT under each condition.

Including the time to answer the question after the 5 m walk, each trial took about 30 seconds. There was a 10-minute break in which the participants could remove the head-mounted devices when half of the trials were completed. Thus, the total experiment time for one participant was about 40 minutes.

6.4.3 Apparatus and Stimuli

The whole environment of the experiment was implemented with Unity using the same head-mounted display (HTC VIVE PRO) as in Experiment 1. To allow for a wide range of movement when walking and to avoid entanglement with the cord connecting the PC to the head-mounted display, we used MSI VR One, a PC that could be carried on the user's back during the experiment.

The scenery, shown in Figure 6.6, consisted of the environment in which the user performed the walking task and the target object that emitted the visuo-auditory cue to the participant. A desert scene was created, as it is an outdoor environment in which fog could appear, Shrubs, trees, and ruins were placed as landmarks in the scene. A straight railroad track was placed to instruct the user the route they should walk, and a rectangular image of a train was placed on the track and accompanied by an engine sound as a visuo-auditory object to manipulate the user's spatial perception. It was assumed that the characteristics of users ' integration of incongruent visuo-auditory cues (MLE) in VR would be invariant regardless of the type of stimulus used. Prerequisite contextual knowledge between visual cues and auditory cues was also considered important for the establishment of multimodal integration. Therefore, the train and engine sound were used as visual cue and auditory cues in Experiment 2, instead of the white sphere and white noise used in Experiment 1. In addition, since the train had a high constraint relationship with the railroad track, it provides a higher manipulation effect of the user's spatial perception. Figure 6.6 shows the case without fog and the case with fog. To prevent the user from identifying their current position using real-world sound, wind sounds were used as the environmental sound. The fog was implemented by using Unity's asset, Dynamic Fog. The alpha value, which is an intra-asset parameter for adjusting transparency, was fixed to 0.98 in the trials with fog. To realize spatialized sound, a head-related transfer function was applied to the engine sounds using Unity's Steam® Audio SDK[2].

Implementation of incongruent visuo-auditory cues

When the visuo-auditory cues were congruent,the engine sound and the train appeared to have the same source. When the visuo-auditory information was incongruent, as shown in Figure 6.7, the relative positions of the engine sound and the user were changed according to the amount the user moved. Before the user began walking, the auditory source of the target object appeared at the same position as

[2]Steam® Audio, Copyright 2017 – 2019, Valve Corp. All rights reserved.

the visual target, but as the user moved forward, it shifted to the right side of the visual target, and the difference in azimuth angle of the visuo-auditory target seen from the user's d_{va} could be given by $d_{va} = 6l/5$. Here, l is the amount the user moved. In other words, after the user walked 5 m, the maximum difference between the relative azimuth angle between the visual and auditory cues of the target object was 6°. We set d_{va} as a continuously increasing value instead of a fixed value. When the relative positions of the visual cue and auditory cue changes continuously, the auditory cue has a higher impact on location perception through visuo-auditory integration.

6.4.4 Results and Discussion

In this experiment, the pseudo-2AFC method was used to investigate the DT of the curvature gain. When the curvature gain was positive ($g_c > 0$), the VR space was rotated to the left, so the participant needed to turn left to walk the straight track in the VR space, and the answer "left" was the correct answer. On the other hand, when the curvature gain was negative ($g_c < 0$), the correct answer was "right". If there was no curvature manipulation creating sensory bias to the left or right, when the curvature gain is not applied ($g_c = 0$), the participants had to guess the direction; thus the probability of answering "left" and "right" was expected to be 50% each.

Figure 6.8 shows the fitted psychometric function and the DT under each condition. There are four conditions consist of the combination of "with visual or without visual noise" and "congruent or incongruent visuo-auditory cues". We fitted the psychometric function using a cumulative normal distribution. The horizontal axis value with a probability of 50% is PSE, and the difference between the horizontal axis value with a probability of 75% and PSE is the threshold. The results of PSE and DT under four conditions are summarized in Table 6.1.

The minimum imperceptible walking radius calculated from the threshold of the curvature gain under the four conditions, based on $r = 1/g_c$, is shown in Table 6.2.

Table 6.1: PSE and DT of visuo-auditory RDW

	without noise		with noise	
	congruent cues	incongruent cues	congruent cues	incongruent cues
PSE	0.661	1.284	0.585	-0.963
DT	2.639	4.739	1.955	5.873

The smaller the minimum imperceptible walking radius, the less noticeable the curvature gain was to the user, so the effect of spatial compression by redirected walking was higher.

The minimum imperceptible walking radius was 21.7 m when there was no visual noise and the visuo-auditory cues were congruent. This value was in agreement with a study of the minimum imperceptible walking radius using visual cues alone [9]. The threshold with the addition of auditory cues was the same as with visual cues alone was due to the visual superiority. This result is also consistent with the research investigating the DT of visuo-auditory rotation manipulation [92]. The minimum imperceptible walking radius of our proposed method reached 9.8 m. In a similar visuo-auditory RDW experiment conducted by Meyer et al. [93], the minimum imperceptible walking radius reached 6.0 m, which is smaller than with our proposed method. There are two major differences between our study and theirs. Meyer et al. used a wave field synthesis (WFS) system to create spatial sounds while we used head-related transfer function (HRTF). Since HRTF is known to have individual differences and we used the same HRTF through out the whole experiment, whether it is compatible with all users is unknown. Furthermore, though both studies considered a psychometric function value of 75% to be the DT, they fitted the psychometric function itself in different ways.

The results showed that the minimum imperceptible walking radius decreased when the visuo-auditory cues were incongruent compared to when the cues were congruent, regardless of the visual noise conditions. This effect may be due to the occurrence of proper visuo-auditory integration and the alteration of users' spatial perception. When the visuo-auditory cues were congruent, the minimum imperceptible walking radius under conditions with visual noise increased compared with

conditions without noise. On the other hand, when the visuo-auditory cues were incongruent, the minimum imperceptible walking radius decreased when visual noise was added. This is due to the reduced visual reliability of an environment with visual noise and because the position perception of the target object is easily affected by auditory cues. Although the effect of spatial perception manipulation was reduced when noise was added, when visuo-auditory cues were congruent, an effect exceeding this reduction was caused by providing incongruent visuo-auditory cues that led to visuo-auditory integration. The curvature manipulation was less noticeable than when the visuo-auditory cues were congruent and there was visual noise.

The PSE under the condition "with visual noise, incongruent visuo-auditory cues" deviated in the negative direction of the curvature gain compared with the other three conditions (Figure 6.8). This perceptual bias may be caused by the direction of curvature manipulation due to the visuo-auditory integration that occurs when the visuo-auditory cue is presented at different positions. Under the condition with incongruent visuo-auditory cues, the auditory cues were always shifted to the right side of the visual cues. Therefore, under the "with visual noise" condition where the location of the target object was easily affected by the auditory cues, the location of the target object was more easily perceived as shifting to the right side. The users inferred that the "target shifting to the right side" phenomenon was the consequence of walking to the left side, which could explain the increased probability of answering "curved to left".

In this study, we conducted visuo-auditory RDW using a sound-emitting object as a target, but it is known that the contribution of environmental sound is also significant in spatial perception [164]. In addition, environmental sounds are considered to be more content-independent. Therefore, it is expected to develop a method to enhance the effect of RDW by using environmental sounds.

Table 6.2: The minimum imperceptible walking radius

	congruent cues	incongruent cues
without visual noise	21.7 m	12.1 m
with visual noise	29.2 m	9.8 m

6.5 Conclusion

In this chapter, in order to explore the possibility of visuo-auditory redirected walking that effectively uses the auditory sense, we first investigated whether MLE could be adapted to incongruent visuo-auditory integration in VR environment. Then, we proposed a novel method that introduced visual noise and incongruence between visual and auditory cues of the object in VR when applying curvature manipulation. We verified the effectiveness of this method by comparing it with existing methods.

Experiment 1 confirmed that the behavior of visuo-auditory integration in VR can be roughly predicted by the MLE model, and that contribution ratio of auditory cues increases as visual noise increases. We showed the possibility of changing the spatial perception according to the auditory sense by presenting the auditory stimulus by lowering the reliability of vision and manipulating the spatial perception of the user in VR.

Experiment 2 introduced visual noise and auditory cues incongruent with visual cues when implementing curvature gain, by which we succeeded in lowering the minimum imperceptible walking radius to 9.8 m, less than half that of the conventional method with only visual cues [9]. Because redirected walking is based on the human perceptual characteristic of integrating incongruent sensory cues, it could be considered as a perceptual phenomenon when the manipulation is under the DT.

Both experiments have shown that manipulations above the DT impose cognitive demands on the user [121]. Thus, redirected walking may not solely be a question of cue integration when the manipulation is noticeable to the user. However, our result did indicate a promising application of incongruent multimodal cues in VR to redirected walking and navigation.

Nevertheless, a certain amount of perceptual bias to the direction of curvature manipulation was observed when presenting users with incongruent visuo-auditory cues of the target object. Bias may result in an uneven DT between curvature manipulation in different directions. Moreover, to perform spatial perception manipulation of the user via visuo-auditory cues, something that emits the visuo-auditory stimulus while moving in front of the user is necessary, and the application scene is limited. Therefore, to realize a more generalizable method, this must be studied in the future. It may be promising to explore a method that manipulates spatial perception by providing auditory cues using environmental sounds that are appropriate for the users' VR content, such as the sound of river water or the sound of birds in a forest content.

Chapter 7

Visuo-Haptic Redirected Walking

7.1 Visuo-Haptic Redirected Walking

Visuo-haptic redirected walking (RDW) is a method to improve the effectiveness of RDW by manipulating the user's proprioceptive sensation by generating visuo-haptic interaction with haptic cues. Figure 7.1 shows a user walking while receiving stimuli from haptic and proprioceptive senses by touching objects placed along a walking path. Simultaneously, first-person view images of the user walking while touching an object placed along the path are generated in a virtual environment. The virtual object differs from the real object and is presented through an HMD. The user believes that she or he is touching the object with a shape that is visually presented to her or him through a visuo-haptic interaction. In this example, the user thinks she or he is touching a flat wall, which can strongly enhance the effect of RDW by thinking she or he is walking straight along a flat wall. We believe that the visuo-haptic RDW enables more effective manipulation of spatial perception than conventional visual manipulation alone.

7.1.1 Evaluation of Curvature Manipulation Using Visuo-Haptic Interaction

In this experiment, we used questionnaires and behavioral indices to verify whether curvature manipulation using visuo-haptic interaction allows to manipulate the spatial perception more effectively than conventional visual-only curvature manipulation. In existing studies on curvature manipulation, only linear walking paths have been presented to participants in virtual environments. In our experiment, we pre-

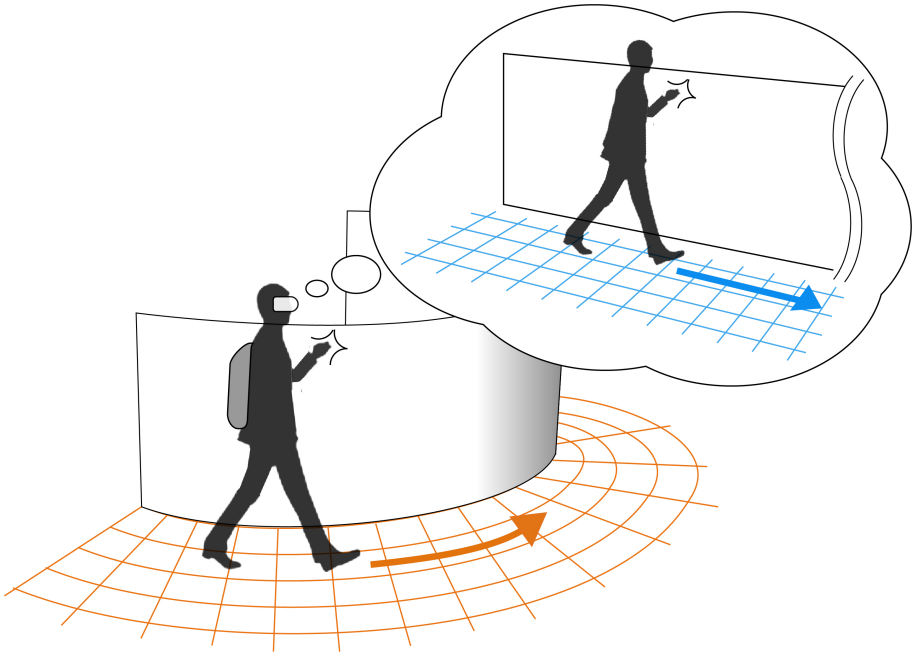

Fig. 7.1: Visuo-haptic Redirected Walking

sented a curved path besides the linear path to hinder the guessing of the purpose of the experiment, thus mitigating preconceptions.

Experimental Design

This experiment comprised $2 \times 4 \times 4$ conditions: two levels, haptic and control conditions, four levels of walking path curvature in the real space, $\chi_{real} \in (0, 0.111, 0.170, 0.372)[m^{-1}]$, and four levels of walking path curvature in the virtual environment, $\chi_{virtual} \in (0, 0.111, 0.170, 0.372)[m^{-1}]$. One trial was conducted per condition, and the order of the trials was randomized. The evaluation items included the subjective curvature calculated based on the amount of rotation felt by the participants during walking, the walking speed, head sway, and the total SSQ score [70]. Given that the purpose of this experiment was to determine the walking path curvature that elicited the perception of walking along a straight line in the virtual environment, the results obtained from curved path perception in the virtual

environment were excluded from the analysis.

Participants

Twelve participants (five females and seven males) participated in this experiment. The participants were healthy and right-handed, and their age ranged from 20 to 24 years (mean, 21.9 years). During the experiment, one participant wore glasses, and three wore contact lenses.

Experimental Setup

The participants wore an Oculus Rift DK2 HMD (horizontal viewing angle of approximately 110 degrees, 75 fps, 9-axis sensor), headphones, and a backpack, as shown in the figure. The backpack carried a laptop computer to which the HMD and headphones were connected, and the participants walked without assistance from the experimenter. A motion capture system consisting of six Optitrack Flex 13 cameras was used to determine the head position of each participant. The measuring range of the motion capture system was 7 $\times$ 4 m with a resolution of 0.1 mm. The posture of the head was obtained from a gyroscope mounted on the HMD. White noise was played through the headphones to prevent the participants from obtaining cues about their own position and posture from environmental sounds. The image presented to the participants was a rendering of the simple virtual environment consisting of walls and floors shown in Figure 7.2. The values in the figure correspond to the walking path curvature in the virtual environment. The right side wall in the environment is 1.6 m in height and 5.4 m long. A curved wall with a radius 0.5 m smaller than that of the walking path in the virtual environment was displayed through the HMD when a curved walking path was presented. Unity was used to render the images presented to each participant at a fixed rate of 30 fps. For rendering, system management, and data recording, we used a computer equipped with an Intel Core i7 processor at 2.6 GHz, 32 GB of main memory, and an NVIDIA GeForce GTX 970M graphics card.

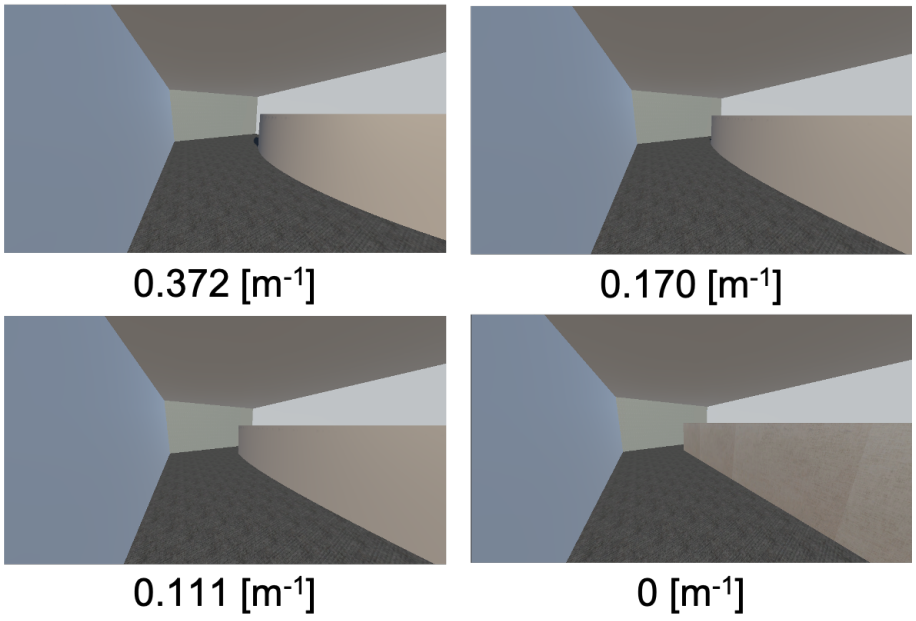

Fig. 7.2: Virtual environments

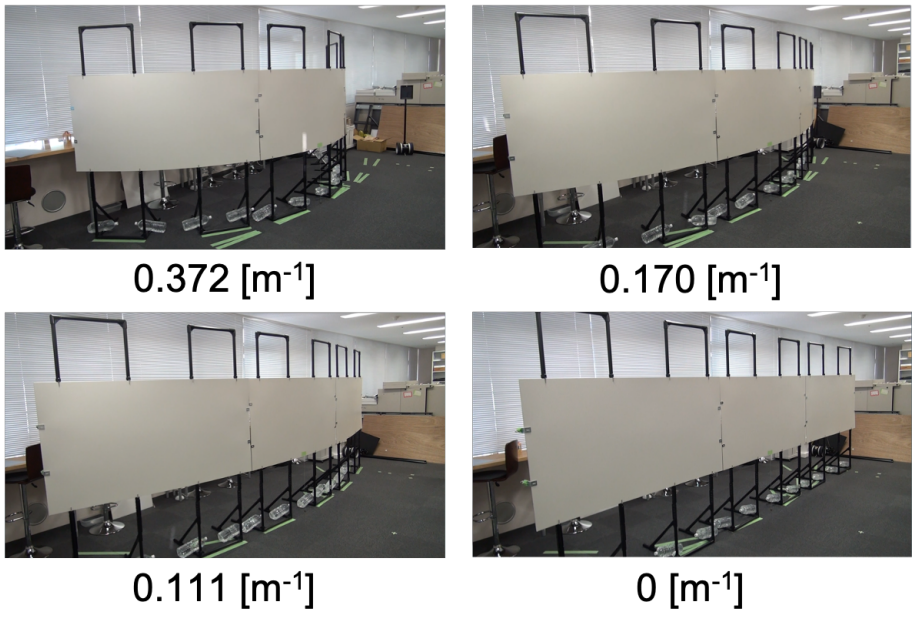

Fig. 7.3: Real environments

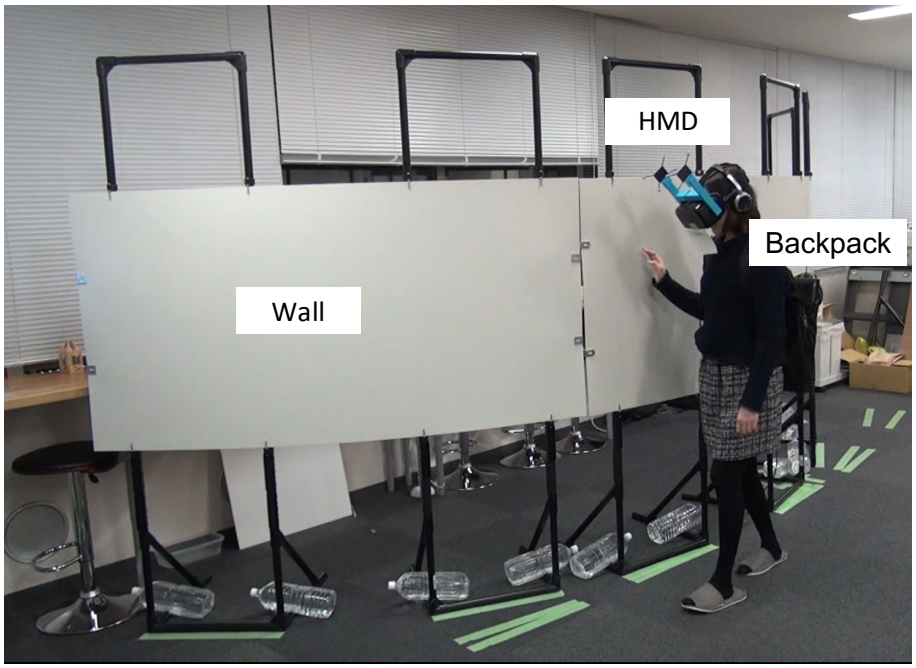

Fig. 7.4: Experimental Overview

Besides the systems, we created a wall that can be given an arbitrary curvature, hereinafter referred to as variable wall, as shown in Figure 7.3. The variable wall provided haptic stimuli when touched by the participants. The values in the figure correspond to the walking path curvature in the real space. The variable wall consists of a plywood board painted on one side (width, 1.8 m; height, 0.9 m; thickness, 5 mm). The board can be convexly warped by applying tension with wires from both ends and placing posts. The participants received haptic stimuli by touching the variable wall with their hands. We constructed a variable wall with a length of 5.4 m by combining three wall segments to match the length of the wall presented in the virtual environment. The average distance from the wall to the center of the participant's body was set to 0.5 m. The radius of the variable wall was 0.5 m smaller than that of the actual walking path, and the variable wall was set with a rightward offset of 0.5 m from the actual walking path. For a straight actual walking path, the variable wall was flattened and offset 0.5 m rightward from the actual walking

path. For curved and flat paths, the height of the variable wall matched that of the wall in the virtual environment.

Experimental Procedures

The duration of the experiment, including the explanation, pre-test questionnaire, main trial, break time, post-test questionnaire, and post-experimental explanation, was 2 h per participant distributed into 2 days with a 1 h session per day. Each participant wore the HMD for approximately 40 min per day. Before the experiment, we explained the purpose of the experiment by claiming that this was an experiment on VR sickness when walking in a virtual environment. This explanation aimed to avoid forming preconceptions in and influencing the responses of the participants regarding the curvature manipulation, which was the real purpose of the study. Then, the participants provided the following information: age, gender, dominant hand, use of glasses or contact lenses, presence or absence of equilibrium sense or visual abnormality. In addition, the participants completed the SSQ.

After answering this pre-test questionnaire, the participants wearing the HMD, headphones, and backpack moved to the initial position 0.5 m away from the variable wall along the radial direction according to the guidance presented by the HMD. Then, they walked for 5 m under each experimental condition. In the control condition, the participants were instructed to walk naturally while maintaining a certain distance from the wall displayed on their righthand side. In the haptic condition, the participants were instructed to walk naturally like in the previous condition and to intermittently touch the variable wall with the palm of their right hand (see Figure 7.4). During the experimental trials, the position and posture of the participants' head were recorded every 0.1 s. After each trial, the participants followed the guidance presented by the HMD and moved to the response seat, where a partition was placed for them not to see the variable wall setup. Then, the HMD was removed for the participants to answer the post-test questionnaire regarding the subjective amount of rotation, sense of immersion, and sickness as they walked through the path.

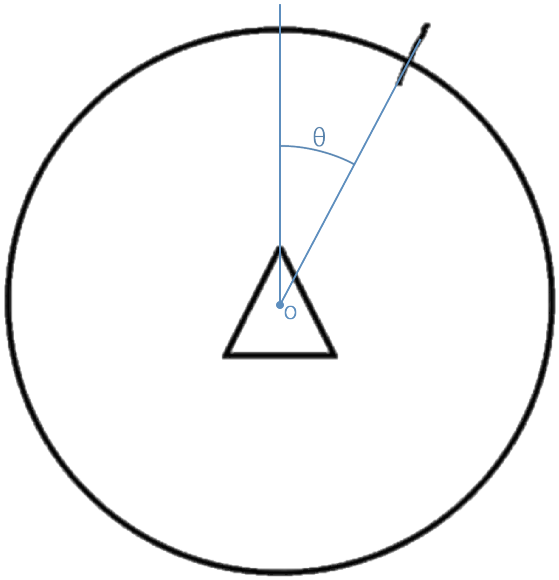

Fig. 7.5: Sample response for subjective amount of rotation. The blue lines are auxiliary lines, o is the center, and θ is the subjective amount of rotation.

The subjective amount of rotation was determined by placing a mark on a graph as that shown in Figure 7.5. The graph consisted of a circle with a radius of 5 cm and an isosceles triangle with a base of 1 cm and a height of 1 cm placed at the center of the circle. The VR sickness experienced by the participants was recorded by using the SSQ. As the participants answered the questionnaire, the experimenter set the variable wall to the curvature corresponding to the walking path of the next trial. After completion of all trials, the participants freely commented on their impressions about the experiment. The experimenter then clarified the true purpose of the experiment to the participants and asked them to answer the questionnaire again. The subjective curvature, $\chi_{sub}[radm^{-1}]$, was calculated from the subjective amount of rotation, $\phi_{sub}[rad]$, obtained from both the questionnaire after each trial and the actual walking distance.

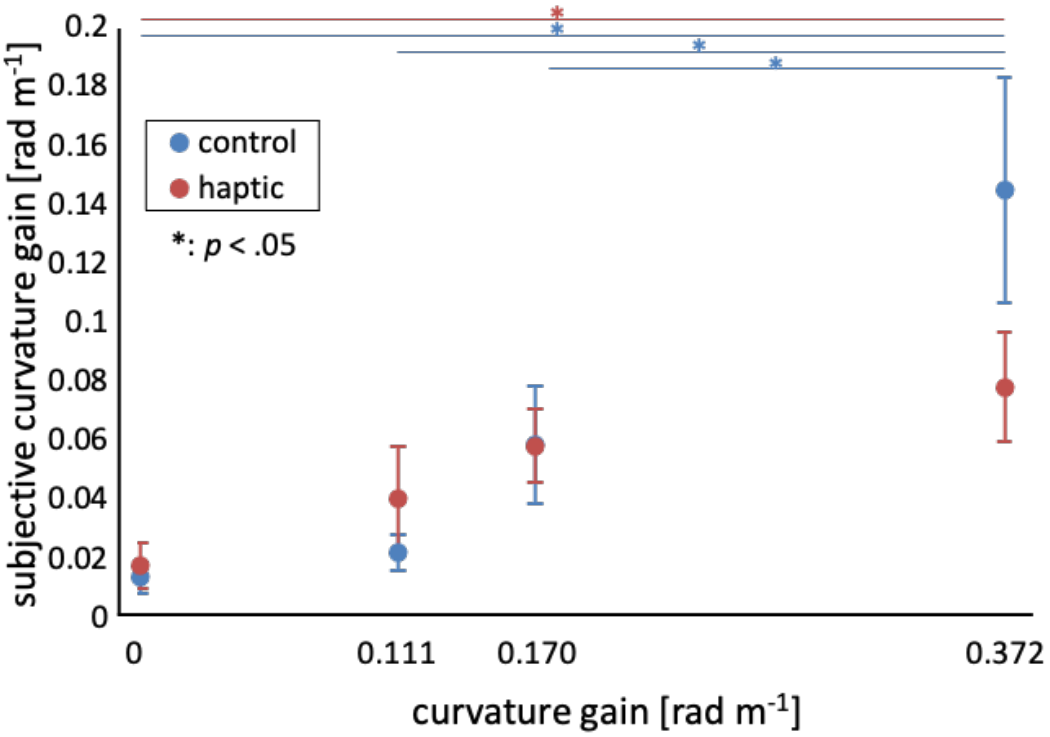

Fig. 7.6: Subjective curvature gains

Results

The mean values and standard errors of the subjective curvatures calculated from the participants' responses according to the curvature gain are shown in Figure 7.6. The red circles and blue squares indicate the haptic and control conditions, respectively. By applying a two-factor within-subjects analysis of variance, we found no significant difference in the main effect of haptic cues but a small effect size ($F(1,11) = .289, p = .601, partial\eta^2 = .026$) regarding the subjective curvature. In addition, we found a significant difference and a large size in the main effect ($F(3,33) = 10.62, p < .001, partial\eta^2 = .491$) regarding the curvature gain. There was also a significant trend and moderate effect size for the interaction ($F(3,33) = 2.61, p = .068, partial\eta^2 = .192$). Next, we performed multiple comparisons regarding haptic conditions and found a significant difference $p = .0309$ only

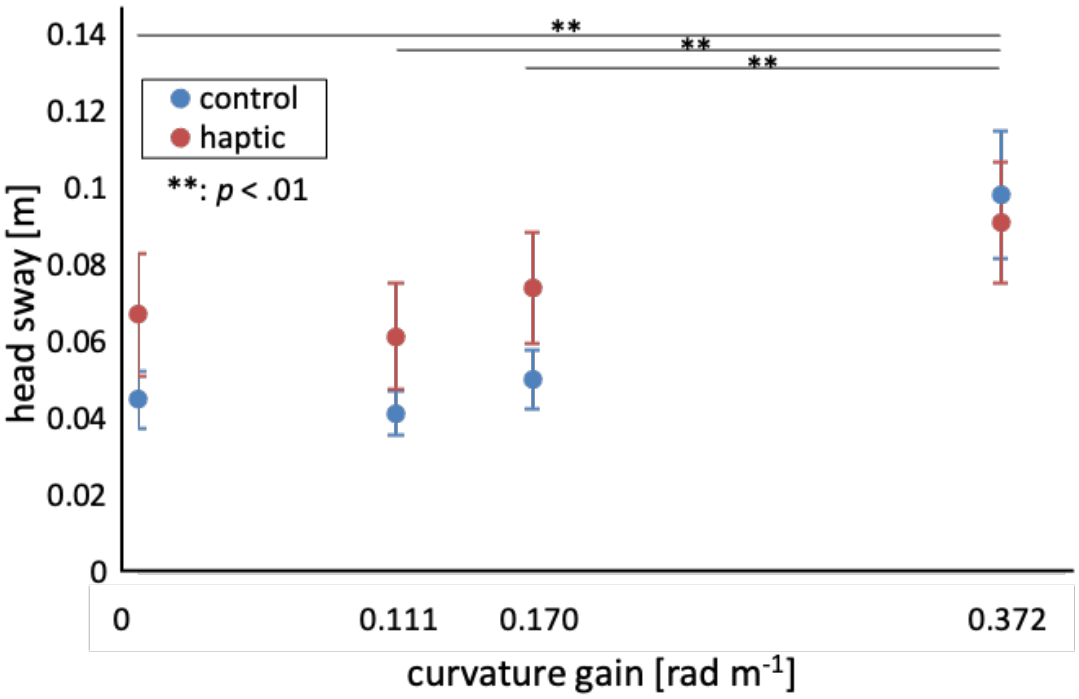

Fig. 7.7: SD of head sway

for curvature gain g_C of (0, 0.372) and no significant difference among the other conditions. There were significant differences in g_C of (0, 0.372), (0.111, 0.372), and (0.170, 0.372)$[m^{-1}]$ ($p = .037$, .037, and .044, respectively) under control conditions.

By applying a two-factor within-subjects analysis of variance to the mean walking speed, we found a significant difference in the main effect of haptic cues ($F(1, 11) = 5.685, p = .036, partial\eta^2 = .341$), no significant difference in the main effect of curvature gain ($F(3, 33) = 1.904, p = .148, partial\eta^2 = .148$), and no significant difference in the interaction ($F(3, 33) = 1.309, p = .287, partial\eta^2 = .106$). The mean walking speed under the haptic conditions was 0.449 $[ms^{-1}]$ and the mean walking speed under the control conditions was 0.4785 $[ms^{-1}]$. Therefore, the presentation of haptic cues decreased the walking speed by 6.2%.

The mean values and standard errors of the head sways according to the curvature gain and haptic conditions are shown in Figure 7.7. By applying a two-factor within-

subjects analysis of variance to the head sway, we found no significant difference in the main effect of haptic cues ($F(1, 11) = 1.042, p = 0.329, partial\eta^2 = .087$) and the interaction ($F(3, 33) = 1.28, p = 0.297, partial\eta^2 = 0.104$) but a significant difference and a large size in the main effect ($F(3, 33) = 10.59, p < .001, partial\eta^2 = .491$) regarding the curvature gain. Multiple comparisons ($\alpha = 0.05$, two-tailed) with the corresponding t-test for the main effect of curvature gains showed that there were significant differences in g_C of (0, 0.372), (0.111, 0.372), and (0.170, 0.372)$[m^{-1}]$ ($p = .002$, .002, and .001, respectively).

By applying a two-factor within-subjects analysis of variance to the total SSQ score, we found no significant difference between the main effect and interaction.

The following participants' comments after the experiment were obtained: "When a straight wall was displayed, I felt as if I was walking along a straight path;" "sometimes, I felt as if I was turning, but I did not intuitively know in which direction I was turning;" "when a curved wall was displayed, I felt as if I was really walking along a curve."

7.1.2 Discussion

When haptic cues were available, the subjective curvature was not significantly different between the straight path and curvature gain $g_C \leq 0.170[m^{-1}]$. On the other hand, in the control conditions, the subjective curvature was significantly different between curvature gain $g_C = 0.372[m^{-1}]$ and $g_C \leq 0.170[m^{-1}]$. These results suggest that the use of haptic cues improves the effectiveness of curvature RDW, particularly when the curvature gain is large. Meanwhile, the presentation of haptic cues significantly decreased the walking speed, which might affect the subjective curvature. Moreover, there was no significant difference in head sway between the haptic and control conditions, but there were significant differences between the curvature gains. The trend of significant differences in head sway was consistent with the trend of significant differences in subjective curvature.

Fig. 7.8: Overview of Unlimited Corridor: Handrail Version. A user sees straight handrails through the head-mounted display (HMD) and feels that they are walking along gripping an ostensibly straight handrail, although they are actually walking along gripping a curved handrail.

7.2 Unlimited Corridor

Unlimited Corridor is a VR system that enables users to explore an immersive corridor freely with touching walls or along the railing [165, 166]. A central feature of the Unlimited Corridor is the improvement of RDW by passive haptic feedback, which makes it possible to freely walk within a large VE even in a small tracked space without unnatural interruptions such as resetting.

The system displays virtual hands through the HMD and synchronizes the timing at which the real/virtual hand touches physical/virtual handrails, as shown in the center of Figure 7.9. These synchronized stimuli generate visuo-haptic interaction and make a user feel that the handrails are straight. This illusion increases the effectiveness of the RDW and makes the user feel as if she/he is walking straight.

Fig. 7.9: Left: first person view of the VE; center: virtual hand gripping a virtual handrail; right: an example walking path in the VE (blue line) and the RE (red line).

Another feature of the Unlimited Corridor is the management of the user's position. Because the VE is larger than the physical tracking space, one point in the physical space corresponds to a several points in the VE. We developed a one-to-many mapping algorithm to control the correspondence between the physical and virtual user's position. We also designed contents for the Unlimited Corridor: a skyscraper environment to justify the situation of walking while gripping handrails.

7.2.1 Visuo-Haptic Redirection

Visuo-haptic interaction is a key technique for the Unlimited Corridor. In the Unlimited Corridor, the radius of curvature is approximately 2.5 m, which is considerably smaller than 22 m [9], 11.6 m, and 6.4 m [10], with which the user does not notice the RDW operation. Schmitz et al. showed that using a wider range of rotation gains than conservative rotation gains does not impair the user's VR experience [98], but the curvature gain applied this time is much larger than that of the conventional ones; thus, it may be considered that a straight walking experience cannot be achieved using only the conventional method. Thus, we focused on visuo-haptic interaction. Matsumoto et al. showed that visuo-haptic interaction could enhance the effects of curvature manipulation and provide an immersive experience [104]. Based on this study, using visuo-haptic interaction, the amount of perceived curvature could be reduced up to 62%. We refer to the RDW method

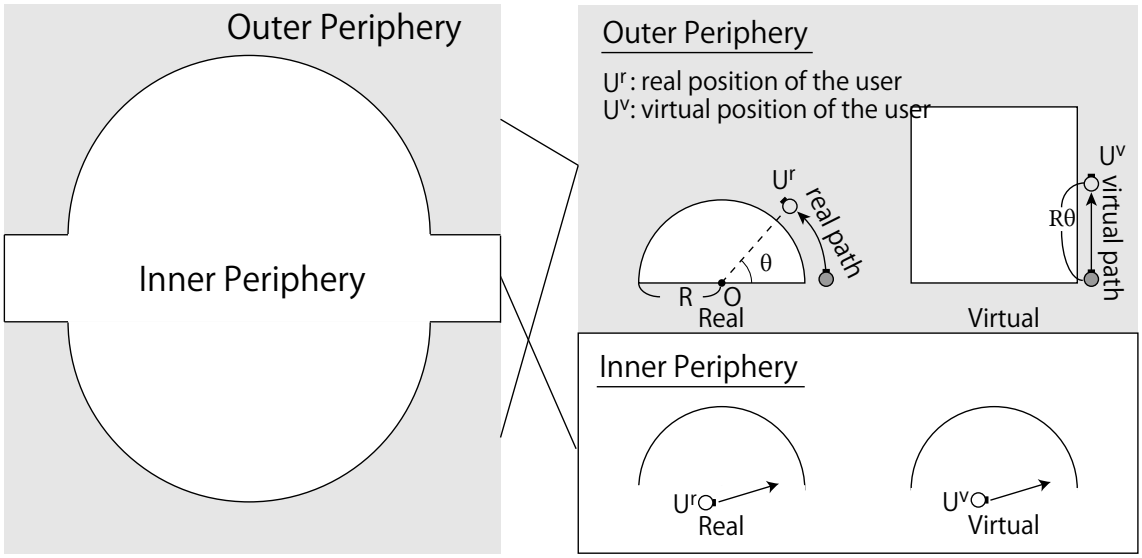

Fig. 7.10: Relationship between user's real position and virtual position (based on [165].)

using visuo-haptic interaction as visuo-haptic redirection.

In our system, we used walls and handrails as haptic stimuli to generate visuo-haptic interaction. The following describes the case of the handrail. A user sees straight virtual handrails through the HMD, and walks along while gripping an ostensibly straight handrail, although they are actually gripping a curved handrail and walking along with it. As a result of synchronization between visual manipulation and passive haptic feedback, visuo-haptic interaction occurs and enhances the effect of RDW. Owing to visuo-haptic redirection, users feel as though they are walking in a straight line, despite walking along a path with a radius of approximately 2.5 m in the real space.

7.2.2 Mapping Algorithm

To realize a branched corridor, we propose dynamically modifying the amount of spatial distortion owing to the actual user's position. The system uses a curvature gain when the user is in the outer periphery, whereas there is no manipulation within the straight central passage. When a user is in the outer periphery (image on the

right in Figure 7.10), the user's virtual position (U^V) is moved by $R\theta$. However, when the user is in the inner periphery (bottom right in Figure 7.10), the system performs one-to-one mapping between the user's real position (U^r) and virtual position. This algorithm can maintain the relative position between the user and the handrails in the real space and VE.

7.2.3 Virtual Path Layout

A virtual corridor comprises straight lines and three-way junctions and looks like a ladder from the top. Figure 7.11 shows two walking routes. In the first route, the user turns left at the first corner, follows the central road, then turns right and goes straight to the next corner. Then, at the corner, the user turns right and follows the central road; they turn left and go straight to the balloons. In the second route, the user turns left at the first corner, follows the central road, then turns right and goes straight to the second corner. Then, at the corner, the user turns right and follows the middle road; they then turn left and go straight to the balloons. The user can take any other route besides these two paths. For example, she/he can run dead ends and come back to the route that she/he once walked. The figure on the right of Figure 7.9 shows the actual walking path of a user. The virtual path is blue, and the real path is red. Furthermore, for smooth demonstrations, we set the start and end points of the VE to be the nearest point in the real world.

7.2.4 System Overview

The tracking space was 8.6 $m \times 7.4$ m. We set up two semi-circular handrails with a diameter of 5.0 m corresponding to the straight virtual handrails arranged in the VR space, as shown in Figure 7.8 and 7.12. The handrails were placed at a height of 0.8 m and they were 34 mm in diameter. The central path was 5.0 m in length and 1.2 m in width.

Users wear an HTC VIVE Pro HMD, which provides a resolution of 1440×1600 pixels per eye, with a diagonal field of view of 110 degrees and a refresh rate of 90

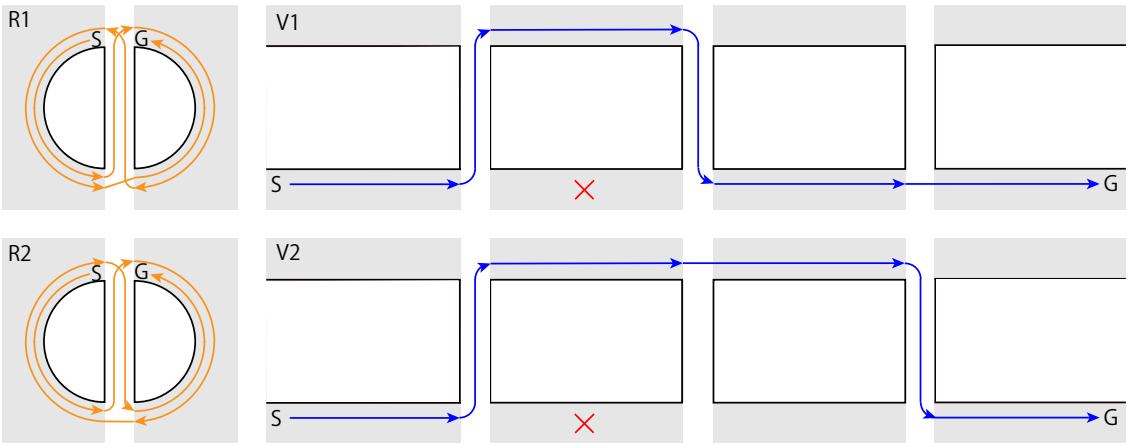

Fig. 7.11: Correspondence between real and virtual routes. The orange paths are the real routes and the blue paths are the virtual routes. 'S' and 'G' indicate the start and goal point, respectively. The gray areas denote the areas where the curvature gain is applied. The red crosses indicate places that cannot be walked on.

Hz. This HMD provides a continuous first-person stereoscopic view of the VE (see the image on the left of Figure 7.9), while a stereo headset provides spatial audio and prevents the user from hearing what happens in the physical space. To detect hand positions, two VIVE Tracker 2.0 devices were attached to the user's hands. Four SteamVR Tracking 2.0 basestations were set to track the user's head and hand positions. The location information of the VIVE Pro HMD and VIVE Trackers measured by the SteamVR Tracking System is sent to Unity3D.

By using the Unlimited Corridor's mapping algorithm, the real space position is associated with the VR space position, and the images and sound corresponding to the VR space position information are rendered and presented to the user through the VIVE Pro HMD.

We used an Intel computer with a 2.7 GHz Core i7 processor and 32 GB of main memory, along with an Nvidia GeForce GTX 1070 graphics card for tracking, rendering, system control, and logging. The VE was rendered using the Unity3D engine at 75 fps.

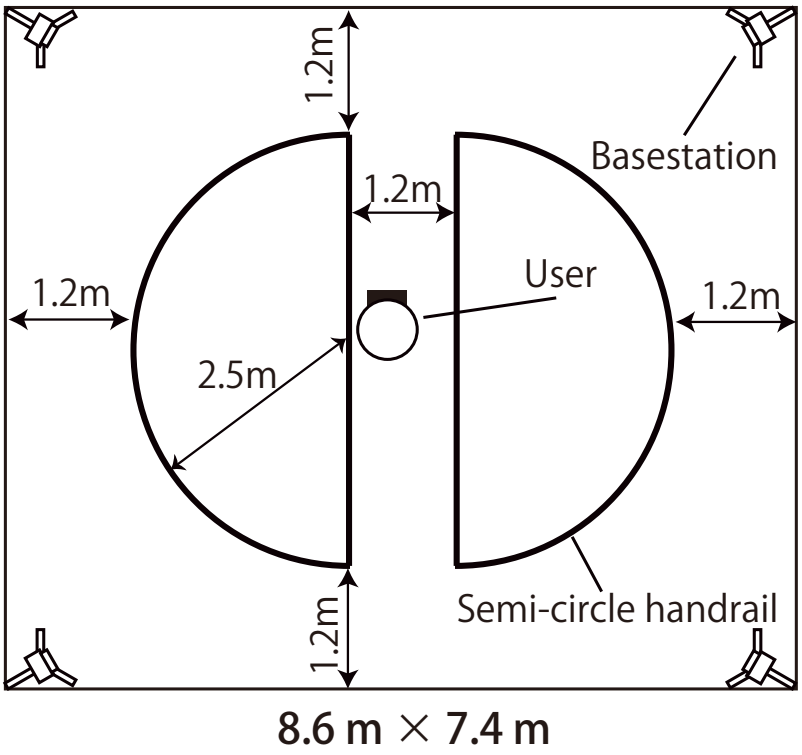

Fig. 7.12: Top view of Unlimited Corridor: Handrail Version.

7.2.5 User Study

The main purpose of the experiment is to measure whether passive haptic stimuli could generate visuo-haptic interaction and enhance the effect of RDW. Our main hypothesis is that walking by gripping the handrails makes the user feel as if they are walking in a straighter direction. As mentioned above, Matsumoto et al. showed that visuo-haptic interaction could enhance the effects of curvature gain manipulation and provide an immersive experience [104], but they did not present virtual hands in their study. Therefore, it is unclear whether visuo-haptic interaction has occurred and that it has affected RDW. In this study, we display virtual hands to examine whether visuo-haptic interaction has occurred and its effect on RDW.

We conducted a within-subject experiment. The experimental conditions are as follows. Non-haptic conditions, the user did not grasp the throughout the experience.

Haptic conditions, the user grabbed the handrail throughout the experience. The order of the non-haptic condition and the haptic condition was adjusted so as to be unbiased.

Participants

22 participants (6 females, 16 males) aged between 22 and 35 years old (mean = 25.7, SD = 3.59) took part in the experiment. All participants had normal or corrected vision, and 20 had previous VR experience. The experimental procedures were approved by local ethics committee.

Questionnaires

The main purpose of the experiment is to measure whether passive haptic stimuli form the handrails could enhance the effect of a curvature manipulation. There are many types of evaluation methods for RDW, such as 2AFC (see section 2.1.5), maximum likelihood estimation [10], and illustration of walking routes [104], but these are methods for estimating the threshold of gains. Therefore, these are not suitable to evaluate the sense of a user who walks in a specific real/virtual route such as that considered in this study. Therefore, we propose new evaluation method, which measures the sensation of straightness with a mean of four seven-point Likert-scale questions. The four questions were as follows.

1. Did you feel that you were walking straight during the VR experience? (1: Strongly disagree, 7: Strongly agree)
2. How often did you feel like you were walking straight during the VR experience? (1: Never, 7: Very frequently)
3. Did you feel that the movements in the VR matched movement in the physical space during the VR experience? (1: Strongly disagree, 7: Strongly agree)
4. How often did you feel that the movements in the VR matched the movements in the physical space during the VR experience? (1: Never, 7: Very frequently)

We also used the Slater-Usoh-Steed presence questionnaire (SUS PQ) [115] to evaluate the presence of users in the IVE. To identify potential influences on the results, participants also completed Kennedy's simulator sickness questionnaire (SSQ) [70] immediately before and after the experiment. Furthermore, we asked participants for a free description of their experiences.

Behavioral Indicators

We focused on walking speed as a behavioral indicator. The walking speed is closely related to the sense of going straight, and it is known that the faster one walks, the more one notices a manipulation [90]. In addition, in the Chapter 4, there is a correlation between individual curvature RDW thresholds and walking speed. The positions and orientations of the user's head and hands in real space and VE were recorded approximately every 0.1 s and the walking speed v_r was calculated from the user's head positions.

Procedure

Each participant conducted a total of two trials, under non-haptic and haptic conditions. Both trials were conducted on the virtual rooftop of the skyscraper environment described in the User Experience section. However, the last falling part was deleted in consideration of its influence on the results. The total time per participant for the experiment was approximately 15 min, which included the pre-questionnaires, instructions, experiment, post-questionnaires, and debriefing. Participants wore the HMD for approximately five minutes.

A participant entered a room with the curved handrails installed, at which time the participant could see its outline. The procedure of the experiment was explained to each participant and they were told that they could abort the experiment at any time. To not disturb the user's natural walking, we did not instruct the participants on how to grip the handrail and left it to them. Furthermore, they were provided with a consent form to sign and an advance questionnaire to complete. Then, they

were asked to complete pre-questionnaires: regarding their gender, age, height, VR experience, eyesight and balance, and pre-SSQ on a laptop. They were subsequently asked to attach the trackers and wear the backpack PC and the HMD. After confirming that the equipment was installed properly, the first trial commenced. At the end of the first trial, the user removed the HMD and answered the questionnaire regarding the sensation of straightness and the SUS PQ on the laptop. Afterward, the user wore the HMD again for the second trial. After the second trial, the user removed the HMD, trackers, and backpack PC and answered the questionnaire about the sensation of straightness, the SUS PQ, and the post-SSQ. After answering the questionnaire, the user was asked to freely describe the whole experience, and the experimenter made a note of this description.

7.2.6 Results

In the free description, everyone stated that the virtual handrails were felt straight. However, six participants reported that the positions of their hand and the handrail were misaligned in the VE although they were touching the handrail in the real environment. Seven participants mentioned that it was easy to notice that they were walking on a bend in the second trial, because they got used to the demo and walked faster during the second trial than the first one.

We checked whether the walking speed differed between the first and second trials. The mean walking speed for the first trial was 0.53 ms^{-1} ($SE = 0.013\ ms^{-1}$) and that of the second trial was 0.58 ms^{-1} ($SE = 0.025\ ms^{-1}$, see Figure 7.13.) We analyzed the walking speed by means of a paired t-test and determined a significant difference between the walking speeds of the first and second trials and moderate effect size ($t(21) = 2.84,\ p = 0.019,\ dz = 0.77$.) As noted by the participants, the walking speed was found to be faster in the second trial than in the first trial by 10%.

We also checked whether the walking speed differed between the non-haptic and haptic conditions. The mean walking speed under the non-haptic condition was

0.60 ($SE = 0.021$), and under the haptic condition, it was 0.56 ($SE = 0.020$, see Figure 7.14.) We analyzed the walking speed by means of a paired t-test and determined that there is no significant difference between non-haptic and haptic walking speeds ($t(21) = 1.57,\ p = 0.26,\ dz = 0.34$.) This result indicates that the experimental conditions were well controlled.

We compared whether the sensation of straightness differed between the first and second trials. The median straightness sensation score in the first trial was 4.38 ($mean = 4.42$) and that of the second trial was 3.63 ($mean = 3.90$, see Figure 7.15.) We analyzed the straightness scores by means of a Wilcoxon signed-rank test and determined that there is no significant difference between first trial and second trial scores ($T = 76.0,\ p = 0.56,\ r = 0.16$.)

We analyzed the differences in the sensation of straightness between the non-haptic and haptic conditions. The median straightness sensation score under the non-haptic condition was 3.38 ($mean = 3.55$), whereas under the haptic condition it was 5.13 ($mean = 4.77$, see Figure 7.16.) We analyzed the straightness scores by means of a Wilcoxon signed-rank test and determined a significant difference between the haptic and non-haptic scores and the moderate effect size ($T = 29.5,\ p = 0.010,\ r = 0.43$.)

The mean SUS PQ score under the non-haptic condition was 5.18 ($SE = 0.32$), and under the haptic condition, it was 5.38 ($SE = 0.27$, see Figure 7.17.) We analyzed the SUS PQ scores by means of a paired t-test and there was no significant difference between the SUS PQ score under the non-haptic and haptic conditions ($t(21) = 0.554,\ p = 0.59,\ dz = 0.12$.)

The SSQ total severity (TS) scores before the experiment averaged 7.48 ($SE = 2.31$, see figure 7.18), while the average post-experiment score was 17.6 ($SE = 4.15$) out of a maximum of 179.52. We analyzed the SSQ TS scores by means of a paired t-test and determined a significant difference between the pre- and post-SSQ scores and moderate effect size ($t(21) = 2.98,\ p = 0.0071,\ dz = 0.64$.)

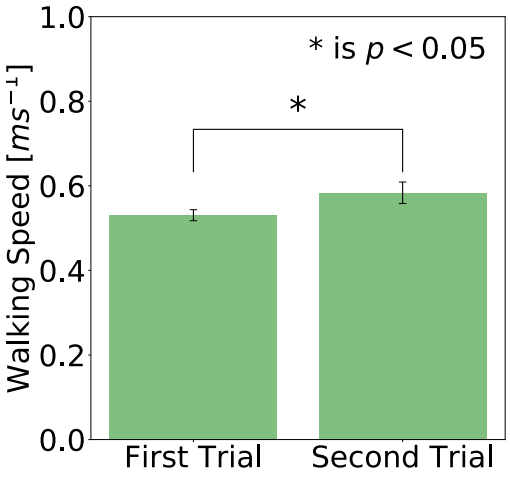

Fig. 7.13: Trial order: Mean walking speed, where the error bars indicate the SE.

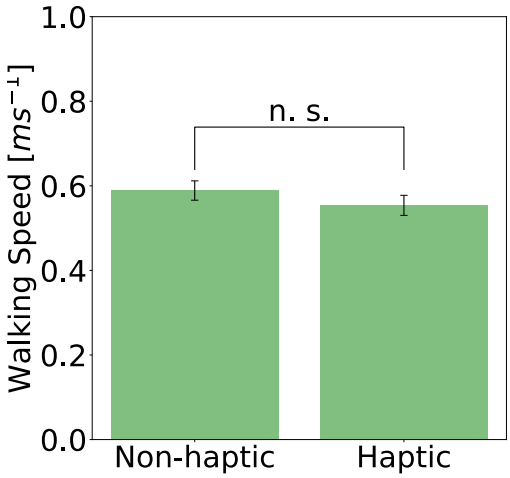

Fig. 7.14: Haptic conditions: Mean walking speed, where the error bars indicate the SE.

7.2.7 Discussion

The reports by users that the handrail felt straight in the free descriptions are evidence that visuo-haptic interaction has occurred. From the comparison of the sensation of straightness under non-haptic and haptic conditions, we found that using passive haptic feedback with handrails significantly improves the sensation of straightness with a moderate effect size. Thus, we concluded that visuo-haptic interaction can enhance the effect of an RDW technique.

The results of the SUS PQ show that the users were immersed in the VE. Although six participants reported that the positions of the handrails and the virtual hands were misaligned sometimes, there was no significant difference in the score of the SUS PQ between non-haptic and haptic conditions.

The results of SSQ showed that the user felt a little VR sickness after the VR experience. Although we cannot clarify the cause of this sickness from this experiment, we estimate that it is owing to the use of the large curvature gain.

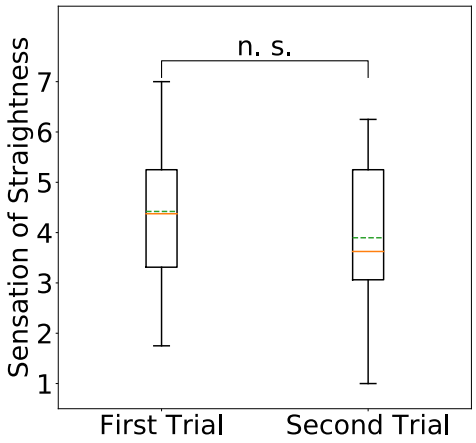

Fig. 7.15: A box plot of straightness sensation according to the questionnaire scores under the first and second trials, where orange lines indicate the median and the green dashed lines indicate the mean.

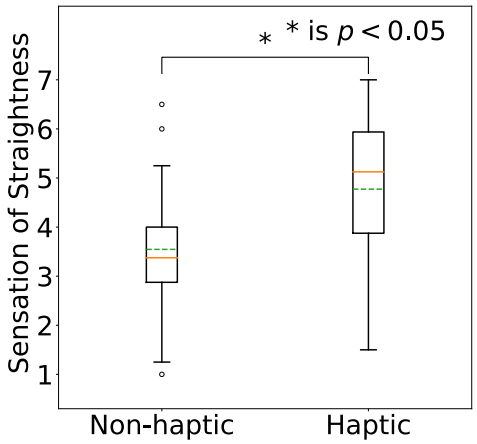

Fig. 7.16: A box plot of straightness sensation according to the questionnaire scores under the non-haptic and haptic conditions, where orange lines indicate the median and the green dashed lines indicate the mean.

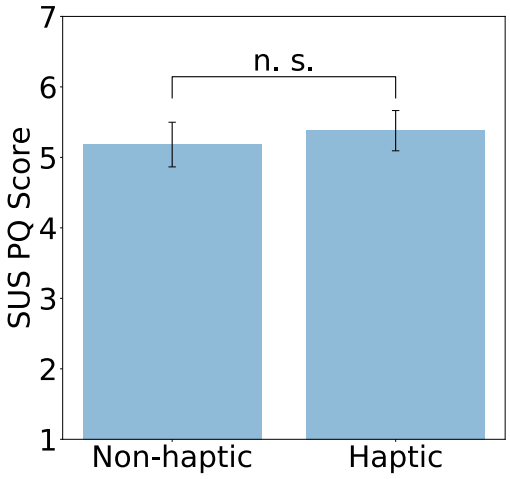

Fig. 7.17: Mean SUS PQ scores, where the error bars indicate the SE.

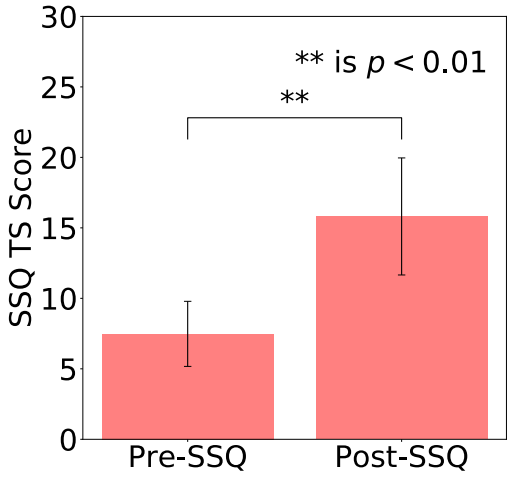

Fig. 7.18: Mean SSQ TS scores, where the error bars indicate the SE.

7.2.8 Contribution, Benefits, Limitations

The main contribution of the Unlimited Corridor is that it can produce large virtual worlds with infinite spaces, without the use of resetting. The study achieved the following: (1) proposal and implementation of a method to improve the effect of redirection using visuo-haptic interaction; (2) proposal and implementation of one-to-many mapping system without unnatural operation such as resetting; and (3) verification to demonstrate the effectiveness of visuo-haptic redirection through a user study.

Our approach also exhibits certain limitations. First, a user needs to touch handrails or walls during the VR experience, which limits the contents of VR. This problem can be addressed to a certain extent by increasing the types of haptic stimuli. For example, users with guided leads can be presented with content to walk a dog, or users with guided objects can be presented with tasks to carry luggage. Second, the shape of the path in the VE is limited to the shape of a ladder. As one solution to this problem, by arranging two central passages as a cross, users can explore a grid-like walking route. It is also possible to walk around with more range by removing the central linear handrail and using the safe walking zone technique [167]. It is possible to change the virtual paths within a certain range by using translation, rotation, and bending gains [74]. Furthermore, by using dynamic props such as those used in TurkDeck [168] and VRHapticDrones [118], it may be possible to present more flexible VEs. Third, this system can only be experienced by one user. As a solution to this problem, by using a blocking algorithm similar to that used in train operation, it can be expanded to multiple users.

7.3 Workshop on VR Exhibition

7.3.1 Background

We have been exhibiting Unlimited Corridor, a VR work that uses space perception manipulation technology, since 2016. This work applies visuo-haptic interaction,

Fig. 7.19: Overview of workshop

in which haptic and proprioceptive sensations are altered through vision, and RDW allows to walk through a vast virtual environment in a narrow real space. Specifically, the users hold onto a circular handrail while walking, but they feel that they are walking along a straight line and holding a straight handrail.

This work has been exhibited at academic conferences, science museums, and art exhibitions in Japan and abroad. Through these exhibitions, the challenges of VR exhibitions unique to museums, which are different from those at academic conferences and science museums, have become apparent. Therefore, we held a review meeting with the developers, museum staff, and visitors to verify the operation of the VR exhibition in a museum (see Figure 7.19).

7.3.2 Participants and Logistics

Four participants, one developer (university lecturer), two museum staff members (curator and staff leader), and one user (journalist) participated in this workshop.

We used the following items in the workshop: imitation vellum, post-its, colored marker pens, computer, lecture slides, text and images from SNS related to the work, and questionnaires.

7.3.3 Workshop Flow

The first part of the workshop was "Good & New," in which participants introduced themselves and shared what they had learned in the past 24 hours. After the ice break, a slide presentation on VR work Unlimited Corridor was presented. Inspired by the photographic reminiscence method, the participants recalled the exhibition by looking at the text and images posted on social networking sites about their experience with the Unlimited Corridor. Next, using the Keep–Problem–Try (KPT) method, which is a typical method applied in retrospective meetings, we orderly wrote down the good things, problems, and trials related to the operation of the VR exhibition and organized them on a piece of paper.

7.3.4 Insights

This workshop brought together people associated with the VR work, namely, curators, attendants, participants, and developers, to discuss the operation and experience of VR media art. After applying the KPT method (see Figure 7.20), we identified the strengths and challenges of VR exhibitions in museums. The strengths of the VR work are that it improved the appearance of the exhibition hall and attracted a new demography of visitors, including young people and children. Except for unexpected problems, the exhibition can be operated by the museum staff by referring to the manual. On the other hand, we found that the challenges of VR exhibitions in museums can be divided into technical, staff, and user layers. One

Fig. 7.20: Deliverable of the KPT method

challenge in the technical layer is the difficulty to predict problems in advance because the technology has not been fully developed. To solve this problem, we should update the manual in cooperation with the developers and attendant staff, particularly regarding early operation. In the staff layer, the burden of troubleshooting is unevenly distributed among the members. Measures to address this challenge include VR equipment, simpler operation, and more technical staff available. In the user layer, we discussed the measures to be taken for various participants such as children, the elderly, and the physically challenged to experience this work. For children, from the perspective of neuroscience, there is no problem with elementary school students and older experiencing VR works, but from the perspective of equipment and safety, we limited it to junior high school students and older. As for the

elderly, those who were able to walk independently were allowed to experience, but due to the risk of falling, the staff walked next to them. Lastly, for the physically-challenged, it was discussed that the staff should support them in moving their wheelchairs. We also found that many visitors, particularly the older ones, were hesitant to experience VR wearing an HMD while the other visitors were watching them. To address this challenge, it was proposed that the attendant staff should promote participation in the VR experience by actively talking with the visitors or demonstrating the experience of the staff.

7.3.5 Discussion

Throughout the workshop, we found that the photographic reminiscence using photographs and texts on SNS is an effective method of reflection. In addition, the KPT method, which was conducted in the last half of the session, allowed to organize the experiences recalled through the photographic reminiscence into good things and problems, and consider improvements to the experience and their implementation.

Although the theme of this session was relatively narrowed down to the operations related to the VR exhibition, the discussion resulted more open-ended than we expected. Topics ranging from VR equipment to the psychology of the participants and the issues involved in holding media art exhibitions at regional museums were exposed.

7.4 Conclusion

In this chapter, we introduce and evaluated visuo-haptic RDW. Visuo-haptic RDW is a method to improve the effectiveness of RDW by manipulating the user's proprioceptive sensation by generating visuo-haptic interaction with haptic cues. The experimental results suggest that the use of haptic cues improves the effectiveness of curvature manipulation in virtual environments. Then, we made the Unlimited Corridor, which enables to create large virtual environments in a relatively small real space without interrupting the experience or reorienting the user.

This is achieved by leveraging visuo-haptic interactions for improved RDW. We exhibited the Unlimited Corridor in museums and conducted a workshop to investigate the operational challenges of this VR exhibition. The workshop provided insights into the challenges to the technology, staff, and users regarding VR exhibitions in museums.

Chapter 8

Discussion

This chapter discusses the contributions of this work by summarizing the findings stated in Chapters 3–7. Then, we discuss the limitations of the study and the promising areas for future research in the field of RDW.

8.1 Contribution

There are two problems in realizing RDW to explore an arbitrary VR space at the room scale while maintaining a natural gait. The first is that the perceptual threshold varies significantly among individuals, and the second is that RDW is not sufficiently effective. In this study, we developed methods for estimating perceptual thresholds based on sensory characteristics and sensory-motor coupling to address the first problem and multimodal RDW methods based on sensory characteristics and sensory integration theory to address the second problem.

Chapter 3 examined the relationship between sensory characteristics and the perceptual threshold of RDW. If the relationship between the sensory characteristics of individuals and perceptual threshold of RDW is known, the effect of RDW can be predicted using questionnaires in advance and the appropriate amount of RDW manipulation can be determined. Adolescent/Adult Sensory Profile (AASP) was used as an index to examine personal characteristics. Experimental results showed that participants with high sensitization had low perceptual thresholds, i.e., they were more likely to notice RDW manipulation. Thus, the amount of RDW manipulation can be adjusted in advance according to the neurological thresholds of each participant based on the sensory profile.

In **Chapter 4**, we attempted to estimate RDW thresholds using physiological

indices (pupil diameter and microsaccades) and behavioral indices (walking speed and head sway). There was no significant correlation between the physiological indices and curvature RDW threshold. However, there was a significant correlation between the behavioral indices and curvature RDW threshold. Although the estimation method that uses behavioral indices is less reliable than the conventional 2AFC method, it provides the advantages that it is not affected by bias in the responses to the questionnaire and it can estimate the threshold online. Thus, the real-time estimation of the RDW threshold using the behavioral indices would make it possible to adjust the amount of RDW manipulation during a VR experience and improve the effectiveness of RDW.

In **Chapter 5**, based on the MLE theory, we hypothesized that adding noise to vestibular sensation would reduce the reliability of the vestibular sensation and improve the effectiveness of RDW by relatively increasing the contribution of vision to spatial perception. The results suggested that nGVS weakly affected the perceptual threshold of curvature gain. In addition, the results of the sensory profile suggested that the effect of nGVS tended to be weaker for users with a higher tendency toward sensory sensitivity. This suggests that the appropriate type of RDW manipulation should be determined according to the sensory characteristics of each user.

In **Chapter 6**, first, we investigated whether MLE could be applied to incongruent visual-auditory integration in a VR environment to explore the possibility of the visual-auditory RDW that effectively uses the auditory sense. Then, we proposed a novel method that introduced visual noise and incongruence between the visual and auditory cues of an object in a VR environment while applying curvature manipulation and verified the effectiveness of this method by comparing it with existing methods. The results showed that the effectiveness of curvature manipulation was improved when users were presented with the incongruent visual-auditory target object. The proposed method limits the range of content that can be presented because it requires a target to move in front of a user while emitting visual and auditory cues. Therefore, it is necessary to consider a highly versatile method that uses environmental sounds.

In **Chapter 7**, we introduced and evaluated visuo-haptic RDW. Visuo-haptic RDW is a method of improving the effectiveness of RDW by manipulating a user's proprioceptive sensation by generating visuo-haptic interaction with haptic cues. Our results suggested that the use of haptic cues improved the effectiveness of curvature manipulation in VEs. We created an RDW demonstration, i.e., Unlimited Corridor, which enabled a user to walk through a large VE in a relatively small tracking space without user interruption or the reorientation phase using visuo-haptic interaction to enhance the effect of RDW. We demonstrated Unlimited Corridor in museums and conducted workshops to investigate the operational challenges of VR exhibitions. The workshop provided insights into the challenges of VR exhibitions and their solutions.

We can summarize the above-mentioned results as follows:

- There is the relationship between sensory characteristics, the perceptual threshold, and optimal sensory modalities in RDW.
- There is the relationship between the behavioral indices and the perceptual threshold of RDW.
- Spatial perception can be manipulated by sensory addition and subtraction based on the sensory integration model.

First, in Chapter 3, the relationship between sensory characteristics and the optimal sensory modality and operation volume in RDW showed that the participants with a higher propensity for sensory sensitivity and sensory avoidance were more likely to notice the RDW techniques. In Chapter 5, it was shown that the effect of nGVS tended to be weaker for users with a higher tendency toward sensory sensitivity. This indicates that sensory sensitivity, among other perceptual characteristics, influences the type and amount of sensory stimuli in RDW. Sensory sensitivity has been linked to the autism spectrum disorder [108, 109], and it is considered to result from the functional features of the parasympathetic nervous system and central nervous system [169]. As the central nervous system is involved in spatial perception, it is expected that the correlation will be higher in participants whose sensory

sensitivity originates from the central nervous system. We may be able to clarify the relationship between neurophysiological mechanisms and responses by examining the responses and brain activity during RDW using various brain function measurements.

Next, in Chapter 4, the relationship between the behavioral indices and the perceptual threshold of RDW showed that there was a significant correlation between the estimated perceptual threshold of RDW, the mean of walking speed, and the standard deviation of head sway. In Chapter 7, it was observed that the tendency of head sway was consistent with the tendency of subjective curvature. These results indicate that the behavioral indices, particularly head sway, correspond to the subjective sense of direction under RDW. The evaluation of RDW effects using the behavioral indices provides several advantages over conventional psychophysical estimation methods. The first is real-time estimation. Psychophysical estimation methods require participants to answer questions after a certain period of an RDW experience. In contrast, the behavioral indices can be obtained during an RDW experience. Even when dynamic gain is used instead of fixed gain, the behavioral indices can provide information with higher temporal resolution. However, time delays must be considered. Second, there is no bias in the responses. In the two-alternative-forced-choice method, which is a typical psychophysical estimation method used to evaluate RDW, a user must select one of two options to respond. However, it is possible that the user will select a specific answer when he or she is confused about the options. As arbitrary judgments by participants do not affect the behavioral indices, bias is unlikely to occur. Third, the participants' experience is not interrupted. The threshold estimation method that uses questionnaires requires the interruption of the VR experience, which may reduce the sense of presence. In contrast, the behavioral indices can estimate the subjective perception of participants without interrupting the VR experience. Therefore, the behavioral indices are expected to be particularly useful for entertainment and training applications.

Last, with regard to the finding that spatial perception was manipulated by sensory addition and subtraction based on the sensory integration model, in Chapter 5,

we showed that the subtraction of vestibular sensation using nGVS led to relative visual dominance and improved the effect of RDW. In Chapter 6, we confirmed that audiovisual integration occurred on the basis of the MLE model while walking in a VR environment and then improved the effect of RDW by adding auditory stimuli. In addition, Chapter 7 showed that the use of haptic stimuli reduced subjective curvature and improved the effectiveness of RDW.

The experimental results described in Chapters 5–7 are consistent with each other and support the hypothesis that the effects of spatial perception manipulation can be modified by sensory addition and subtraction based on the sensory integration model. In addition, as shown in Figure 8.1, each multimodal RDW technique can be mapped in terms of the applicable scale and contextual constraints. In general, high-context techniques can be more effective; however, they are less versatile. In contrast, even though low-context techniques are less effective than high-context techniques, they can be applied to various environments. Among the methods proposed in this dissertation, visuo-haptic RDW is a high-context method. However, it has the potential to present a certain level of walking experience even in a room-scale real space. Auditory RDW is a moderate-context method, and it can be applied to a VR space ranging from the room scale to a few tens of meters, where sounds can be heard. In addition, nGVS RDW is a low-context method, and it can be used in VR spaces with sizes ranging from the room scale to unlimited size.

Next, we discuss this study in relation to the sensory-motor couplingFigure 8.2 shows the relationship between this study and the motor control system. In Chapter 3, we discussed the characteristics of sensory processing from a sensory input to behavior. In the motor control model, sensory sensitivity is considered to be a large difference between the desired state and the estimated actual state constructed by a sensory input, or an excessive reaction to the difference. For example, in RDW, there is a difference between the desired state, which consists of an attempt to walk in a straight line in a VR space, and the estimated actual state, which consists of the vestibular and somatosensory feedback that the person is actually walking on a curved line. People with high sensory sensitivity tend to notice RDW because

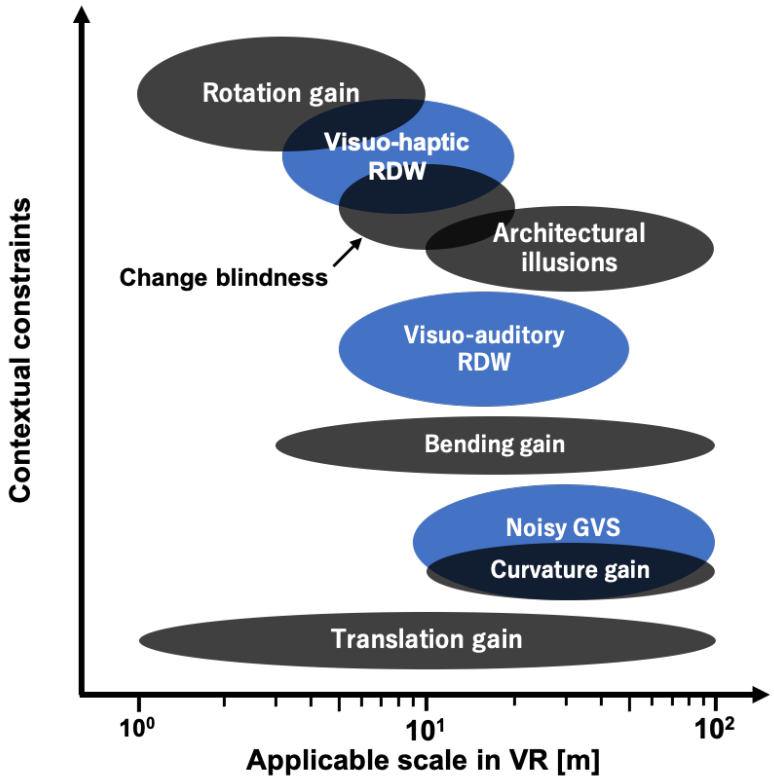

Fig. 8.1: Mapped redirection techniques in terms of contextual constraints and applicable scale.

this circuit is common. In Chapter 4, we discussed the relationship between the behavioral indices and RDW, and In Chapter 7, we also found a relationship between the behavioral indices and the subjective curvature RDW threshold. The difference between the desired state and estimated actual state caused by RDW is fed back to the controllers. It is considered that this feedback reflects a user's internal state of RDW to movement via motor commands.

In Chapter 5–7, we discussed multisensory stimulation and RDW using the sensory integration theory. It is considered that sensory integration is related to sensory feedback to estimate the actual state in behavioral control models. It can be interpreted that the sensory integration of multisensory stimuli can improve the effect of RDW by bringing the estimated actual state closer to the desired state.

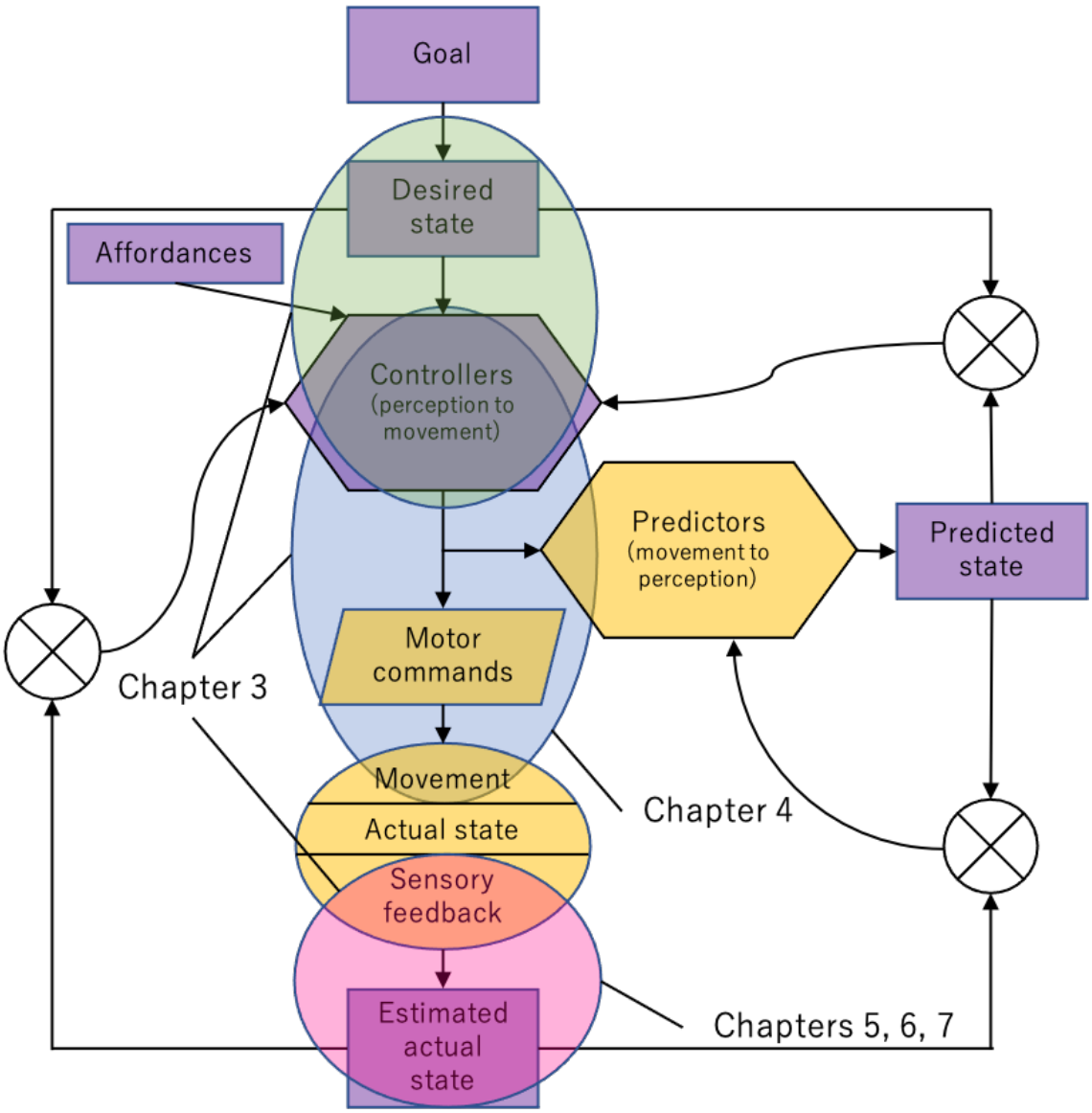

Fig. 8.2: Relationship between the research objects in this dissertation and the motor control system based on Frith et al [41] and Blakemore et al [42]

If we consider RDW based on the behavioral control system, it is possible to improve the effectiveness of RDW using approaches other than the proposed method. One approach is to make the predicted state and estimated actual state closer. The predicted state is constructed using predictors, which receive input from controllers. The feedback is the error between the estimated actual state and predicted state.

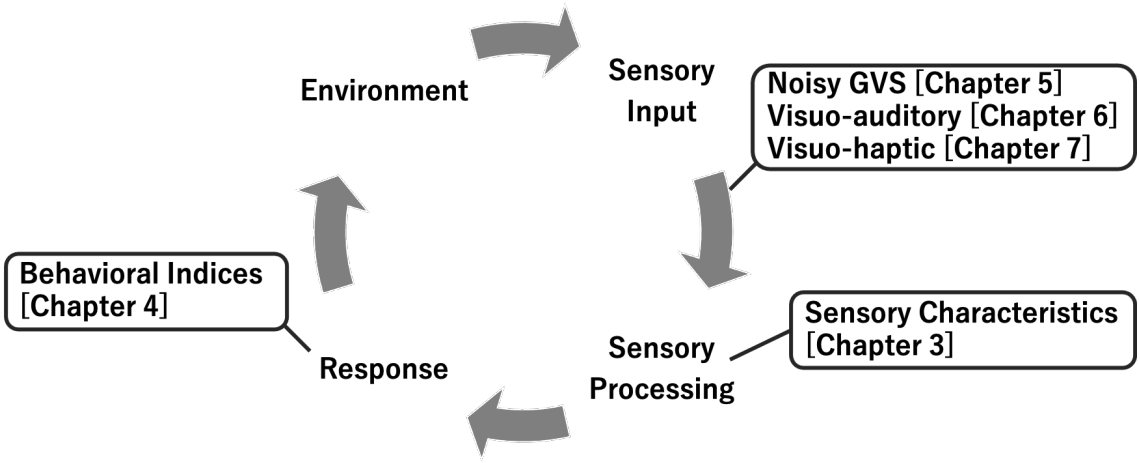

Fig. 8.3: Relationship between the research objects in this dissertation and the system that performs multimodal RDW by optimizing the type and amount of stimuli according to the sensory characteristics and behavioral responses.

The internal model of predictors is updated based on feedback error learning [170]. Therefore, it is possible to improve the effectiveness of RDW by updating the internal model optimized for RDW through motion learning. Specifically, experiencing a certain RDW manipulation for a long period or gradually increasing the amount of RDW manipulation might extend the effect range of RDW. Experiments performed over multiple days with a constant RDW showed an increase in the RDW threshold [95, 171].

Therefore, the results obtained from this study can contribute not only to the field of VR but also to neuroscience and psychology. The correlation of sensory characteristics with the perceptual thresholds of RDWs and the effects of specific sensory manipulations may be applicable to interactions with neurodiverse people. Conversely, it might be possible to explore neurological diversity by measuring the effects of sensory manipulation techniques such as RDW.

8.2 Limitation

As mentioned in section 8.1, the contributions of this study are as follows: (1) the relationship between sensory characteristics, optimal sensory modalities, and manipulation volume in RDW is determined; (2) the relationship between the behavioral indices and the perceptual threshold of RDW is determined; (3) spatial perception can be manipulated by sensory addition and subtraction based on the sensory integration model. By integrating these findings, we can realize a system that performs multimodal RDW by optimizing the type and amount of stimuli according to the sensory characteristics of users and behavioral responses (see Figure 8.3). However, there are a few problems in realizing this system. In Chapters 3 and 5, we found correlations between the effects of the threshold, stimulus type, and sensory characteristics. However, we did not investigate the causal relationships. In addition, individual differences are too large to estimate thresholds from sensory characteristics. Furthermore, there are large errors in the estimation of thresholds using the behavioral indices, as compared with conventional psychophysical estimation methods. A possible solution to this problem is to combine the estimation of sensory characteristics and behavioral indices with the Likert questionnaire on subjective curvature proposed in Chapter 4. The Likert questionnaire shows extremely high correlations with the values obtained by conventional estimation methods, even if the estimates are based on only a few trials. Therefore, after starting the RDW experience, the threshold of RDW can be estimated by conducting Likert questionnaires several times, and then the threshold can be updated by behavioral indices.

With respect to the finding that spatial perception can be manipulated by sensory addition and subtraction based on the sensory integration model, additive methods are content constrained and subtractive methods are not highly effective. This problem can be solved by developing an effective RDW method for various types of content by applying an additive method for vestibular sensation and a subtractive method for somatosensory sensation in addition to the proposed method. Foot sensation is considered to be important in posture control and walking [172–174].

Therefore, a method of manipulating the somatosensory system by physically or electrically stimulating the sole of the foot may be effective.

In addition to perceptual thresholds, we assessed individual cybersickness. However, there was no correlation between cybersickness and the perceptual characteristics or behavioral indices. This is interesting because cybersickness and the RDW threshold are related to the inconsistency between senses. The reason for no correlation may be that different neural systems are involved in the perceptual threshold and cybersickness.

In the context of cybersickness, aftereffects should also be considered. For example, users could experience problems such as not being able to drive after RDW. A previous work showed that cybersickness occurred immediately after an RDW experience but eased ten minutes after RDW [175]. Therefore, cybersickness could be resolved by taking a short break after an RDW experience. Aftereffects, such as the effect of RDW on the sense of direction, should be examined in future.

In addition, even though this is not the scope of this study, the effects of developmental differences on individual differences in sensation must be considered. Specifically, the issue of whether children and the elderly can experience RDW, which was also discussed in the workshop in Chapter 7, should be examined. There are limited studies on VR use by children. According to the report of Children and Virtual Reality[1], a 20 min VR experience for children aged 8–12 years might affect the binocular vision system of a few children and adversely affect their sense of balance. In addition, there is a concern that RDW may adversely affect the development of the nervous system because different stimuli are applied to the senses. However, according to Scammon's developmental curve, almost 100% of the nervous system completes development by the age of 12 years [176]. Thus, there should be no significant problem in terms of nervous system development. Most HMD devices that allow for RDW are intended for the ages of 12[2] or 13[3] years and above. Therefore, the age at which children can experience RDW should be the minimum age for

[1]http://childrenvr.org/
[2]https://www.playstation.com/en-us/legal/health-warning/
[3]https://www.oculus.com/safety-center/

which devices are designed. The use of RDW by the elderly was studied by Janeh et al [6]. They showed that there was no difference in presence or VR sickness between younger and older adults during RDW experiences. However, in the pace and phase domains, older adults walked in an extremely similar manner in the real world and VE. This was not observed in the case of younger adults. Therefore, elderly people with no problems in the walking function should not experience issues in the use of RDW. Children and the elderly must be supervised by family members and staff to prevent accidents during an RDW experience.

8.3 Future Work

This work proposed estimation methods for RDW and multimodal RDW based on sensory characteristics and sensory-motor coupling and evaluated these methods using psychophysical experiments and behavioral indices. However, the overall goal of RDW research is to present a general solution to allow for unconstrained natural walking in any VR space. The following approaches might contribute to further progress in this field:

- Online optimization: The findings presented in Chapters 3–7 can be integrated to provide the online estimates of the effects of RDW and achieve RDW with the optimal type and amount of sensory manipulation for individuals. For example, nGVS can be used to apply a larger amount of manipulation for users whose sensory characteristics suggest that nGVS is likely to improve the effectiveness of RDW. In contrast, other methods such as visuo-auditory RDW can be used instead of nGVS for users for whom nGVS is not likely to be effective. Furthermore, the online acquisition of behavioral indices under RDW manipulation would enable the dynamic optimization of the stimulus type the and amount of manipulation. This method is expected to be used in the process where the interaction between movement and the environment is fed back to sensations, which is not included in the cybernetic loop in this study.

- Habituation to RDW: A previous study reported that prolonged experience with curvature manipulation, which is a type of RDW, expanded the threshold for curvature manipulation [95]. This indicates that habituation to RDW may expand the perceptual threshold and enable a larger amount of manipulation to be applied to a user. A constant manipulation gain is applied in most conventional RDW techniques. According to the findings of adaptation in neurophysiology [177], by gradually increasing the manipulation gain (e.g., walking along a clothoid curve in curvature manipulation), users may become accustomed to the RDW technique and expand their perceptual detection threshold.

- Stimulation of the nervous system: The stimulation of the nervous system, particularly electromagnetic stimulation, is a promising approach because it can directly intervene in the sensory system. This might help resolve the inconsistencies between senses such as vision, vestibular, and proprioception. A previous study proposed the use of transcranial direct-current stimulation (tDCS) for RDW [94] and reported that tDCS did not improve the effect of RDW. However, our experiment suggests that nGVS may improve the effect of RDW (Chapter5). Therefore, it is quite possible that the effect of RDW can be improved by electromagnetic stimulation.

Figure 8.4 shows the correspondence between the future research targets and the research target discussed in this dissertation, i.e., the cybernetic loop. The cybernetic loop is expected to be completed, and improved RDW is expected to be realized through online optimization, which is one of the future research targets.

Therefore, it is expected that the methods discussed in this dissertation will further improve the VR experience. A few of the most interesting applications of these methods are as follows:

- Entertainment and training: RDW, particularly multimodal RDW such as visuo-haptic RDW (Chapter 7), is ideal for location-based VR experiences. The real-time estimation along with the proposed behavioral indices can be

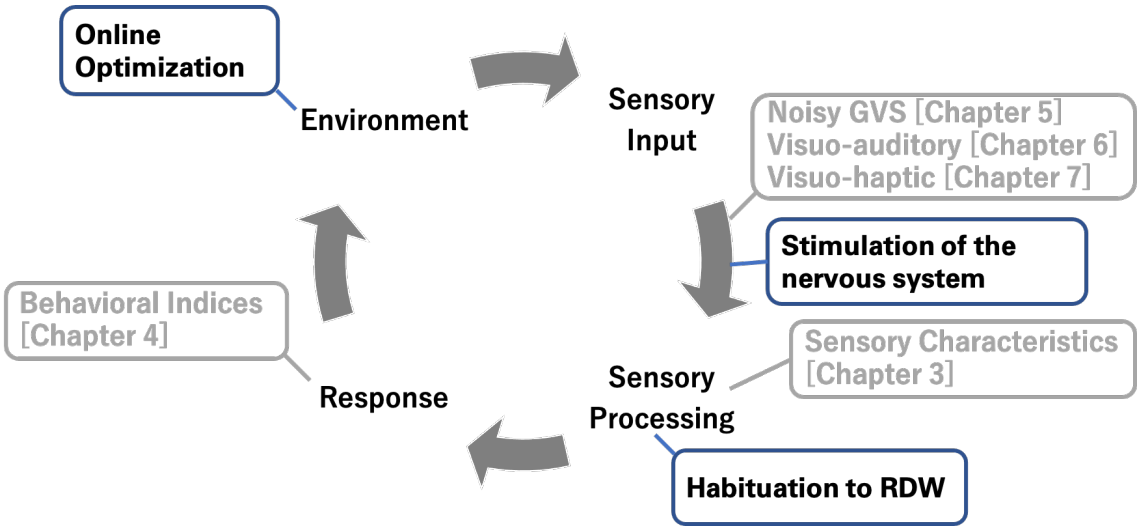

Fig. 8.4: Relationship between the future research targets and the cybernetic loop

used to apply optimal RDW to VR experiences where presence is important, such as haunted houses, safety education, and hazard simulations.

- Psychological and physiological investigation: RDW has the potential to be used for investigating sensory characteristics and sensory-motor coupling. In particular, as the proposed multimodal RDW can present different stimuli between senses, it will be possible to experiment with a wider range of sensory integration compared to previous studies. In addition, the participants' responses to RDW are expected to be useful in elucidating sensory-motor coupling.

- Exercise and rehabilitation: The proposed methods are expected to be used for exercise and gait rehabilitation. Regarding exercise, it is possible to optimize the type and intensity of exercise according to the perceptual load and motor load by applying the proposed evaluation method of RDW using the behavioral indices. Furthermore, the multisensory presentation method used in Chapters 5–7 is expected to improve the effectiveness of rehabilitation for people with sensory and motor impairments.

Chapter 9

Conclusion

In this dissertation, to explore an arbitrary virtual reality (VR) space in a real space of room-scale size while maintaining a natural gait, redirected walking (RDW) techniques are investigated, developed, and evaluated on the basis of the perceptual characteristics and sensory-motor coupling.

In Chapter 2, perception theory and research related to RDW are presented. Moreover we introduce spatial abilities, perception models, and psychophysics. Furthermore, we also discuss a wide range of RDW-related topics, from elemental technologies to control algorithms.

In Chapter 3, we test the hypothesis that there is an association between neurological features, the RDW threshold, and cybersickness. We use Dunn's sensory processing model to evaluate neurological thresholds, behavioral responses, and self-regulation. We also describe a psychophysical experiment in which participants' detection thresholds for curvature gain were estimated. The results suggest that participants with a low sensory threshold tend to notice RDW techniques.

In Chapter 4, the relationship between perceptual thresholds and physiological and behavioral indices is explored. The results suggest that there is an association between the behavioral indices and perceptual threshold; however, use of behavioral indices is less reliable than conventional methods because of large individual differences in the behavioral indices. In contrast, for some manipulations that are difficult to measure with conventional questionnaires, such as continuous changes in gain, use of the behavioral index has significant advantages. Therefore, one should integrate the questionnaire and the behavioral indices to estimate perceptual threshold online.

In Chapter 5, we review the theory that perception is the application of maximum likelihood estimation (MLE) to sensory input data. On this basis, we hypothesize

that reducing the reliability of a vestibular sensation will increase the efficacy of RDW and minimize cybersickness. Noisy galvanic vestibular stimulation (nGVS) is chosen as the means to reduce vestibular sensation reliability. The findings indicate that nGVS may influence the detection thresholds for curvature gain.

Chapter 6 discusses a method to improve the effectiveness of an RDW using auditory stimuli based on the principle of maximum likelihood estimation. We also propose a novel method introducing visual noise and incongruence between visual and auditory cues regarding an object in VR when applying curvature gain. The effectiveness of this method was confirmed by comparing it with existing methods.

In Chapter 7, we explore the possibility of RDW that effectively using the haptic sense. The experimental results suggest that the use of haptic cues improved the effectiveness of curvature manipulation. Then, we propose an RDW demonstration, i.e., Unlimited Corridor, using visuo-haptic RDW. We also held a workshop to investigate the operational challenges of this RDW demonstration.

Chapter 8 summarizes the contributions made in Chapters 3–7, and discusses the limitations and future prospects of the method proposed in this paper. We also discuss the relationship between the sensory-motor coupling and the proposed methods.

In summary, this dissertation examines the relationships among RDW, perceptual characteristics, and sensory-motor coupling; it also contains proposals for novel multimodal RDW methods. Our findings highlight the importance of personalizing the type and intensity of stimuli in the design of virtual experiences, depending on individual perceptual characteristics.

Based on this study's findings, a user-friendly RDW technique with stimulus types and stimulus amounts optimized for each individual will be realized in the near future. These findings are expected to be applied to not only the RDW field but also neurophysiological studies and rehabilitation of people with sensory and motor impairments.

References

[1] Ivan E Sutherland. The ultimate display. *Multimedia: From Wagner to virtual reality*, Vol. 1, , 1965.

[2] Mel Slater, Martin Usoh, and Anthony Steed. Taking steps: the influence of a walking technique on presence in virtual reality. *ACM Transactions on Computer-Human Interaction (TOCHI)*, Vol. 2, No. 3, pp. 201–219, 1995.

[3] Rudolph P Darken, William R Cockayne, and David Carmein. The omni-directional treadmill: a locomotion device for virtual worlds. In *Proceedings of the 10th annual ACM symposium on User interface software and technology*, pp. 213–221, 1997.

[4] Martin Usoh, Kevin Arthur, Mary C. Whitton, Rui Bastos, Anthony Steed, Mel Slater, and Frederick P. Brooks. Walking >walking-in-place >flying, in virtual environments. In *Proceedings of the 26th Annual Conference on Computer Graphics and Interactive Techniques*, SIGGRAPH '99, p. 359–364, USA, 1999. ACM Press/Addison-Wesley Publishing Co.

[5] Sharif Razzaque, Zachariah Kohn, and Mary C Whitton. Redirected Walking. In *Proceedings of EUROGRAPHICS*, pp. 289–294, 2001.

[6] Omar Janeh, Gerd Bruder, Frank Steinicke, Alessandro Gulberti, and Monika Poetter-Nerger. Analyses of Gait Parameters of Younger and Older Adults during (Non-)Isometric Virtual Walking. Technical Report 10, 2018.

[7] Omar Janeh, Eike Langbehn, Frank Steinicke, Gerd Bruder, Alessandro Gulberti, and Monika Poetter-Nerger. Walking in Virtual Reality. *ACM Transactions on Applied Perception*, Vol. 14, No. 2, pp. 1–15, 2017.

[8] Niels Christian Nilsson, Tabitha Peck, Gerd Bruder, Eri Hodgson, Stefania Serafin, Mary Whitton, Frank Steinicke, and Evan Suma Rosenberg. 15 years of research on redirected walking in immersive virtual environments. *IEEE computer graphics and applications*, Vol. 38, No. 2, pp. 44–56, 2018.

[9] F. Steinicke, G. Bruder, J. Jerald, H. Frenz, and M. Lappe. Estimation of detection thresholds for redirected walking techniques. *IEEE Transactions on Visualization and Computer Graphics*, Vol. 16, No. 1, pp. 17–27, Jan 2010.

[10] Timofey Grechkin, Jerald Thomas, Mahdi Azmandian, Mark Bolas, and Evan Suma. Revisiting detection thresholds for redirected walking. *Proceedings of the ACM Symposium on Applied Perception - SAP '16*, pp. 113–120, 2016.

[11] Michael Rietzler, Jan Gugenheimer, Teresa Hirzle, Martin Deubzer, Eike Langbehn, and Enrico Rukzio. Rethinking Redirected Walking: On the Use of Curvature Gains beyond Perceptual Limitations and Revisiting Bending Gains. *Proceedings of the 2018 IEEE International Symposium on Mixed and Augmented Reality, ISMAR 2018*, No. October, pp. 115–122, 2019.

[12] Russell L DeValois and Karen K DeValois. *Spatial vision*, Vol. 14. Oxford university press, 1990.

[13] Robert Sekuler, Scott NJ Watamaniuk, and Randolph Blake. Motion perception. *Stevens' Handbook of Experimental Psychology*, 2002.

[14] Hermann von Helmholtz. *Treatise on physiological optics*, Vol. 3. Courier Corporation, 2013.

[15] Michael N Geuss, Jeanine K Stefanucci, Sarah H Creem-Regehr, and William B Thompson. Effect of viewing plane on perceived distances in real and virtual environments. *Journal of Experimental Psychology: Human Perception and Performance*, Vol. 38, No. 5, p. 1242, 2012.

[16] Etienne Peillard, Thomas Thebaud, Jean-Marie Norrnand, Ferran Argelaguet, Guillaume Moreau, and Anatole Lécuyer. Virtual objects look farther on the sides: The anisotropy of distance perception in virtual reality. In *2019 IEEE Conference on Virtual Reality and 3D User Interfaces (VR)*, pp. 227–236. IEEE, 2019.

[17] Helen E Ross and Cornelis Plug. The history of size constancy and size illusions. 1998.

[18] Lloyd Kaufman and James H Kaufman. Explaining the moon illusion. *Proceedings of the National Academy of Sciences*, Vol. 97, No. 1, pp. 500–505, 2000.

[19] Heiner Deubel, Werner X Schneider, and Ingo Paprotta. Selective dorsal and ventral processing: Evidence for a common attentional mechanism in reaching and perception. *Visual cognition*, Vol. 5, No. 1-2, pp. 81–107, 1998.

[20] Allen William Mills. On the minimum audible angle. *The Journal of the Acoustical Society of America*, Vol. 30, No. 4, pp. 237–246, 1958.

[21] Brian Brown. Dynamic visual acuity, eye movements and peripheral acuity for moving targets. *Vision research*, Vol. 12, No. 2, pp. 305–321, 1972.

[22] Michiko Ohkura, Yasuyuki Yanagida, Taro Maeda, and Susumu Tachi. Measurement of auditory alleys in a virtual environment and their mathematical models. *Systems and Computers in Japan*, Vol. 31, No. 4, pp. 12–21, 2000.

[23] Gregory Hickok and David Poeppel. The cortical organization of speech processing. *Nature reviews neuroscience*, Vol. 8, No. 5, pp. 393–402, 2007.

[24] Uwe Proske and Simon C Gandevia. The proprioceptive senses: their roles in signaling body shape, body position and movement, and muscle force. *Physiological reviews*, Vol. 92, No. 4, pp. 1651–1697, 2012.

[25] Marc A Sommer and Robert H Wurtz. Brain circuits for the internal monitoring of movements. *Annu. Rev. Neurosci.*, Vol. 31, pp. 317–338, 2008.

[26] Roger Wolcott Sperry. Neural basis of the spontaneous optokinetic response produced by visual inversion. *Journal of comparative and physiological psychology*, Vol. 43, No. 6, p. 482, 1950.

[27] Sarah A Burnett, David M Lane, and Lewis M Dratt. Spatial visualization and sex differences in quantitative ability. *Intelligence*, Vol. 3, No. 4, pp. 345–354, 1979.

[28] Mark G McGee. Human spatial abilities: Psychometric studies and environmental, genetic, hormonal, and neurological influences. *Psychological bulletin*, Vol. 86, No. 5, p. 889, 1979.

[29] Marcia C Linn and Anne C Petersen. Emergence and characterization of sex differences in spatial ability: A meta-analysis. *Child development*, pp. 1479–1498, 1985.

[30] Irwin Silverman and Marion Eals. Sex differences in spatial abilities: Evolutionary theory and data. In *Portions of this paper were presented at the meetings of the International Society for Human Ethology in Binghamton, NY, Jun 1990, the Human Behavior and Evolution Society in Los Angeles, CA, Aug 1990, and the European Sociobiological Society in Prague, Czechoslovakia, Aug 1991.* Oxford University Press, 1992.

[31] Daniel Voyer, Susan Voyer, and M Philip Bryden. Magnitude of sex differences in spatial abilities: a meta-analysis and consideration of critical variables. *Psychological bulletin*, Vol. 117, No. 2, p. 250, 1995.

[32] Herman A Witkin and Solomon E Asch. Studies in space orientation. iv. further experiments on perception of the upright with displaced visual fields. *Journal of experimental psychology*, Vol. 38, No. 6, p. 762, 1948.

[33] Jean Piaget, Bärbel Inhelder, Frederick John LANGDON, and JL LUNZER. *La Représentation de L'espace Chez L'enfant. The Child's Conception of Space... Translated... by FJ Langdon & JL Lunzer. With Illustrations.* New York; Routledge & Kegan Paul: London; printed in Great Britain, 1956.

[34] Jack M Loomis, Joshua M Knapp, et al. Visual perception of egocentric distance in real and virtual environments. *Virtual and adaptive environments*, Vol. 11, pp. 21–46, 2003.

[35] Bob G Witmer and Paul B Kline. Judging perceived and traversed distance in virtual environments. *Presence*, Vol. 7, No. 2, pp. 144–167, 1998.

[36] Claudia Armbrüster, Marc Wolter, Torsten Kuhlen, Will Spijkers, and Bruno Fimm. Depth perception in virtual reality: distance estimations in peri-and extrapersonal space. *Cyberpsychology & Behavior*, Vol. 11, No. 1, pp. 9–15, 2008.

[37] Rebekka S Renner, Boris M Velichkovsky, and Jens R Helmert. The perception of egocentric distances in virtual environments-a review. *ACM Computing Surveys (CSUR)*, Vol. 46, No. 2, pp. 1–40, 2013.

[38] Roger N. Shepard and Jacqueline Metzler. Mental Rotation of 3D objects, 1971.

[39] Timothy A Salthouse, Renee L Babcock, Eric Skovronek, Debora RD Mitchell, and Roni Palmon. Age and experience effects in spatial visualization. *Developmental Psychology*, Vol. 26, No. 1, p. 128, 1990.

[40] Mary Hegarty, Anthony E Richardson, Daniel R Montello, Kristin Lovelace, and Ilavanil Subbiah. Development of a self-report measure of environmental spatial ability. *Intelligence*, Vol. 30, No. 5, pp. 425–447, 2002.

[41] Christopher D Frith, Sarah-Jayne Blakemore, and Daniel M Wolpert. Abnormalities in the awareness and control of action. *Philosophical Transactions of the Royal Society of London. Series B: Biological Sciences*, Vol. 355, No. 1404, pp. 1771–1788, 2000.

[42] Sarah-Jayne Blakemore, Daniel M Wolpert, and Christopher D Frith. Abnormalities in the awareness of action. *Trends in cognitive sciences*, Vol. 6, No. 6, pp. 237–242, 2002.

[43] Daniel M Wolpert and Zoubin Ghahramani. Computational principles of movement neuroscience. *Nature neuroscience*, Vol. 3, No. 11, pp. 1212–1217, 2000.

[44] Charles Spence. Crossmodal correspondences: A tutorial review. *Attention, Perception, & Psychophysics*, Vol. 73, No. 4, pp. 971–995, 2011.

[45] Barry E Stein and Terrence R Stanford. Multisensory integration: current issues from the perspective of the single neuron. *Nature reviews neuroscience*, Vol. 9, No. 4, pp. 255–266, 2008.

[46] Christophe Lalanne and Jean Lorenceau. Crossmodal integration for perception and action. *Journal of Physiology-Paris*, Vol. 98, No. 1-3, pp. 265–279, 2004.

[47] James Joseph Clark and Alan L Yuille. Data fusion for sensory information processing systems. 1990.

[48] Marc O. Ernst and Martin S. Banks. Humans integrate visual and haptic information in a statistically optimal fashion. *Nature*, Vol. 415, No. 6870, pp. 429–433, 2002.

[49] Marc O Ernst. A bayesian view on multimodal cue integration. *Human body perception from the inside out*, Vol. 131, pp. 105–131, 2006.

[50] David Alais and David Burr. The ventriloquist effect results from near-optimal bimodal integration. *Current biology*, Vol. 14, No. 3, pp. 257–262, 2004.

[51] Hannah B Helbig and Marc O Ernst. Optimal integration of shape information from vision and touch. *Experimental brain research*, Vol. 179, No. 4, pp. 595–606, 2007.

[52] Peter W. Battaglia, Robert A. Jacobs, and Richard N. Aslin. Bayesian integration of visual and auditory signals for spatial localization. *Journal of the Optical Society of America A*, Vol. 20, No. 7, p. 1391, 2003.

[53] Shinsuke Shimojo, Gerald H Silverman, and Ken Nakayama. Occlusion and the solution to the aperture problem for motion. *Vision research*, Vol. 29, No. 5, pp. 619–626, 1989.

[54] Yair Weiss, Eero P Simoncelli, and Edward H Adelson. Motion illusions as optimal percepts. *Nature neuroscience*, Vol. 5, No. 6, pp. 598–604, 2002.

[55] G A. GESCHEIDER, JM Thorpe, J Goodarz, and SJ Bolanowski. The effects of skin temperature on the detection and discrimination of tactile stimulation. *Somatosensory & motor research*, Vol. 14, No. 3, pp. 181–188, 1997.

[56] Ernst Heinrich Weber. *Anatomia comparata nervi sympathici, cum tabulis aeneis*. 1817.

[57] Selig Hecht. The visual discrimination of intensity and the weber-fechner law. *The Journal of general physiology*, Vol. 7, No. 2, p. 235, 1924.

[58] CJBJoP Spearman. The method of right and wrong cases (constant stimuli) without gauss's formulae. *British Journal of Psychology*, Vol. 2, No. 3, p. 227, 1908.

[59] Tom N Cornsweet. The staircase-method in psychophysics. *The American journal of psychology*, Vol. 75, No. 3, pp. 485–491, 1962.

[60] George A Gescheider. *Psychophysics: the fundamentals*. Psychology Press, 2013.

[61] Nicolaas Prins, et al. *Psychophysics: a practical introduction*. Academic Press, 2016.

[62] Eike Langbehn, Frank Steinicke, Markus Lappe, Gregory F. Welch, and Gerd Bruder. In the blink of an eye - Leveraging blink-induced suppression for imperceptible position and orientation redirection in virtual reality. *ACM Transactions on Graphics*, Vol. 37, No. 4, p. 11, 2018.

[63] Yoonhee Jang, John T Wixted, and David E Huber. Testing signal-detection models of yes/no and two-alternative forced-choice recognition memory. *Journal of Experimental Psychology: General*, Vol. 138, No. 2, p. 291, 2009.

[64] Robert B Welch and David H Warren. Immediate perceptual response to intersensory discrepancy. *Psychological bulletin*, Vol. 88, No. 3, p. 638, 1980.

[65] Alain Berthoz. *The brain's sense of movement*, Vol. 10. Harvard University Press, 2000.

[66] Gregg H Recanzone. Auditory influences on visual temporal rate perception. *Journal of neurophysiology*, Vol. 89, No. 2, pp. 1078–1093, 2003.

[67] Joseph J LaViola Jr. A discussion of cybersickness in virtual environments. *ACM Sigchi Bulletin*, Vol. 32, No. 1, pp. 47–56, 2000.

[68] Eugenia M Kolasinski. *Simulator sickness in virtual environments*, Vol. 1027. US Army Research Institute for the Behavioral and Social Sciences, 1995.

[69] Séamas Weech, Sophie Kenny, and Michael Barnett-Cowan. Presence and cybersickness in virtual reality are negatively related: a review. *Frontiers in psychology*, Vol. 10, p. 158, 2019.

[70] Robert S Kennedy, Norman E Lane, Kevin S Berbaum, and Michael G Lilienthal. Simulator Sickness Questionnaire: An Enhanced Method for Quantifying Simulator Sickness. *The International Journal of Aviation Psychology*, Vol. 3, No. 3, pp. 203–220, 1993.

[71] Niels Chr. Nilsson. *Walking Without Moving: An exploration of factors influencing the perceived naturalness of Walking-in-Place techniques for locomotion in virtual environments*. PhD thesis, 2015. Rolf Nordahl, Principal supervisor Stefania Serafin, Secondary supervisor.

[72] Evan A. Suma, Gerd Bruder, Frank Steinicke, David M. Krum, and Mark Bolas. A taxonomy for deploying redirection techniques in immersive virtual environments. *Proceedings - IEEE Virtual Reality*, pp. 43–46, 2012.

[73] Frank Steinicke, Gerd Bruder, Luv Kohli, Jason Jerald, and Klaus Hinrichs. Taxonomy and implementation of redirection techniques for ubiquitous passive haptic feedback. In *Proceedings of the 2008 International Conference on Cyberworlds, CW 2008*, pp. 217–223, 2008.

[74] E. Langbehn, P. Lubos, G. Bruder, and F. Steinicke. Bending the curve: Sensitivity to bending of curved paths and application in room-scale vr. *IEEE Transactions on Visualization and Computer Graphics*, Vol. 23, No. 4, pp. 1389–1398, 2017.

[75] Ayaka Nishi, Keisuke Hoshino, and Hiroyuki Kajimoto. Straightening walking path using redirected walking technique. In *ACM SIGGRAPH 2016 Posters*, pp. 1–2. 2016.

[76] Christopher You, Evan Suma Rosenberg, and Jerald Thomas. Strafing gain: A novel redirected walking technique. In *Symposium on Spatial User Interaction*, SUI '19, New York, NY, USA, 2019. Association for Computing Machinery.

[77] Evan A. Suma, Seth Clark, David Krum, Samantha Finkelstein, Mark Bolas, and Zachary Warte. Leveraging change blindness for redirection in virtual environments. In *Proceedings - IEEE Virtual Reality*, pp. 159–166, 2011.

[78] Khrystyna Vasylevska, Hannes Kaufmann, Mark Bolas, and Evan A. Suma. Flexible spaces: Dynamic layout generation for infinite walking in virtual environments. *IEEE Symposium on 3D User Interface 2013, 3DUI 2013 - Proceedings*, pp. 39–42, 2013.

[79] Betsy Williams, Gayathri Narasimham, Bjoern Rump, Timothy P. McNamara, Thomas H. Carr, John Rieser, and Bobby Bodenheimer. Exploring large virtual environments with an HMD when physical space is limited. *Proceedings of the 4th*

symposium on Applied perception in graphics and visualization - APGV '07, Vol. 1, No. 212, p. 41, 2007.

[80] Eric Hodgson, Eric Bachmann, and David Waller. Redirected walking to explore virtual environments: Assessing the potential for spatial interference. *ACM Transactions on Applied Perception*, Vol. 8, No. 4, pp. 1–22, 2011.

[81] Eric Hodgson and Eric Bachmann. Comparing four approaches to generalized redirected walking: Simulation and live user data. *IEEE Transactions on Visualization and Computer Graphics*, Vol. 19, No. 4, pp. 634–643, 2013.

[82] Michael A. Zmuda, Joshua L. Wonser, Eric R. Bachmann, and Eric Hodgson. Optimizing constrained-environment redirected walking instructions using search techniques. *IEEE Transactions on Visualization and Computer Graphics*, Vol. 19, No. 11, pp. 1872–1884, 2013.

[83] Thomas Nescher, Ying Yin Huang, and Andreas Kunz. Planning redirection techniques for optimal free walking experience using model predictive control. *IEEE Symposium on 3D User Interfaces 2014, 3DUI 2014 - Proceedings*, pp. 111–118, 2014.

[84] Dang Yang Lee, Yang Hun Cho, and In Kwan Lee. Real-time optimal planning for redirected walking using deep q-learning. *26th IEEE Conference on Virtual Reality and 3D User Interfaces, VR 2019 - Proceedings*, pp. 63–71, 2019.

[85] Yuchen Chang, Keigo Matsumoto, Takuji Narumi, Tomohiro Tanikawa, and Michitaka Hirose. Redirection controller using reinforcement learning. *arXiv preprint arXiv:1909.09505*, 2019.

[86] Ryan R Strauss, Raghuram Ramanujan, Andrew Becker, and Tabitha C Peck. A steering algorithm for redirected walking using reinforcement learning. *IEEE Transactions on Visualization and Computer Graphics*, Vol. 26, No. 5, pp. 1955–1963, 2020.

[87] Wataru Shibayama and Shinichi Shirakawa. Reinforcement learning-based redirection controller for efficient redirected walking in virtual maze environment. In *Computer Graphics International Conference*, pp. 33–45. Springer, 2020.

[88] Lucie Kruse, Eike Langbehn, and Frank Stelnlcke. I Can See on My Feet while Walking: Sensitivity to Translation Gains with Visible Feet. *25th IEEE Conference on Virtual Reality and 3D User Interfaces, VR 2018 - Proceedings*, pp. 305–312, 2018.

[89] Benjamin Bolte and Markus Lappe. Subliminal Reorientation and Repositioning in Immersive Virtual Environments using Saccadic Suppression. *IEEE Transactions on Visualization and Computer Graphics*, Vol. 21, No. 4, pp. 545–552, 2015.

[90] Christian T. Neth, Jan L. Souman, David Engel, Uwe Kloos, Heinrich H. Bülthoff, and Betty J. Mohler. Velocity-dependent dynamic curvature gain for redirected walking. *IEEE Transactions on Visualization and Computer Graphics*, Vol. 18, No. 7, pp. 1041–1052, 2012.

[91] Jingxin Zhang, Eike Langbehn, Dennis Krupke, Nicholas Katzakis, and Frank Steinicke. Detection thresholds for rotation and translation gains in 360 ° video-based telepresence systems. *IEEE Transactions on Visualization and Computer Graphics*, Vol. 24, No. 4, pp. 1671–1680, 2018.

[92] Niels Christian Nilsson, Evan Suma, Rolf Nordahl, Mark Bolas, and Stefania Serafin. Estimation of detection thresholds for audiovisual rotation gains. *Proceedings - IEEE Virtual Reality*, Vol. 2016-July, No. January, pp. 241–242, 2016.

[93] Florian Meyer, Malte Nogalski, and Wolfgang Fohl. Detection thresholds in audio-visual redirected walking. In *Proc. Sound and Music Comp. Conf.(SMC)*, Vol. 16, pp. 17–27, 2016.

[94] Eike Langbehn, Frank Steinicke, Ping Koo-Poeggel, Lisa Marshall, and Gerd Bruder. Stimulating the brain in vr: Effects of transcranial direct-current stimulation on redirected walking. In *ACM Symposium on Applied Perception 2019*, SAP '19, New York, NY, USA, 2019. Association for Computing Machinery.

[95] Luke Boelling, Niklas Stein, Frank Steinicke, and Markus Lappe. Shrinking Circles: Adaptation to Increased Curvature Gain in Redirected Walking. *IEEE Transactions on Visualization and Computer Graphics*, Vol. 2626, No. c, pp. 1–1, 2019.

[96] Nguyen Thi Anh Ngoc, Yannick Rothacher, Peter Brugger, Bigna Lenggenhager, and Andreas Kunz. Estimation of individual redirected walking thresholds using standard perception tests. *Proceedings of the ACM Symposium on Virtual Reality Software and Technology, VRST*, Vol. 02-04-November-2016, pp. 329–330, 2016.

[97] Courtney Hutton, Shelby Ziccardi, Julio Medina, and Evan Suma Rosenberg. Individualized calibration of rotation gain thresholds for redirected walking. In *ICAT-EGVE*, pp. 61–64, 2018.

[98] Patric Schmitz, Julian Hildebrandt, Andre Calero Valdez, Leif Kobbelt, and Martina Ziefle. You spin my head right round: Threshold of limited immersion for rotation gains in redirected walking. *IEEE Transactions on Visualization and Computer Graphics*, Vol. 24, No. 4, pp. 1623–1632, 2018.

[99] Yannick Rothacher, Anh Nguyen, Bigna Lenggenhager, Andreas Kunz, and Peter Brugger. Visual capture of gait during redirected walking. *Scientific Reports*, Vol. 8, No. 1, p. 17974, 2018.

[100] Eike Langbehn. *Walking in Virtual Reality: Perceptually-inspired Interaction Techniques for Locomotion in Immersive Environments*. PhD thesis, 2019.

[101] Stefania Serafin, Niels C. Nilsson, Erik Sikstrom, Amalia De Goetzen, and Rolf Nordahl. Estimation of detection thresholds for acoustic based redirected walking techniques. *Proceedings - IEEE Virtual Reality*, No. March, pp. 161–162, 2013.

[102] Tobias Feigl, Eliise Kõre, Christopher Mutschler, and Michael Philippsen. Acoustical manipulation for redirected walking. *Proceedings of the ACM Symposium on Virtual Reality Software and Technology, VRST*, Vol. Part F131944, , 2017.

[103] Luv Kohli, Eric Burns, Dorian Miller, and Henry Fuchs. Combining passive haptics with redirected walking. *ACM International Conference Proceeding Series*, Vol. 157, No. 4, pp. 253–254, 2005.

[104] Keigo Matsumoto, Yuki Ban, Takuji Narumi, Tomohiro Tanikawa, and Michitaka Hirose. Curvature manipulation techniques in redirection using haptic cues. In *2016 IEEE Symposium on 3D User Interfaces (3DUI)*, pp. 105–108. IEEE, 2016.

[105] Anh Nguyen, Yannick Rothacher, Bigna Lenggenhager, Peter Brugger, and Andreas Kunz. Individual differences and impact of gender on curvature redirection thresholds. In *Proceedings of the 15th ACM Symposium on Applied Perception - SAP '18*, Vol. 18, pp. 1–4. ACM, 2018.

[106] Amitta Shah and Uta Frith. Why do autistic individuals show superior performance on the block design task? *Journal of Child Psychology and Psychiatry*, Vol. 34, No. 8, pp. 1351–1364, 1993.

[107] M-J Caron, L Mottron, C Rainville, and S Chouinard. Do high functioning persons with autism present superior spatial abilities? *Neuropsychologia*, Vol. 42, No. 4, pp. 467–481, 2004.

[108] Winnie Dunn. The impact of sensory processing abilities on the daily lives of young children and their families: A conceptual model. *Infants and young children*, Vol. 9, pp. 23–35, 1997.

[109] Winnie Dunn. *Sensory profile: User's manual*. Psychological Corporation San Antonio, TX, 1999.

[110] Catana Brown and Winnie Dunn. *Adolescent/adult sensory profile*. Pearson San Antonio, TX:, 2002.

[111] Eric F Rieke and Diane Anderson. Adolescent/adult sensory profile and obsessive–compulsive disorder. *American Journal of Occupational Therapy*, Vol. 63, No. 2, pp. 138–145, 2009.

[112] 萩原拓, 岩永竜一郎, 伊藤大幸, 谷伊織. Aasp 青年・成人感覚プロファイル ユーザーマニュアル 日本文化科学社. 2015.

[113] T Schubert, F Friedmann, and H Regenbrecht. Igroup presence questionnaire, 2001.

[114] Bob G Witmer and Michael J Singer. Measuring presence in virtual environments: A presence questionnaire. *Presence*, Vol. 7, No. 3, pp. 225–240, 1998.

[115] Martin Usoh, Ernest Catena, Sima Arman, and Mel Slater. Using presence questionnaires in reality. *Presence: Teleoperators & Virtual Environments*, Vol. 9, No. 5, pp. 497–503, 2000.

[116] Valentin Schwind, Pascal Knierim, Nico Haas, and Niels Henze. Using presence questionnaires in virtual reality. In *Proceedings of the 2019 CHI Conference on Human Factors in Computing Systems*, pp. 1–12, 2019.

[117] Weiya Chen, Nicolas Ladevèze, Wei Hu, Shiqi Ou, and Patrick Bourdot. Comparison Between the Methods of Adjustment and Constant Stimuli for the Estimation of Redirection Detection Thresholds. *Lecture Notes in Computer Science (including subseries Lecture Notes in Artificial Intelligence and Lecture Notes in Bioinformatics)*, Vol. 11883 LNCS, pp. 226–245, 2019.

[118] Matthias Hoppe, Pascal Knierim, Thomas Kosch, Markus Funk, Lauren Futami, Stefan Schneegass, Niels Henze, Albrecht Schmidt, and Tonja Machulla. Vrhapticdrones: Providing haptics in virtual reality through quadcopters. *ACM International Conference Proceeding Series*, pp. 7–18, 2018.

[119] Anh Nguyen and Andreas Kunz. Discrete scene rotation during blinks and its effect on redirected walking algorithms. *Proceedings of the ACM Symposium on Virtual Reality Software and Technology, VRST*, 2018.

[120] M. Zank and A. Kunz. Eye tracking for locomotion prediction in redirected walking. In *2016 IEEE Symposium on 3D User Interfaces (3DUI)*, pp. 49–58, 2016.

[121] Gerd Bruder, Paul Lubos, and Frank Steinicke. Cognitive resource demands of redirected walking. *IEEE transactions on visualization and computer graphics*, Vol. 21, No. 4, pp. 539–544, 2015.

[122] Anh Nguyen, Yannick Rothacher, Evdokia Efthymiou, Bigna Lenggenhager, Peter Brugger, Lukas Imbach, and Andreas Kunz. Effect of cognitive load on curvature redirected walking thresholds. In *26th ACM Symposium on Virtual Reality Software and Technology*, pp. 1–5, 2020.

[123] Dag Alnæs, Markus Handal Sneve, Thomas Espeseth, Tor Endestad, Steven Harry Pieter van de Pavert, and Bruno Laeng. Pupil size signals mental effort deployed during multiple object tracking and predicts brain activity in the dorsal attention network and the locus coeruleus. *Journal of vision*, Vol. 14, No. 4, pp. 1–1, 2014.

[124] Kenneth R Boff, Lloyd Kaufman, and James P Thomas. Handbook of perception and human performance. volume 2. cognitive processes and performance. Technical report, HARRY G ARMSTRONG AEROSPACE MEDICAL RESEARCH LAB WRIGHT-PATTERSON AFB OH, 1994.

[125] Arthur F Kramer. Physiological metrics of mental workload: A review of recent progress. *Multiple-task performance*, pp. 279–328, 1991.

[126] Jackson Beatty. Task-evoked pupillary responses, processing load, and the structure of processing resources. *Psychological bulletin*, Vol. 91, No. 2, p. 276, 1982.

[127] Sylvia Ahern and Jackson Beatty. Pupillary responses during information processing vary with scholastic aptitude test scores. *Science*, Vol. 205, No. 4412, pp. 1289–1292, 1979.

[128] Susana Martinez-Conde, Stephen L Macknik, and David H Hubel. The role of fixational eye movements in visual perception. *Nature reviews neuroscience*, Vol. 5, No. 3, pp. 229–240, 2004.

[129] Eva Siegenthaler, Francisco M Costela, Michael B McCamy, Leandro L Di Stasi, Jorge Otero-Millan, Andreas Sonderegger, Rudolf Groner, Stephen Macknik, and Susana Martinez-Conde. Task difficulty in mental arithmetic affects microsaccadic rates and magnitudes. *European Journal of Neuroscience*, Vol. 39, No. 2, pp. 287–294, 2014.

[130] Krzysztof Krejtz, Andrew T Duchowski, Anna Niedzielska, Cezary Biele, and Izabela Krejtz. Eye tracking cognitive load using pupil diameter and microsaccades with fixed gaze. *PloS one*, Vol. 13, No. 9, p. e0203629, 2018.

[131] Richard Fitzpatrick and DI McCloskey. Proprioceptive, visual and vestibular thresholds for the perception of sway during standing in humans. *The Journal of physiology*, Vol. 478, No. 1, pp. 173–186, 1994.

[132] Corinne GC Horlings, Mark G Carpenter, Ursula M Küng, Flurin Honegger, Brenda Wiederhold, and John HJ Allum. Influence of virtual reality on postural stability during movements of quiet stance. *Neuroscience letters*, Vol. 451, No. 3, pp. 227–231, 2009.

[133] Justin Munafo, Meg Diedrick, and Thomas A Stoffregen. The virtual reality head-mounted display oculus rift induces motion sickness and is sexist in its effects. *Experimental brain research*, Vol. 235, No. 3, pp. 889–901, 2017.

[134] Ralf Engbert and Reinhold Kliegl. Microsaccades uncover the orientation of covert attention. *Vision research*, Vol. 43, No. 9, pp. 1035–1045, 2003.

[135] Ralf Engbert. Microsaccades: A microcosm for research on oculomotor control, attention, and visual perception. *Progress in brain research*, Vol. 154, pp. 177–192, 2006.

[136] Susana Martinez-Conde, Stephen L Macknik, Xoana G Troncoso, and David H Hubel. Microsaccades: a neurophysiological analysis. *Trends in neurosciences*, Vol. 32, No. 9, pp. 463–475, 2009.

[137] Robert J Peterka. Sensorimotor integration in human postural control. *Journal of neurophysiology*, Vol. 88, No. 3, pp. 1097–1118, 2002.

[138] Daniel L Wardman and Richard C Fitzpatrick. What does galvanic vestibular stimulation stimulate? In *Sensorimotor Control of Movement and Posture*, pp. 119–128. Springer, 2002.

[139] Daniel L Wardman, Janet L Taylor, and Richard C Fitzpatrick. Effects of galvanic vestibular stimulation on human posture and perception while standing. *The Journal of physiology*, Vol. 551, No. 3, pp. 1033–1042, 2003.

[140] Sudipto Pal, Sally M. Rosengren, and James G. Colebatch. Stochastic galvanic vestibular stimulation produces a small reduction in sway in Parkinson's disease. *Journal of Vestibular Research: Equilibrium and Orientation*, Vol. 19, No. 3-4, pp. 137–142, 2009.

[141] Shinichi Iwasaki, Yoshiharu Yamamoto, Fumiharu Togo, Makoto Kinoshita, Yukako Yoshifuji, Chisato Fujimoto, and Tatsuya Yamasoba. Noisy vestibular stimulation improves body balance in bilateral vestibulopathy. *Neurology*, Vol. 82, No. 11, pp. 969–975, 2014.

[142] Chisato Fujimoto, Yoshiharu Yamamoto, Teru Kamogashira, Makoto Kinoshita, Naoya Egami, Yukari Uemura, Fumiharu Togo, Tatsuya Yamasoba, and Shinichi Iwasaki. Noisy galvanic vestibular stimulation induces a sustained improvement in body balance in elderly adults. *Scientific Reports*, Vol. 6, No. October, pp. 1–8, 2016.

[143] Max Wuehr, Julian Decker, and Roman Schniepp. Noisy galvanic vestibular stimulation: an emerging treatment option for bilateral vestibulopathy. *Journal of Neurology*, Vol. 264, No. s1, pp. 81–86, 2017.

[144] Richard C Fitzpatrick, Daniel L Wardman, and Janet L Taylor. Effects of galvanic vestibular stimulation during human walking. *The Journal of Physiology*, Vol. 517, No. Pt 3, p. 931, 1999.

[145] Richard C Fitzpatrick and Brian L Day. Probing the human vestibular system with galvanic stimulation. *Journal of applied physiology*, Vol. 96, No. 6, pp. 2301–2316, 2004.

[146] Kazuma Aoyama, Hiroyuki Iizuka, Hideyuki Ando, and Taro Maeda. Four-pole galvanic vestibular stimulation causes body sway about three axes. *Scientific Reports*, Vol. 5, pp. 1–4, 2015.

[147] Kathrin S Utz, Violeta Dimova, Karin Oppenländer, and Georg Kerkhoff. Electrified minds: transcranial direct current stimulation (tdcs) and galvanic vestibular stimulation (gvs) as methods of non-invasive brain stimulation in neuropsychology—a review of current data and future implications. *Neuropsychologia*, Vol. 48, No. 10, pp. 2789–2810, 2010.

[148] Kazuma Aoyama, Daiki Higuchi, Kenta Sakurai, Taro Maeda, and Hideyuki Ando. Gvs ride: Providing a novel experience using a head mounted display and four-pole galvanic vestibular stimulation. In *ACM SIGGRAPH 2017 Emerging Technologies*, SIGGRAPH '17, New York, NY, USA, 2017. Association for Computing Machinery.

[149] Misha Sra, Abhinandan Jain, and Pattie Maes. Adding proprioceptive feedback to virtual reality experiences using galvanic vestibular stimulation. In *Proceedings of the 2019 CHI Conference on Human Factors in Computing Systems*, pp. 1–14, 2019.

[150] 前田太郎, 安藤英由樹, 渡邊淳司, 杉本麻樹. 前庭感覚電気刺激を用いた感覚の提示. バイオメカニズム学会誌, Vol. 31, No. 2, pp. 82–89, 2007.

[151] Sudipto Pal, Sally M Rosengren, and James G Colebatch. Stochastic galvanic vestibular stimulation produces a small reduction in sway in parkinson's disease. *Journal of Vestibular Research*, Vol. 19, No. 3, 4, pp. 137–142, 2009.

[152] Ajitkumar P Mulavara, Matthew J Fiedler, Igor S Kofman, Scott J Wood, Jorge M Serrador, Brian Peters, Helen S Cohen, Millard F Reschke, and Jacob J Bloomberg. Improving balance function using vestibular stochastic resonance: optimizing stimulus characteristics. *Experimental brain research*, Vol. 210, No. 2, pp. 303–312, 2011.

[153] Luca Gammaitoni, Peter Hänggi, Peter Jung, and Fabio Marchesoni. Stochastic resonance. *Reviews of modern physics*, Vol. 70, No. 1, p. 223, 1998.

[154] Chisato Fujimoto, Naoya Egami, Takuya Kawahara, Yukari Uemura, Yoshiharu Yamamoto, Tatsuya Yamasoba, and Shinichi Iwasaki. Noisy galvanic vestibular stimulation sustainably improves posture in bilateral vestibulopathy. *Frontiers in Neurology*, Vol. 9, No. OCT, 2018.

[155] Aram Keywan, Hiba Badarna, Klaus Jahn, and Max Wuehr. No evidence for after-effects of noisy galvanic vestibular stimulation on motion perception. *Scientific Reports*, Vol. 10, No. 1, pp. 1–7, 2020.

[156] R Zink, SF Bucher, A Weiss, Th Brandt, and M Dieterich. Effects of galvanic vestibular stimulation on otolithic and semicircular canal eye movements and perceived vertical. *Electroencephalography and clinical neurophysiology*, Vol. 107, No. 3, pp. 200–205, 1998.

[157] 永谷直久, 吉積将, 杉本麻樹, 稲見昌彦ほか. 前庭感覚電気刺激により生起される主観的視野運動の計測. 情報処理学会論文誌, Vol. 53, No. 4, pp. 1372–1379, 2012.

[158] Michael I Posner, Mary J Nissen, and Raymond M Klein. Visual dominance: an information-processing account of its origins and significance. *Psychological review*, Vol. 83, No. 2, p. 157, 1976.

[159] Herbert L Pick, David H Warren, and John C Hay. Sensory conflict in judgments of spatial direction. *Perception & Psychophysics*, Vol. 6, No. 4, pp. 203–205, 1969.

[160] Stefania Serafin, Niels C Nilsson, Erik Sikstrom, Amalia De Goetzen, and Rolf Nordahl. Estimation of detection thresholds for acoustic based redirected walking techniques. In *2013 IEEE Virtual Reality (VR)*, pp. 161–162. IEEE, 2013.

[161] Bela Julesz. Foundations of cyclopean perception. 1971.

[162] PO Bishop. Can random-dot stereograms serve as a model for the perception of depth in relation to real three-dimensional objects? *Vision research*, Vol. 36, No. 10, pp. 1473–1477, 1996.

[163] Dora E Angelaki and Bernhard JM Hess. Self-motion-induced eye movements: effects on visual acuity and navigation. *Nature Reviews Neuroscience*, Vol. 6, No. 12, p. 966, 2005.

[164] Nicolas Misdariis, Antoine Minard, Patrick Susini, Guillaume Lemaitre, Stephen McAdams, and Etienne Parizet. Environmental sound perception: Metadescription and modeling based on independent primary studies. *EURASIP Journal on Audio, Speech, and Music Processing*, Vol. 2010, pp. 1–26, 2010.

[165] Keigo Matsumoto, Yuki Ban, Takuji Narumi, Yohei Yanase, Tomohiro Tanikawa, and Michitaka Hirose. Unlimited corridor: Redirected walking techniques using visuo haptic interaction. In *ACM SIGGRAPH 2016 Emerging Technologies, SIGGRAPH 2016*, pp. 1–2, 2016.

[166] Keigo Matsumoto, Takuji Narumi, Yuki Ban, Yohei Yanase, Tomohiro Tanikawa, and Michitaka Hirose. Unlimited corridor: A visuo-haptic redirection system. In *The 17th International Conference on Virtual-Reality Continuum and its Applications in Industry*, pp. 1–9, 2019.

[167] Paul Lubos, Gerd Bruder, and Frank Steinicke. Safe Walking Zones: Visual Guidance for Redirected Walking in Confined Real-World Spaces. In Gerd Bruder, Shunsuke Yoshimoto, and Sue Cobb, editors, *ICAT-EGVE 2018 - International Conference on Artificial Reality and Telexistence and Eurographics Symposium on Virtual Environments*. The Eurographics Association, 2018.

[168] Lung-Pan Cheng, Thijs Roumen, Hannes Rantzsch, Sven Köhler, Patrick Schmidt, Robert Kovacs, Johannes Jasper, Jonas Kemper, and Patrick Baudisch. TurkDeck: Physical Virtual Reality Based on People. *Proceedings of the 28th Annual ACM Symposium on User Interface Software & Technology - UIST '15*, pp. 417–426, 2015.

[169] Hiroshi Fukuyama, Shin-ichiro Kumagaya, Kosuke Asada, Satsuki Ayaya, and Masaharu Kato. Autonomic versus perceptual accounts for tactile hypersensitivity in autism spectrum disorder. *Scientific reports*, Vol. 7, No. 1, pp. 1–12, 2017.

[170] Mitsuo Kawato, Kazunori Furukawa, and Ryoji Suzuki. A hierarchical neural-network model for control and learning of voluntary movement. *Biological cybernetics*, Vol. 57, No. 3, pp. 169–185, 1987.

[171] Ben J. Congdon and Anthony Steed. Sensitivity to rate of change in gains applied by redirected walking. *Proceedings of the ACM Symposium on Virtual Reality Software and Technology, VRST*, 2019.

[172] Matthew A Nurse and Benno M Nigg. The effect of changes in foot sensation on plantar pressure and muscle activity. *Clinical Biomechanics*, Vol. 16, No. 9, pp. 719–727, 2001.

[173] Eric Eils, Stefan Nolte, Markus Tewes, Lothar Thorwesten, Klaus Völker, and Dieter Rosenbaum. Modified pressure distribution patterns in walking following reduction of plantar sensation. *Journal of biomechanics*, Vol. 35, No. 10, pp. 1307–1313, 2002.

[174] Hylton B Menz, Meg E Morris, and Stephen R Lord. Foot and ankle characteristics associated with impaired balance and functional ability in older people. *The Journals of Gerontology Series A: Biological Sciences and Medical Sciences*, Vol. 60, No. 12, pp. 1546–1552, 2005.

[175] Julian Hildebrandt, Patric Schmitz, André Calero Valdez, Leif Kobbelt, and Martina Ziefle. Get well soon! human factors' influence on cybersickness after redirected walking exposure in virtual reality. In *International Conference on Virtual, Augmented and Mixed Reality*, pp. 82–101. Springer, 2018.

[176] Richard E Scammon. The first seriatim study of human growth. *American Journal of Physical Anthropology*, Vol. 10, No. 3, pp. 329–336, 1927.

[177] Michael Davis and Allan R Wagner. Habituation of startle response under incremental sequence of stimulus intensities. *Journal of comparative and physiological psychology*, Vol. 67, No. 4, p. 486, 1969.

Achievements

Original Papers

[1] Ryohei Nagao, **Keigo Matsumoto**, Takuji Narumi, Tomohiro Tanikawa, and Michitaka Hirose: Ascending and descending in virtual reality: Simple and safe system using passive haptics. IEEE transactions on visualization and computer graphics 24 (4), 1584-1593. 2018.

[2] **松本啓吾**，鳴海拓志，伴祐樹，谷川智洋，廣瀬通孝．視触覚間相互作用を用いた曲率操作型リダイレクテッドウォーキング．日本バーチャルリアリティ学会論文誌, vol.23, no.3, pp.129–138. 2018. [* Chapter 7 is based on this publication]

[3] 山本達己，**松本啓吾**，鳴海拓志，谷川智洋，廣瀬通孝．ヨー方向とロール方向の複合的視点操作によるリダイレクテッドウォーキング．日本バーチャルリアリティ学会論文誌, vol.23, no.3, pp.159–168. 2018.

International Conferences (Peer-reviewed)

[1] Peizhong Gao, **Keigo Matsumoto**, Takuji Narumi, Michitaka Hirose: Visual-Auditory Redirection: Multimodal Integration of Incongruent Visual and Auditory Cues for Redirected Walking, 2020 IEEE International Symposium on Mixed and Augmented Reality, pp. 639-648. 2020.
DOI:https:doi.org/10.1109/ISMAR50242.2020.00092. [* Chapter 6 is based on this publication]

[2] **Keigo Matsumoto**, Eike Langbehn, Takuji Narumi and Frank Steinicke: Detection Thresholds for Vertical Gains in VR and Drone-based Telepresence Systems, 2020 IEEE Conference on Virtual Reality and 3D User Interfaces (VR), pp. 101-107. 2020.
DOI:https://doi.org/10.1109/VR46266.2020.00028.

[3] **Keigo Matsumoto**, Takuji Narumi, Yuki Ban, Yohei Yanase, Tomohiro Tanikawa, and Michitaka Hirose: Unlimited Corridor: A Visuo-haptic Redirection System, In The 17th International Conference on Virtual-Reality Continuum and its Applications in Industry (VRCAI '19). pp. 1-9. 2019.
DOI:https://doi.org/10.1145/3359997.3365705. [* Chapter 7 is based on this publication]

[4] Junya Mizutani, **Keigo Matsumoto**, Ryohei Nagao, Takuji Narumi, Tomohiro Tanikawa, and Michitaka Hirose: Error Correction in Redirection: Rotational Manipulation for Natural Walking and Control of Walking Paths. ICAT-EGVE 2018 - International Conference on Artificial Reality and Telexistence and Eurographics Symposium on Virtual Environments 2018. DOI:https://doi.org/10.2312/egve.20181313.

[5] **Keigo Matsumoto**, Yuki Ban, Takuji Narumi, Tomohiro Tanikawa and Michitaka Hirose: Curvature Manipulation Techniques in Redirection Using Haptic Cues, 2016 IEEE Symposium on 3D User Interfaces (3DUI), pp. 105-108, 2016. DOI:https://doi.org/10.1109/3DUI.2016.7460038.

Demonstrations (Peer-reviewed)

[1] **Keigo Matsumoto***, Nami Ogawa*, Hiroyuki Inou, Shizuo Kaji, Yutaka Ishii, Michitaka Hirose: Polyvision: 4D space manipulation through multiple projection, SIGGRAPH Asia '19 Emerging Technologies, Brisbane, Australia, Nov. 2019. (*: equally contributed)

[2] Tatsuki Yamamoto, Junya Shimatani, Isamu Ohashi, **Keigo Matsumoto**, Takuji Narumi, Tomohiro Tanikawa, and Michitaka Hirose: Mobius Walker: Pitch And Roll Redirected Walking, SIGGRAPH Asia 2017, demo & talk, Nov. 2017. (Best Demonstration)

[3] **Keigo Matsumoto**, Takeru Hashimoto, Junya Mizutani, Hibiki Yonahara, Ryohei Nagao, Takuji Narumi, Tomohiro Tanikawa, and Michitaka Hirose: Magic Table: Deformable Props using Visuo Haptic Redirection, SIGGRAPH Asia 2017, demo & talk, Nov. 2017.

[4] Ryohei Nagao, **Keigo Matsumoto**, Takuji Narumi, Tomohiro Tanikawa, and Michitaka Hirose: Infinite Stairs: simulating stairs in virtual reality based on visuo-haptic interaction, SIGGRAPH 2017, demo, Aug. 2017.

[5] **Keigo Matsumoto**, Yuki Ban, Takuji Narumi, Yohei Yanase, Tomohiro Tanikawa, and Michitaka Hirose: Unlimited Corridor: redirected walking techniques using visuo haptic interaction, SIGGRAPH 2016, demo, Aug. 2016.

Poster Presentations (Peer-reviewed)

[1] Ko Tsai-Yen, Su Li-wen, Chang Yuchen, **Keigo Matsumoto**, Takuji Narumi, Michitaka Hirose: Evaluate Optimal Redirected Walking Planning Using Reinforcement Learning, IEEE ISMAR '20 Posters, VirBELA, Virtual Reality, Nov. 2020.

[2] Junya Mizutani, **Keigo Matsumoto**, Ryohei Nagao, Takuji Narumi, Tomohiro Tanikawa, Michitaka Hirose: Estimation of Detection Thresholds for Redirected Turning, IEEE VR '19 Posters, Osaka, Japan, Mar. 2019.

[3] **Keigo Matsumoto**, Ayaka Yamada, Anna Nakamura, Yasushi Uchmura, Keitaro Kawai, Tomohiro Tanikawa: Biomechanical Parameters Under Curvature Gains and Bending Gains in Redirected Walking, IEEE VR '18 Posters, Reutlingen, Germany, Mar. 2018.

[4] Tasuya Yamamoto **Keigo Matsumoto**, Takuji Narumi, Tomohiro Tanikawa, Michitaka Hirose: Adopting the Roll Manipulation for Redirected Walking, IEEE VR '18 Posters, Reutlingen, Germany, Mar. 2018.

[5] **Keigo Matsumoto**, Takuji Narumi, Yohei Yanase, Yuki Ban, Tomohiro Tanikawa, Michitaka Hirose: Visuo-Haptic Redirected Walking Using Handrail, ICAT-EGVE '18 Poster, Limassol, Cyprus, Nov. 2018.

[6] **Keigo Matsumoto**, Masahumi Muta, Kelvin Cheng, and Soh Masuko: Selecting Moving Targets in AR using Head Orientation, ICAT-EGVE '17 Poster, Adelaide, Australia, Nov. 2017. [Best Poster]

[7] Ryohei Nagao, **Keigo Matsumoto**, Takuji Narumi, Tomohiro Tanikawa, and Michitaka Hirose: Walking up virtual stairs based on visuo-haptic interaction, SIGGRAPH '17 Poster, Los Angeles, CA, Aug. 2017.

[8] **Keigo Matsumoto**, Takuji Narumi, Tomohiro Tanikawa, and Michitaka Hirose: Walking Uphill and Downhill: Redirected Walking in the Vertical Direction, SIGGRAPH '17 Poster, Los Angeles, CA, Jul. 2017.

[9] **Keigo Matsumoto**, Takuji Narumi, Yuki Ban, Tomohiro Tanikawa, and Michitaka Hirose: Turn physically curved paths into virtual curved paths, IEEE VR '17 Poster, Los Angeles, CA, Mar. 2017.

国内会議口頭発表（査読なし）

[1] 迫野弘明，**松本啓吾**，鳴海拓志，葛岡英明．連続的な曲率変化下でのリダイレクテッドウォーキング，第 25 回日本バーチャルリアリティ学会大会．2020 年 9 月

[2] 谷崎充，**松本啓吾**，鳴海拓志，葛岡英明．実空間歩行における視覚刺激の速度操作と歩行速度変化の関係性，第 25 回日本バーチャルリアリティ学会大会．2020 年 9 月

[3] **松本啓吾**，鳴海拓志，葛岡英明，廣瀬通孝．バーチャル障害物を用いた Redirected Walking 手法の検討，第 24 回日本バーチャルリアリティ学会大会．2019 年 9 月

[4] 水谷純也，**松本啓吾**，鳴海拓志，葛岡英明，廣瀬通孝．旋回量操作型リダイレクション手法の検討，第 24 回日本バーチャルリアリティ学会大会．2019 年 9 月

[5] 張祐禎，**松本啓吾**，鳴海拓志，葛岡英明，廣瀬通孝．強化学習を用いた回転量操作型リダイレクションコントローラの構築，第 24 回日本バーチャルリアリティ学会大会．2019 年 9 月

[6] 高培鐘，**松本啓吾**，鳴海拓志，葛岡英明，廣瀬通孝．VR 環境下における方向認識の視聴覚統合，第 24 回日本バーチャルリアリティ学会大会．2019 年 9 月

[7] **松本啓吾**，鳴海拓志，谷川智洋，廣瀬通孝．バーチャルハンドの視触覚提示が曲率操作型リダイレクションに与える効果の検討，第 23 回日本バーチャルリアリティ学会大会．2018 年 9 月

[8] 山本達己，**松本啓吾**，鳴海拓志，谷川智洋，廣瀬通孝．勾配ゲインと曲率ゲインを固定化したリダイレクション，第 23 回日本バーチャルリアリティ学会大会．2018 年 9 月

[9] 水谷純也，長尾涼平，**松本啓吾**，鳴海拓志，谷川智洋，廣瀬通孝．身体と環境との整合性を考慮した回転量操作型リダイレクションに関する基礎検討，ヒューマンインタフェース学会 (SIGDeMO)．2018 年 6 月

[10] **松本啓吾**，長尾涼平，鳴海拓志，谷川智洋，廣瀬通孝．並進移動量操作を用いた坂昇降感覚提示手法の研究，第 22 回日本バーチャルリアリティ学会大会．2017 年 9 月

[11] 長尾涼平，**松本啓吾**，鳴海拓志，谷川智洋，廣瀬通孝．視触覚間相互作用を用いた疑似上昇感覚提示の基礎検討．マルチメディア・仮想環境基礎研究会（MVE）.2017 年 6 月

Invited Talks

[1] Eike Langbehn, **Keigo Matsumoto**, etc. Walking in Circles - Two Decades of Redirected Walking. ICAT EGVE 2020. Dec. 2020. (to attend)

[2] 石井晃，鈴木一平，**松本啓吾**，阿部達矢，遠藤雅伸，小林頼子．VR が更新するリアリティ．第 20 回文化庁メディア芸術祭．2017 年 9 月

[3] 小川奈美，**松本啓吾**．VR で探り，活用する，人の知覚の仕組み．Unite 2017 Tokyo．2017 年 5 月

Books

[1] 廣瀬 通孝 (監修)，東京大学バーチャルリアリティ教育研究センター（編集）. トコトンやさしい VR の本．日刊工業新聞社, 2019.（分担執筆）

Patent

[1] 「画像処理装置、画像処理方法、およびプログラム」牟田 将史，**松本啓吾**，チェング ケルビン カ シン，益子 宗　特許 6581748（令和 1 年 9 月 6 日　登録）

Exhibitions

[1] Unlimited Corridor，文化庁メディア芸術祭　長崎展，長崎県庁舎，2020 年 1 月 8 日-1 月 19 日

[2] Unlimited Corridor，文化庁メディア芸術祭 やんばる展 『見えるものと見えないものと』，大宜味村立旧塩屋小学校，2018 年 12 月 15 日-2019 年 1 月 20 日

[3] Unlimited Corridor,「めがねと旅する美術」展，静岡県立美術館，2018 年 11 月 23 日-2019 年 1 月 27 日

[4] Unlimited Corridor,「めがねと旅する美術」展，島根県立石見美術館，2018 年 9 月 15 日-11 月 12 日

[5] Unlimited Corridor,「めがねと旅する美術」展，青森県立美術館，2018 年 7 月 20 日-9 月 2 日

[6] Unlimited Corridor, FILE São Paulo 2018 ”The body is the message”, FIESP Cultural Center, 04 July to 12 August 2018

[7] Unlimited Corridor，第 20 回文化庁メディア芸術祭，東京オペラシティ，2017 年 9 月 16 日-28 日

[8] Change Feather，第 18 回東京大学制作展 ”Fake Future”，東京大学，2016 年 11 月 17 日-11 月 21 日

[9] Unlimited Corridor，経済産業省 Innovative Technologies 2016，日本科学未来館，2016 年 10 月 27 日-30 日

[10] Alice in Wander Around, 東京大学制作展 EXTRA 2016 ”補助線”，東京大学, 2016 年 7 月 8 日-7 月 11 日

Awards

[1] 視触覚間相互作用を用いた曲率操作型リダイレクテッドウォーキング，日本バーチャルリアリティ学会　論文賞，2019 年 3 月

[2] 東京大学　総長賞，2018 年 3 月

[3] Unlimited Corridor, 第 20 回文化庁メディア芸術祭　エンターテインメント部門優秀賞，2017 年 9 月